

EPSRC

Engineering and Physical Sciences
Research Council



University Defence Research Collaboration (UDRC)

**Engineering and Physical Sciences Research Council
& Defence Science Technology Laboratory**

**Loughborough, Surrey, Strathclyde, Cardiff and Newcastle
(LSSCN) Consortium**

**“Signal Processing Solutions for the
Networked Battlespace”**

**Fourth Year Progress Report
March 2017**

Director: Professor Jonathon Chambers FEng

Deputy Director: Professor John Soraghan



Contents

Reporting to Sponsors in Year IV	p 3
Technical Highlights for Year IV	p 4
Vision Statement, Sub-Tasks & Gantt Chart.....	pp 5-7
L-WP1 Anomaly Detection	pp 8-38
L-WP2 Handling Uncertainty & Domain Knowledge	pp 39-53
L-WP3 Source Separation & Broadband Beamforming	pp 54-77
L-WP4 MIMO and Distributed Sensing	pp 78-97
L-WP5 Efficient Implementation	pp 98-117

Reporting to Sponsors in Year IV

The fourth year of the operation of the LSSCN consortium as part of UDRC II has been very successful. Our progress is recorded jointly in the 11th progress report which was provided to Dstl and EPSRC in September 2016 and this fourth-year annual report which is again delivered ahead of the 31st March 2017 deadline.

Earlier in March 2017 we were also required by the EPSRC to update Researchfish with our outputs for the last year. We are pleased to report that it is now populated with 131 published outputs for the first four years of UDRC II, composed of some 40 journal articles, 85 conference works, 1 book chapter and 5 PhD theses completed by UDRC graduates. It is particularly noteworthy that the world-class training provided to these UDRC PhD graduates has resulted in them progressing to new academic and industrial career positions both in the UK and internationally.

In terms of academic staff and research assistants the consortium has been essentially stable over the last year. However, Dr Miao Yu (L_WP2) has recently accepted a permanent lectureship in Machine Learning at the University of Lincoln, and so we are in the process of recruiting a replacement for the final year of UDRC II. We wish Miao every success in this new role and thank him for his major contributions over the last four years.

The LSSCN consortium has continued to contribute to all activities forming UDRC II, including the annual SSPD conference and vacation school, together with knowledge transfer and themed days, and challenges. Moreover, building upon the success of the new PEVD MATLAB toolbox for polynomial matrix eigenvalue decompositions generated from within our consortium, we are indebted to Professor John McWhirter FRS and Dr Stephan Weiss for running a unique workshop on Polynomial Matrix Decompositions and their Applications at The Royal Society, Kavli International Research Centre, Chicheley Hall, 25th-26th August 2016 which benefitted both academic and industrial delegates. We have also played a major part in running the 11th IMA Mathematics in Signal Processing Conference at the IET Austin Court, Birmingham, 12th-14th December 2016, in order that a wider community benefits from the progress in UDRC II.

Our consortium also continues to enjoy excellent support from our industrial partners including Atlas Elektronik, Leonardo, Mathworks, QinetiQ, and Thales, and we wish to thank them all for their outstanding commitment to ensuring the success of our consortium. We also welcome Kaon Ltd who have also formally joined the LSSCN consortium in 2016.

We remain very grateful to the Dstl team for their help; of particular value this year has been in working with researchers on L_WP1 to provide access to the WASABI and related datasets, and guidance in network anomaly and surveillance tasks. The generosity of the national and international independent experts within the consortium has also been invaluable.

In conclusion, we are very much looking forward to the fifth and final year of our operation, and pushing further for the exploitation of our findings, thereby benefiting the technical advantage of our armed services and the security of the UK.

Technical Highlights for Year IV

Full details can be found in ensuing workpackage reports:

- **L_WP1 (Anomaly Detection)** 1) anomaly detection in ship behaviour using a displacement model based on Gaussian processes; 2) cyber port scanning attack detection based on exploiting contextual information in the form of a pattern of life model; 3) human activity recognition using a novel temporal hierarchy model to represent complex activities in video.
- **L_WP2 (Handling Uncertainty and Domain Knowledge)** 1) ballistic missile tracking with a generalized state-dependent interactive multiple model based particle filter; 2) chemical, biological and radiological (CBR) dispersion source estimation using a new information theoretic search strategy "Entrotaxis", exploiting maximum entropy sampling principles; 3) multistatic radar resource allocation based upon a Bayesian Game Theoretic approach; 4) robust waveform design for multistatic cognitive radars.
- **L_WP3 (Source Separation and Broadband Beamforming)** 1) a novel proof to better understand the second order sequential best rotation algorithm for diagonalising Para-Hermitian polynomial matrices; 2) minimising the sensors in hydrophone arrays through compressed sensing; 3) overcoming sensor failures in hydrophone arrays through sparsity promoting optimisation; 4) acoustic reflector localisation and its exploitation in acoustic source separation.
- **L_WP4 (MIMO and Distributed Sensing)** 1) ambiguity function for MIMO radar systems; 2) prototype and experimental evaluation of a fractional Fourier based waveform for a joint radar-communication system and comparison with OFDM; 3) a new space debris detection and monitoring system based on a bistatic passive radar deployed on a CubeSAT flying in low earth orbit; 4) GUAPO - GNSS based UAV monitoring system using passive radar observations.
- **L_WP5 (Efficient Implementation)** 1) improved computational performance and algorithm speed-up of the PEVD algorithms; 2) multiple shift algorithms for polynomial matrices such as a multiple-shift QR decomposition for polynomial matrices; 3) exploiting parallelisation through partitioning of covariance matrices to handle BIG PEVDs such as in towed sonar array applications; 4) linking with L_WP1 to provide an FPGA implementation of an evolving GMM for image segmentation.
- Premier journal outputs for example in IEEE Trans. Aerospace and Electronic Systems, Multimedia and Signal Processing continue to be generated and presentations are being delivered at leading international conferences such as ICASSP and Radar 2017.

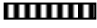


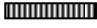
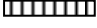




Vision Statement for Consortium

The future battlespace will be a complex environment characterised by known and unknown threats, modern and legacy sensor systems, a congested RF spectrum, and mobile and static forces. Information is key in warfare but future conflicts are likely to be characterised by an increased level of complexity in intelligence gathering and analysis. Unless such complexity can be overcome, the effectiveness of critical decision making and operational actions will be reduced.

Legacy, current and future sensor systems will provide ever more data for subsequent analysis hence advances in technology will be essential to ensure that they can be optimally exploited. The outputs of sensors of different modalities, capabilities and locations within the battlespace will need to be combined in multiple ways so that such optimal exploitation can be ensured in a wide variety of operations at all levels of conflict. However, at the same time, the electronic environments in which such conflicts will take place are likely to pose greater problems as the availability of bandwidth becomes ever more restricted.

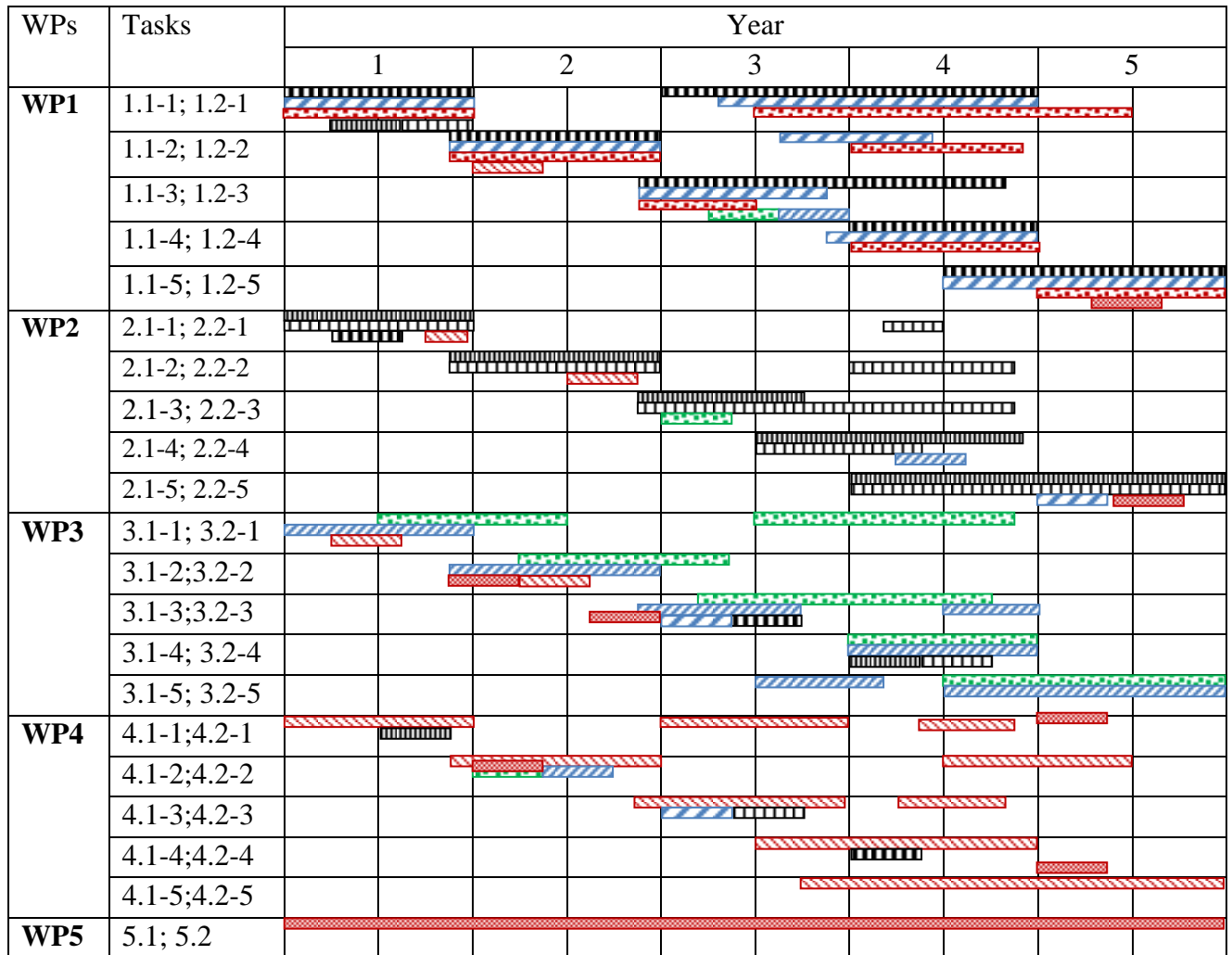
On the basis of a unique consortium of academic experts from Loughborough, Surrey, Strathclyde, Cardiff and Newcastle Universities, we will provide transformational new signal processing solutions which exploit multi-sensor and multimodal data, whilst retaining bandwidth and computational efficiency, to maximize the UK's defence capabilities and its broader academic and industrial skill-base in signal and data processing. In particular, we believe that networked-enabled distributed sensing might provide new capabilities such as combating stealth. However this potentially increases the complexity of the processing task. This might be mitigated by new signal-separation/beamforming algorithms possibly utilising sparsity concepts. Control of distributed sensors could be costly in terms of network traffic so systems that are able to interact without central control would be preferable. Networking also allows for new types of data to be available such as GIS data in a tracking problem. This could be used to enhance sensor processing but requires a new approach to handling uncertainty. Increased information implies the need for something like anomaly detection in order to reduce operator work load. Finally, in order to protect this new networked-enhanced sensing paradigm, aspects of cyber-security will be important.

Sub-Tasks and Main Research Staff for each Work Package

WPs, PDRAs & PSs	Sub-Tasks
WP1 Anomaly Detection NU-PDRA1*,  SU-PDRA4,  CU-PDRA8,  LU-PS1,	1.1-1 Baseline system (and adaptation to any new datasets, e.g. the Wasabi dataset); 1.2-1 Contextual model inference (and adaptation to any new datasets, e.g. the Wasabi dataset) 1.1-2 Radar SAM mode change detection (and Ballistic missile detection); 1.2-2 Data quality modelling 1.1-3 Discriminative anomaly detection; 1.2-3 Incongruence detection 1.1-4 Fusion of multiple anomaly detectors; 1.2-4 System integration 1.1-5 Adv. anomaly detect. sys. design; 1.2-5 Comp. netwk. anomaly detect.
WP2 Handling Uncertainty LU-PDRA2,  LU-PDRA3,  LU-PS2	2.1-1 World modelling; 2.2-1 Convex optimization and robust SP 2.1-2 Pooling data sources; 2.2-2 Radar and sensor applications 2.1-3 New adaptive algorithms; 2.2-3 Dynamic modelling of uncertainty 2.1-4 Bayesian inference; 2.2-4 Game theory; 2.1-5 Multiple sensor platforms; 2.2-5 Bayesian games
WP3 Signal Sep. & BF SU-PDRA5,  CU-PS7,  NU-PS3, SU-PS4, SU-PS5,	3.1-1 Multichan. SS with PEVD; 3.2-1 Sparse recovery and comp. sensing 3.1-2 Low-rank approx. IC in BF; 3.2-2 Adaptive dictionary learning & SS 3.1-3 PM-SVD & Sparse PEVD; 3.2-3 Noise robust T-F masking 3.1-4 Semi-blind SS & domain know.; 3.2-4 Variational Bayesian modelling 3.1-5 Complex applications and evaluations; 3.2-5 Multimodal signals
WP4 MIMO & Distributed Sensing ST-PDRA6,  ST-PS6, ST-PS7, ST-PS8	4.1-1 Waveform design for DMRS; 4.2-1 Ballistic missile classification; 4.1-2 Sparsity in DMRS; 4.2-2 DMRS based clutter mitigation; 4.1-3 Pruned OMP; 4.2-3 Information fusion in DMRS; 4.1-4 Complexity reduction; 4.2-4 Advanced ATR for DMRS 4.1-5 Passive DMRS; 4.2-5 Decentralised processing for DMRS
WP5 Efficient Implementation. ST-PDRA7 	5.1 Polynomial matrix decompositions; 5.2 Computationally efficient realizations
<i>* PDRA1 was based in Loughborough in the first three years, and then in Newcastle in the final two years.</i>	

Fourth-Year Gantt Chart (following the Jan 2017 CMT Meeting)

This will be refined following the March 2017 CSG Meeting in Strathclyde.



L_WP1 (AD) Automated Statistical Anomaly Detection and Classification in High Dimensions for the Networked Battlespace

1 Staffing

Work Package Leaders: Prof. Josef Kittler (SU), Prof. Jonathon Chambers (NU) and Dr. Yulia Hicks (CU)

Research Associates: Dr. Cemre Zor (SU), Dr. Francisco Aparicio-Navarro (LU),

Dr. Ioannis Kaloskampis (CU)

Lead Project Partner: Mr. Angus Johnson (Thales)

Other Project Partners: Mr. John Griffin and Mr. George Matich (Leonardo)

Dstl contacts: Mr. Alasdair Hunter, Mr. Richard Green, Dr. Stephen Barrington, Mr. Matthew Rixson, and Dr Jordi Barr

2 Aims and Introduction

Work Package 1 (L_WP1) is concerned with the development of algorithms for automatic detection of anomalies from multidimensional, under-sampled, non-complete datasets and unreliable sources.

The aim is to advance the state of the art in anomaly detection by developing a methodology that is not only effective and computationally efficient, but also provides insight into the nature and statistical characteristics of the detected anomalies in complex high-dimensional network environments, which include interference, communications and video signals and cyber-attacks.

3 Data

Currently, we have access to the following data sets:

- Portsmouth harbour ship monitoring data (Thales)
- Tank and helicopter data (DSTL)
- Wright-Patterson dataset (DSTL)
- WASABI dataset
- Video segmentation VSB100 benchmark
- Breakfast dataset
- Engineering activities dataset
- Glucometer calibration dataset
- IEEE 802.11 network traffic dataset (LU)
- Netflow measurements from a virtual network testbed (LU)
- LTE emulation measurements collected at Cobham/Aeroflex (Aeroflex, 2017) (LU)
- Netflow measurements from a partly virtualised network (DSTL)
- Ethernet traffic measurements from a real Local Area Network testbed (LU)

4 Outline of the Research Approach

We proposed a comprehensive methodology for anomaly detection, which builds on mechanisms that would enhance the efficiency of the detection, and allow various types of anomaly and their nuances to be identified and distinguished. The proposed mechanism includes sub-units responsible for data quality assessment, classifier outlier detection, classifier decision confidence assessment, model-drift detection and classifier incongruence detection in addition to the main operational system. In our case, the main operational system is a machine perception system interpreting input sensor data in a hierarchical manner by engaging non-contextual and contextual labelling processes.

The methodological advances in anomaly detection offered by the proposed anomaly detection system architecture are expected to be validated on diverse applications. These applications include: 1) Detection of anomalous ship behaviour using information retrieved from Automated Identification System (AIS) to aid maritime traffic control, safety and surveillance in Portsmouth harbour. 2) Network anomaly detection with the aim to increase the efficiency of flagging network intrusion. 3) Anomaly detection in surveillance videos with the objective of developing an accurate, data-driven methodology which is computationally efficient and can incorporate domain knowledge.

L_WP1 has two strands as given in Table 1.

1.1-1 Baseline system	1.2.-1 Contextual model inference
1.1-2 Radar SAM mode	1.2-2 Data quality modelling
1.1-3 Discriminative AD	1.2-3 Incongruence detection
1.1-4 Fusion of ADs	1.2-4 System integration
1.1-5 Advanced AD system	1.2-5 Communications network AD

Table 1 Two strands of L_WP1

5 Overview of the Technical Progress in Years 1-3

The advances on the baseline systems concerning anomaly detection applications and the contributions in terms of theoretical foundations, which took place in the first three years of the project, can be summarised as follows:

- A novel anomaly detection system architecture has been proposed which includes several distinct mechanisms such as classifier incongruence detection, data quality assessment, classifier confidence gauging, model-drift detection to detect anomalous events and facilitates their characterisation.
- As a part of the anomaly detection framework, three novel measures to be used in detecting incongruence, namely Δ_{avg} , Δ_{max} and D_{Δ} have been sequentially proposed. The comparisons of the proposed measures with some baseline methods are carried out, and the superiority of the delta divergence (D_{Δ}) is experimentally demonstrated. Theoretical analyses including error sensitivity have also been performed and the results have led to guidelines on determining an appropriate threshold for incongruence detection.

- For maritime anomaly detection application, an initial methodology developed for detecting anomalies in ship behaviour exhibited in the main shipping lanes has been extended to cover other vessels including ferries. The initial technique is based on Gaussian Mixture Models (GMMs), whereas the extended methodology employs Markov chains based on spatial grids. Both methods utilize the sailing direction information.
- For the network anomaly detection system, the focus was to develop methods to automatically generate labelled network traffic datasets. We developed a novel approach, based on the outcome of an anomaly-based Intrusion Detection System (IDS), to automatically label frames as malicious and non-malicious within the analysed network traffic datasets. Work was also undertaken to implement an automatic feature selection process for metric selection. A genetic algorithm based approach was developed to select the set of metrics that provide the best intrusion detection results, using the resulting labelled datasets. All these activities are in line with objectives of this project defined in the sub-task 1.2-2 Data Quality Modelling.
- The effort during the second and third year concentrated on developing different approaches to incorporate contextual information, user's cognitive information, and Situational Awareness (SA) into the intrusion detection process to increase the efficiency of the developed anomaly-based IDS. We proposed three approaches, based on the use of a Fuzzy Cognitive Map (FCM) in conjunction with our anomaly-based IDS. The activities carried out during the second year tackled the objectives defined in the sub-task 1.2-1 Contextual Model Inference, contributed in the ongoing sub-task 1.1-3 Discriminative Anomaly Detection defining novel algorithms to effectively differentiate between malicious and non-malicious information in communication networks.
- In the area of anomaly detection in surveillance videos, an accurate, data-driven and computationally efficient system was developed, which can handle heterogeneous spatio-temporal data and can incorporate domain knowledge to detect anomalies. The proposed system features: i) a low-level feature extraction component; ii) a mid-level feature representation component which organises the extracted features in an efficient manner, incorporating techniques such as dimensionality reduction, feature clustering (depending on the application, video segmentation, bag-of-words, or Fisher vectors may be used); iii) a situational assessment component which fuses low and mid-level feature representations from various sources and infers the current system state (ontologies and sequence formulation techniques may be utilised); iv) a high-level inference model which encodes the temporal dependencies between different system states, characterises the event underlying the input data (event/activity recognition and anomaly detection) and predicts the future system states.
- As part of the system's mid-level feature representation component, a video segmentation algorithm has been developed. The algorithm can handle the research problems of spatial coherence in segmentation, high dimensionality and exploiting motion in video segmentation.
- A situational assessment component based on ontologies to detect anomalous behaviour in videos of road scenes was proposed, where anomalies are related to the

degree of risk of collision. In this case, mid-level feature representations extracted with our video segmentation algorithm were used as input.

- As part of the system's high-level inference model, a new temporal model capable of recognising complex human behaviour has been developed and successfully tested with high dimensional low-level video features.
- The system has been evaluated using standard, publicly available datasets. The developed algorithms have also been applied to several defence-related datasets, including video streams from UAVs (in collaboration with WP2 - Loughborough) and the tank dataset provided by DSTL.

6 Technical Progress in Year 4

6.1 Overview

Within the fourth year of the project, the progress taken place for each sub-task annotated in Table 1 can be summarised as follows:

a) 1.1-1 Baseline system

Progress has been made on the anomaly detection systems used in communication networks, spatio-temporal video datasets and AIS maritime monitoring.

For anomaly detection in maritime data, new features such as displacement over time have been taken into consideration in addition to the already utilized sailing direction information. The new features are modelled using Gaussian Processes (GPs) to form up the final decision mechanism together with the existing Markov chain classification information. GP regression is performed together with Median Absolute Deviation to account for contaminated training data. The proposed method is applicable to ferries, with a potential extension to generic vessel types.

For anomaly detection in video, the novel framework for complex human activity recognition and anomaly detection in heterogeneous streams was finalised. The main component of the framework is the temporal hierarchy model (THIM), a formal mathematical model which represents complex activities. Highlights from the framework's final development stage are: (i) an efficient parameter learning algorithm for THIM based on sampling from the Dirichlet distribution was proposed, (ii) the framework can work with the state-of-the-art improved dense trajectory features and also STIP features, (iv) the state-of-the-art Fisher vector mid-level representation was integrated into the framework, (v) the framework is suitable for work with large datasets (>1500 videos), where the localisation and recognition of primitive actions is hard and there is a large number of missing, unrecognised or incorrectly recognised actions. Due to these improvements, the framework currently achieves state-of-the-art performance in three publicly available datasets featuring complex human behaviour.

The developed algorithms were applied to defence-related datasets, including the WASABI dataset (DSTL) and the Wright-Patterson Air Force Base 2009 (WPAFB09)

dataset. The preliminary results for WASABI were presented in the project meeting on 5 October 2016, held in Newcastle. As there were trajectory registration issues in the WASABI dataset, which will be resolved by the DSTL scientists, the algorithms are currently being applied to the WPAFB09 dataset.

b) 1.2-1 Contextual model inference

Progress has been made at Newcastle in the context of anomaly detection in communication networks to improve the detection performance of our unsupervised anomaly-based IDS. We have used Fuzzy Cognitive Maps (FCMs) in conjunction with our IDS to add contextual information into the intrusion detection process. The work conducted during the fourth year extended the analysis of the methodology that we previously proposed last year for the use of FCMs to add contextual information into the intrusion detection process. In particular, we have implemented a novel scheme to construct the FCM using high-level information extracted from the network users, with a process that is completely transparent to them. We have made use of the Pattern-of-Life (PoL) of the network usage as the main source of contextual information.

Secondly, as part of the collaboration between WP1-Cardiff and WP2-Surrey, a contextual classifier for human action and activity recognition was developed by Cardiff based on the Cardiff framework for anomaly detection in video and the HTK stream analysis system. The classifier is capable of outputting confidence scores for multiple classes both for action and activity recognition. This output will be further utilised by the components of the proposed anomaly detection system (i.e. contextual decision confidence assessment, contextual model outlier detector and incongruence detector).

Recent advances in autonomous vehicle technology pose an important problem of anomaly detection in videos of road scenes. In our work anomalies are related to the risk of collision, which are detected using a novel framework based on ontologies developed in the third year of the project (Mohammad et al., 2015). In the fourth year, the framework was improved by integrating a novel algorithm for automatic road detection from video, building on the video segmentation algorithm developed previously (Kaloskampis & Hicks, ISCCSP 2014). The new algorithm is described in (Kaloskampis et al. 2016).

c) 1.1-2 Radar SAM mode change detection (*discontinued at the start of the project*)

d) 1.2-2 Data quality modelling

Earlier work on data quality modelling was carried out at Loughborough in the context of anomaly detection in communication networks. During this reporting period the focus of the work at Surrey was on using signal quality measurements as a basis for detecting spoofing attacks on biometric security systems. The following table lists the image quality measures used as features for decision making using different classification methods, including sparse representation based classification. The security system attack

was formulated as an anomaly detection problem using quality measurements as features. The solution based on this formulation was then compared with conventional system attack approaches formulated as two or multiclass classification problems, relying on training data being available for each type of attack. The anomaly detection performance achieved using one class classifiers using the image quality features for outlier detection is promising. The study showed that signal quality can serve multiple purposes. In addition to identifying the situations where it may not be sensible to attempt to detect anomalies, image quality measurements may also be relevant as a source of discriminatory information for anomaly detection. This has implications on the anomaly detection framework investigated by the project.

#	Type	Name
1	R	Mean Square Error
2	R	Peak Signal to Noise Ratio
3	R	Signal to Noise Ratio
4	R	Structural Content
5	R	Maximum Difference
6	R	Average Difference
7	R	Normalized Absolute Error
8	R	R-Averaged Maximum Difference
9	R	Laplacian Mean Square Error
10	R	Normalized Cross-Correlation
11	R	Mean Angle Similarity
12	R	Mean Angle Magnitude Similarity
13	R	Total Edge Difference
14	R	Total Corner Difference
15	R	Spectral Magnitude Error
16	R	Spectral Phase Error
17	R	Gradient Magnitude Error
18	R	Gradient Phase Error
19	R	Structural Similarity Index
20	R	Visual Information Fidelity
21	R	Reduced Ref. Entropic Difference
22	B	JPEG Quality Index
23	B	High-Low Frequency Index
24	B	Blind Image Quality Index
25	B	Naturalness Image Quality Estimator

e) 1.1-3 Discriminative anomaly detection

Progress has been made at Newcastle in the context of anomaly detection in communication networks to improve the detection performance of our IDS. We have developed and evaluated a novel scheme to construct the FCM using contextual information extracted from the PoL of the network usage. The results confirm that the use of the contextual information improves the effectiveness of the IDS, and indicate that by utilising only measureable information from the network without considering the available contextual information, the IDS may reach a wrong conclusion, leading to an overall low accuracy. We have used different modes of port scanning attacks to evaluate the approaches that we propose. This task will continue with the development of the

detection system throughout the project duration, as new functionalities are proposed and evaluated.

As for the progress in Cardiff, anomaly detection is handled by the high-level inference THIM model. The proposed model possesses discriminative feature capabilities, as it discovers recurring actions in discrete time sequences representing activities.

The framework's discriminative capabilities were enhanced with the inclusion of the Fisher vectors, a mid-level representation which discovers underlying patterns within the extracted features.

The properties of the combination of discriminative and generative classifiers for the bridge design dataset were investigated in (Kaloskampis & Hicks, 2016) and improvement of performance was demonstrated when these two types of classifiers were combined.

f) 1.2-3 Incongruence detection

Although this task is now considered completed, the work on incongruence detection continued via a collaborative activity carried out by a visitor to CVSSP, Surrey, Dr. Moacir Ponti from the University of Sao Paulo in Brazil and his student. We developed a variant of the Kullback-Leibler divergence, named Decision-Cognizant Kullback-Leibler (DC-KL). The proposed measure reduces the impact of the minority classes, which obscure the true degree of classifier incongruence. The amount of clutter of the non-dominant hypotheses is reduced by merging them into a single event.

The properties of DC-KL have been analytically and experimentally investigated and the measure has been demonstrated to be more robust to minority class clutter than the classical KL divergence. Moreover, its sensitivity to estimation noise is also shown to be considerably lower than that of the KL divergence.

Concerning the application of incongruence detection within a generic domain anomaly detection framework, a collaboration between University of Surrey (SU) and Cardiff University (CU) has been set up. The aim is to use the surprise measures proposed by SU within the baseline video anomaly detection framework proposed by CU, where contextual and non-contextual classifiers are being used for the detection of activities and actions. This work is currently in progress on the breakfast dataset.

g) 1.1-4 Fusion of multiple anomaly detectors

In collaboration with a Brazilian visitor, Surrey worked on motion anomaly detection using the University of California San Diego Ped 2 dataset (video of pedestrians passing a pedestrian area). A novel representation of optical flow features based on empirical mode decomposition has been developed. This particular signal processing approach has the advantage that it is applicable to non-periodic, non-stationary signals, and does not assume linearity as do wavelets, PCA and Singular Spectrum Analysis. The representation achieved improved anomaly detection results. Currently this representation

is used in conjunction with other information (appearance) to develop an anomaly detection system exploiting incongruence detection and information fusion.

h) 1.2-4 System Integration

System integration activity takes place organically in connection with each of the anomaly detection applications described in the various workpackage tasks (ship behaviour anomaly, detection of anomalies in video, and detection of anomalies in communication networks).

i) 1.1-5 Advanced anomaly detection system design

The design of the advanced detection system is evolving in the context of anomaly detection in communication networks throughout the project duration. A single piece of software is being built as new functionalities are proposed and evaluated. All these functionalities have been implemented and incorporated into our unsupervised anomaly-based IDS, initially at Loughborough University and now continues at Newcastle University.

j) 1.2-5 Complex network anomaly detection

During this fourth year, effort has been made to evaluate our anomaly-based IDS on networks comprising multiple and heterogeneous communication technologies. In particular, we have moved towards the detection of anomalies and attacks in wired Ethernet networks. On the one hand, we have gathered our own network traffic dataset comprising traces of different modes of port scanning attacks in an Ethernet Local Area Network (LAN) testbed. On the other hand, Dstl have shared with us a Netflow dataset, generated in a partly virtualised wired network. This dataset contains traces of different type of attacks, such as Denial-of-Service (DoS) attacks and scanning attacks. The efficiency of our IDS detecting attacks in wired environment complements to the efficient results that we previously obtained detecting attacks in wireless networks. This is an ongoing task.

6.2 Technical Highlights

In this section, technical highlights concerning the sub-tasks *1.1-1 Baseline system* and *1.1-3 Discriminative anomaly detection* will be provided.

6.2.1 Anomaly Detection in Ship Behaviour in Portsmouth Area (Sub-task 1.1-1)

As part of Task 1.1-1, the anomaly detection framework previously developed for maritime AIS data provided by Thales has been improved further.

In the first three years of the project, a methodology for detecting anomalies in the tracks recorded by transport vehicles and ferries was implemented by making use of approaches such as Gaussian Mixture Models (GMMs) and Markov chains based on hierarchical spatial

grids. The framework was built by utilizing the sailing direction as the main information source.

In the fourth year, we have expanded the framework by exploiting more features such as time and displacement in addition to the direction information. The modelling capacity and flexibility of the framework has been enhanced by adopting Gaussian Processes (GPs) model. A novel feature of our GP approach is the use of a training data-cleaning system. As the unlabelled training data may be corrupted by anomalies, it is purified from any outliers by using Median Absolute Deviation (MAD) based on time grids, prior to GP modelling.

The output of the GP based anomaly detection system is combined with the decisions of the previously implemented Markov chain based classifier, such that if any of the two classifiers considers a track as anomalous, it is confirmed as anomalous. Experimental results summarised in terms of Receiver Operating Curves, show that the method can successfully detect all anomalies with a False Positive Rate of 6%.

Although the approach is extendable to generic ship types, in this report we concentrate on ferry track anomaly detection.

Displacement Model Based on Gaussian Processes – Technical Details

In order to define the characteristics of a track, we exploit the displacement of a ferry from its departure port, over the total time it takes for the trip. This way, it becomes possible to map the tracks into a unified form, where three critical features: time, displacement and therefore speed are taken into account jointly.

The input data for anomalous ship movement detection is expected to be composed of location information reported in the form $[V_k, V_l]$ for a given ship at any time, where V_k denotes the longitude and V_l the latitude. Given that a ferry operates between the ports O_1 and O_2 we initially carry out an automatic extraction of the so-called “one-way trips” between any combination of these ports. (Any trip where the ferry is coming back to the departure port without visiting the destination is considered to be anomalous, and such trips are left out from the training set.)

Without loss of generality, we can define a ferry's displacement from the departure port O^1 for a given trip α , as a function of the time it spent after the departure:

$$T_1^\alpha(\bar{t}) = \sqrt{(V_k^\alpha(\bar{t}) - O_k^1)^2 + (V_l^\alpha(\bar{t}) - O_l^1)^2} \quad \text{Equation 1}$$

where O_k^1 and O_l^1 are the latitude and longitude coordinates for O^1 and \bar{t} is the elapsed time. If the duration of the whole journey is given by t_j , then the displacement over normalized time becomes

$$f^a(s) = f^a\left(\frac{\bar{t}}{t_1}\right) = T_1^a(\bar{t}) \quad \text{Equation 2}$$

where $0 \leq s \leq 1$. From Equation 2, it can be observed that for each value of s , $f^a(s)$ takes different values depending on a . This scenario can be interpreted as having a function $f(s)$ whose value at each s is a random variable.

Gaussian Process regression is a method for stochastically modelling the target value of a variable, by employing a function drawn from a probability distribution. Using s as the variable, the function f can then be denoted as

$$f(s) \sim \text{GP}(b(s), k(s, s)) \quad \text{Equation 3}$$

where $b(s)$ is the mean of the probability distribution at a given realization of s and $k(s, s)$ is the covariance function which represents the similarity between two different realizations, such that

$$k(s_p, s_q) = \text{cov}(f(s_p), f(s_q)) \quad \text{Equation 4}$$

Equation 4 shows that the covariance between the outputs is given as a function of the inputs. The choice of the covariance matrix should be made according to the requirements of the system. In our approach, we use the squared exponential function. Under the assumption of having observations corrupted by independently and identically distributed Gaussian noise with zero mean and σ_c^2 variance, the noisy target values can be denoted with variable ω such that $\omega = f(s) + \varepsilon$. This corruption changes the covariance function into

$$\text{cov}(\omega_p, \omega_q) = k(s_p, s_q) + \sigma_c^2 \delta_{p,q} \quad \text{Equation 5}$$

with δ being the Kronecker delta function which is one if and only if $p=q$.

Let us denote the vector of means belonging to the distributions at each element of the training set, S , by $B(S)$; and the matrix obtained after applying the covariance function to all pairs of elements within S as $K(S, S)$. Accordingly, we denote the vector of covariances calculated between a single test point, s^* , and S as $K(S, s^*)$. Then, given S , the distribution informing the prediction at s^* , namely $f(s^*)$, can be gauged as a Gaussian distribution with the mean and variance

$$\bar{f}(s^*) = b(s^*) + K(S, s^*)^T [K(S, S) + \sigma_c^2 I]^{-1} (\Omega - B(S)) \quad \text{Equation 6}$$

$$\text{var}(f(s^*)) = k(s^*, s^*) - K(S, s^*)^T [K(S, S) + \sigma_c^2 I]^{-1} K(S, s^*) \quad \text{Equation 7}$$

where the vector of target values is denoted by Ω and I is the identity matrix. The parameters h , σ_f^2 and σ_c^2 are called the hyper-parameters and need to be estimated from the anomaly-free training data. As our training set may be contaminated by anomalies, its initial cleaning has to

be carried out before modelling normality, from which deviations will be classified as anomaly.

The cleaning is applied using Median Absolute Deviation from Median (MAD). While dealing with sampled data which is prone to outliers, MAD allows to robustly estimate the standard deviation of the underlying distribution, i.e. it is more resilient to outliers compared to the standard deviation computed from the sampled population space. In our strategy, we discretize the input domain $s \in [0,1]$ into 200 cells, and apply MAD on the target values falling within each cell. MAD is calculated as the median of the absolute differences between the points and their median:

$$MAD(\Omega_e) = c \left(med(abs(\Omega_e - med(\Omega_e))) \right) \quad \text{Equation 8}$$

where Ω_e is the vector of target variables in a given cell, e , and c is the consistency constant that is equal to 1.4826 when the underlying distribution function is assumed to be Gaussian (as in our case). By setting a cut-off value, v , any corrupted data point, ω_e^c , which satisfies $(abs(\omega_e^c - med(\Omega_e)) / MAD(\Omega_e)) > v$ is removed from the training set.

After the application of MAD followed by GP regression, the testing of anomaly for s^* is carried out by setting a multiplier r for the desired confidence interval such that

$$g = \begin{cases} 1 & \omega^* > \bar{f}(s^*) + r \text{var}(f(s^*)) \\ 1 & \omega^* < \bar{f}(s^*) - r \text{var}(f(s^*)) \\ 0 & \text{o.w.} \end{cases} \quad \text{Equation 9}$$

where g is the flag for anomaly, ω^* is the target value for the test sample and $r=2.57$ for 99% confidence interval. An input trip a is labelled as anomalous if more than $p\%$ of its time stamps are detected as anomalous, where p is a suitable threshold.

Experimental Results

The experimental study has been conducted on the AIS dataset collected by Thales UK Ltd. at the Solent area between 20/07/2012 and 19/08/2012. For each ferry, the dataset is split into training and test at a rate of 1:6 respectively, via randomly choosing 4 days for training and 24 for test, and this sampling procedure is repeated.

Initially, we note that after the application of MAD cleaning by setting the confidence constant $c=1.4826$, 3.4% of the training data has been detected as anomalous/corrupted.

By using the cleaned training dataset, we carry out an assessment of the tracks that are classified as anomalous together with those that are labelled normal by the proposed algorithm. As given in in Figure 1, for an example test set, the tracks labelled anomalous are

provided in dark shade (red) whereas the normal tracks are given in lighter colour (yellow). Using a 90% confidence interval during the GP regression, a threshold of $r=0.0005$ for the MC direction classifier, and an anomaly threshold of $p = 30$ for both classifiers, we obtain a 93% detection rate for anomalies, and 2% false positive rate (FPR). It is also possible to detect all anomalies with FPR=6%. The ROC curve using confidence intervals [1, 0.99, 0.95, 0.90, 0.85, 0.80, 0.75, 0.50] is given in Figure 2.

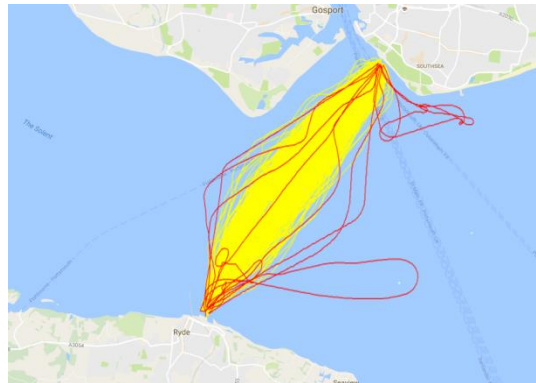


Figure 1: Detected anomalies plotted on top of normalities (dark shade on light)

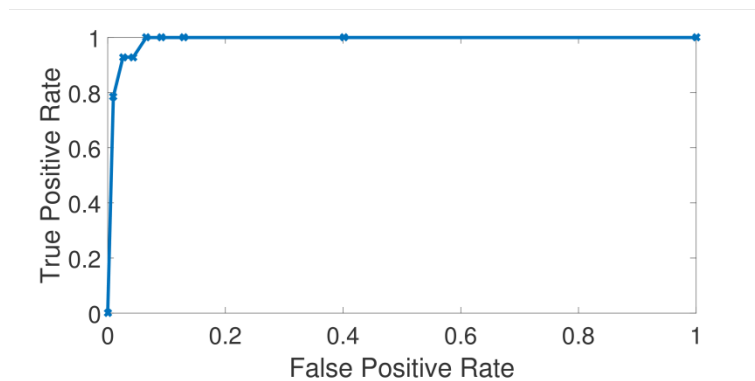


Figure 2: ROC analysis for the proposed methodology

6.2.2 Network Anomaly Detection (Sub-task 1.1-3) Contextual Information & Port Scanning Attack Detection

The focus of the work during the fourth year was to continue developing and evaluating novel algorithms to efficiently differentiate between malicious and non-malicious information in communication networks. We have extended the analysis of the methodology

that we previously proposed in (Aparicio-Navarro, 2016) for the use of FCMs to add high-level information into the intrusion detection process. This methodology builds upon the design of the unsupervised anomaly-based IDS that we previously presented in (Kyriakopoulos, 2014). The outcome of the FCM is used to fine-tune the techniques used by the anomaly-based IDS to assign evidence of attack at different stages of the detection process.

We have implemented a novel scheme to construct the FCM using high-level information extracted from the network users, with a process that is completely transparent to them. We have made use of the PoL of the network usage as the main source of contextual information. The concept of PoL refers to the information generated by observing repeated behaviours over an extended period of time. In order to characterise the PoL of the network usage and to generate useful contextual information, we have correlated the number of researchers present in the monitored offices with the time of the day and the usage of the network resources.

In order to allow the FCM to adapt to changes in the network usage, depending on the time of the day, different timeframes were defined, which define some of the concepts that compose the modelled FCM. Similarly, in order to characterise the usage of the network, a number of thresholds that define levels of normal usage of the network resources are defined. Since the network traffic would present variable levels of usage depending on the PoL (i.e. the cycles of the PoL), the defined thresholds allow the system to adapt to changes in the network usage. In turn, each of these thresholds also defines some of the concepts that compose the modelled FCM. Finally, two additional concepts are defined as the two possible outcomes of the FCM (i.e. *Normal* and *Abnormal*). The FCM weight values associated with the last two concepts are used to incorporate the contextual information into the detection process of our IDS.

We have evaluated three different approaches that employ an FCM to incorporate the PoL of the network usage into the detection process. Figure 3 shows the schematic representation of the structure of the IDS, including the extraction of the different metrics, the automatic generation of the BPA values and the data fusion process. Additionally, the figure also indicates the different stages at which each of the proposed approaches adds the contribution of the FCM into the detection process.

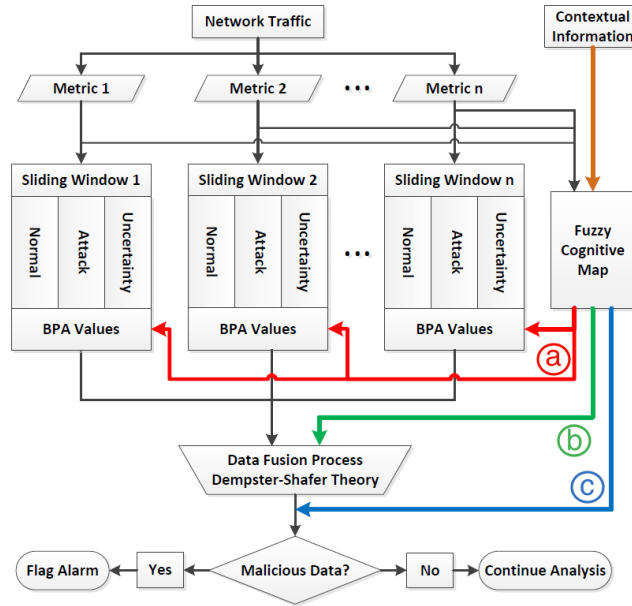


Figure 3 Schematic structure of the IDS, including the extraction of the metrics, the generation of the BPAs, the data fusion process and the addition of contextual information into the detection process by using an FCM.

a) BPA Adjustment Using the FCM Prior Data Fusion

The first approach is based on the adjustment of the BPA values assigned prior to the data fusion process, by using the outcome of the FCM. This is represented by the red channel (a) in Figure 3. Once the BPA values have been computed as explained in (Kyriakopoulos, 2014), the outcome of the FCM will be used to adjust these accordingly. Once the FCM process has ended, the outcome weights associated to FCM concepts *Normal* and *Abnormal* are used to adjust the BPA values assigned to the D-S hypotheses *Normal* and *Abnormal*. Then, the adjusted BPA values in *Normal* and *Abnormal* are used to compute the new BPA value in *Uncertainty*. After all the BPA values have been adjusted, the data fusion process is carried out using the Dempster's rule and the final decision is taken. It is worth noting that, although the same weight values are used to adjust all of the considered metrics, it is unlikely for these metrics to have the same BPA value. Therefore, the adjustments would impact each of the metrics differently.

b) Extra BPA Values Using the FCM

The second approach, represented by the green channel (b) in Figure 3, is based on the use of the output of an FCM to construct an additional metric to be fused by D-S. The outcome weights associated to the FCM concepts *Normal* and *Abnormal* are used to provide the BPAs for the hypotheses *Normal* and *Abnormal*, respectively, to yield an extra metric to be fused. These values are then used to infer the BPA in the hypothesis *Uncertainty*. Once the three BPAs have been computed, these values are merged with D-S, along with the rest of the considered network traffic metrics, using the Dempster's rule. It is worth noting that for this second approach, in contrast to the one that adjusts the BPAs prior to the fusion process, the

contextual information might have less influence over the final IDS decision, as its contribution is reduced to one set of BPAs to be fused.

c) BPA Adjustment After Data Fusion Process

The last approach, represented by the blue channel (c) in Figure 3, is based on the use of the outcome of the FCM to adjust the BPA values after the D-S data fusion process. The IDS carries out the detection process using solely the measurable information. The different BPA values are computed and fused using the Dempster’s rule. Only after the data fusion process has ended, the contextual information is used to adjust the resulting BPA values, by adding the outcome of the FCM. The adjustment is implemented over the final outcome of the IDS, hence the addition of the outcome of the FCM is prone to dominate the entire detection decision.

New network traffic has been collected from a larger and more complex network than the one use in (Aparicio-Navarro, 2016). We have collected data traffic from our own LAN testbed. Figure 4 shows the logical topology of the testbed LAN. The PCs in two distinct labs are connected to the same office LAN. In addition, two additional PCs have been connected to a testbed LAN in order to implement the attacks: an attacker launches the attack using the network mapping tool Nmap (Lyon, 2016), and a victim is in charge of gathering all the network traffic using the network packets analyser Tcpcdump (Jacobson, 2016) in pcap format.

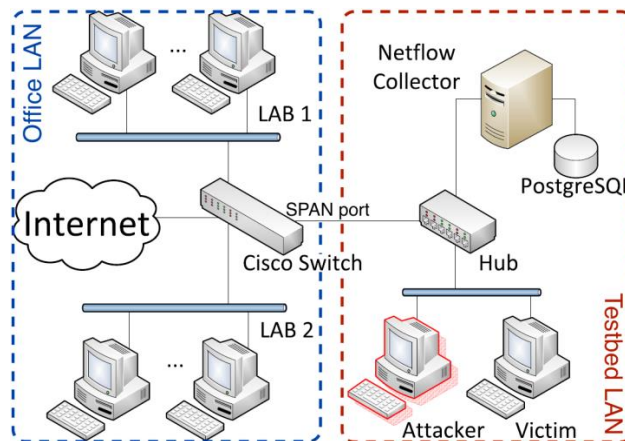


Figure 4 Logical topology of the testbed LAN; PCs on the left generate the background traffic, while those on the right are involved in the port scanning attacks implementation, and detection process.

In total, 160 GBytes of network traffic have been gathered during the 9 days that the experiment lasted. This traffic dataset comprises 99.40% of non-malicious traffic (i.e. 696638 data instances) and 0.60% of malicious traffic (i.e. 4220 data instances). Four different metrics have been computed from the dataset. These metrics are Communication Rate (COM), the number of frames transmitted per second; Throughput (THR), the number of transmitted bytes per second; Destination Port Distribution (DPD), the number of unique

destination ports per second; and Source Port Distribution (SPD), the number of unique source ports per second. These metrics are represented in Figure 5-Figure 7. The figures present cyclic patterns in the metric measurements. These cycles correspond to the PoL and the time of the day at which the network is being utilised by more users. The section in blue corresponds to the non-malicious traffic, while the section in red corresponds to the traces of port scanning attacks. Additionally, a zoomed in representation of the day 1 of the THR is shown in Figure 8. We can differentiate the different PoL depending on the time of the day, and we can also see that the traces of port scanning attack could not be easily identified by using a simple signature or threshold in all the instances.

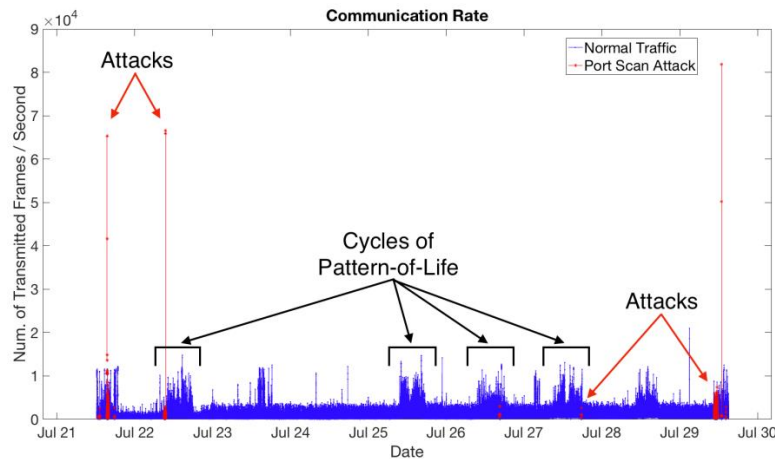


Figure 5 COM- Communication Rate (number of transmitted frames per second) collected over 9 days.

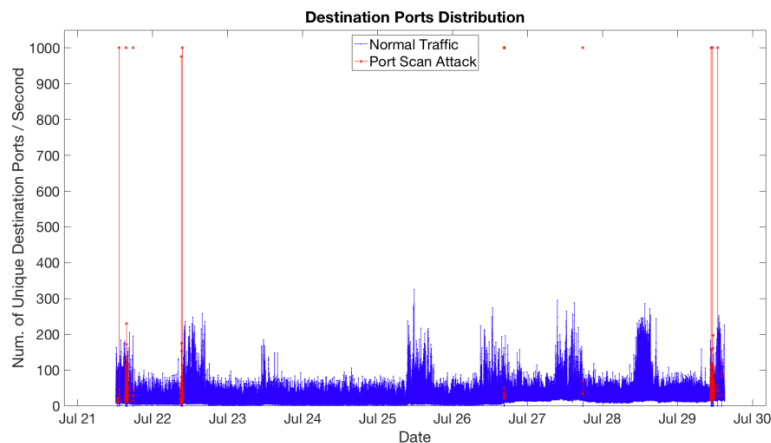


Figure 6 DPD- Destination Ports Distribution (number of unique destination ports per second) collected over 9 days.

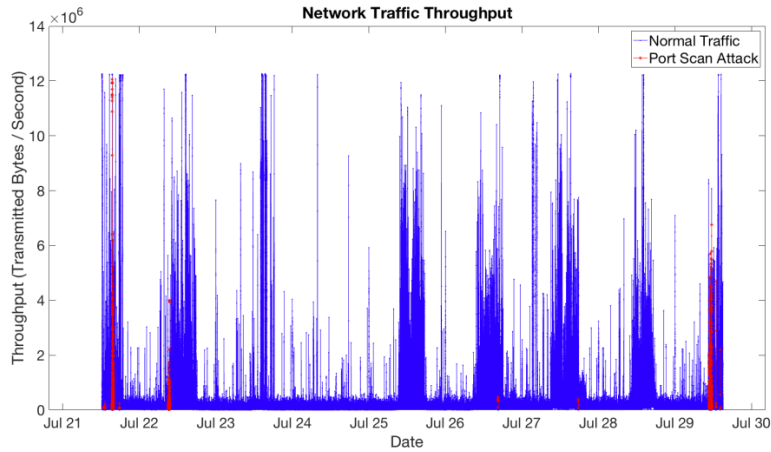


Figure 7 THR- Throughput (bytes per second) collected over 9 days.

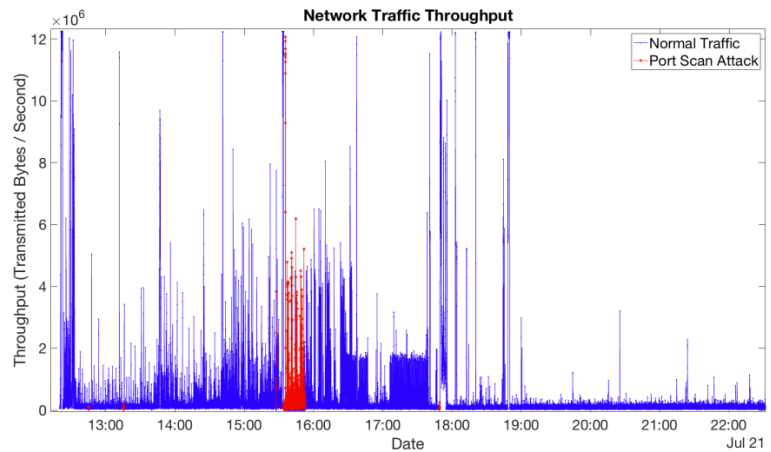


Figure 8 THR- Throughput gathered over 1 day, showing a zoomed in representation the normal traffic and malicious traffic, as well as the PoL.

The effectiveness of the IDS has been evaluated using four well-known parameters, True Positive (TP), True Negative (TN), False Positive (FP), and False Negative (FN). These parameters are essential to calculate the following performance metrics, which quantify the effectiveness of the IDSs: Detection Rate (DR), which is the proportion of anomalies correctly classified among the anomalous data; False Positive Rate (FPr), which is the proportion of normal data misclassified among all the data; and Overall Success Rate (OSR), which is the proportion of all the data correctly classified among all the data. The experimental results are presented in the form of bar charts, in Figure 9-Figure 14. The dataset has been analysed for all the possible combinations of metrics. The Y-axis of the graphs represents the results in percentage, while the X-axis of the graphs represents the index of the used metrics. Each index corresponds to one possible combination of metrics, with #1 being a single metric set and #15 the set that combines all the considered metrics. Therefore, the overall best results are to be expected from the set index #15. The indexes of all the possible combinations of metrics are presented in Table 2.

1 – DPD	6 – THR-DPD	11 – THR-SPD-DPD
2 – SPD	7 – THR-SPD	12 – CON-SPD-DPD
3 – THR	8 – COM-DPD	13 – COM-THR-DPD
4 – COM	9 – COM-SPD	14 – COM-THR-SPD
5 – SPD-DPD	10 – COM-THR	15 – COM-THR-SPD-DPD

Table 2 Index of the Combination of Metrics

The DR results of the IDS without the use of an FCM and with the application of all the proposed approaches are compared in Figure 9. The metric used to construct the FCM for these results was the THR. As we can see, with regards to the DR, there is no evident difference between all the approaches, using similar combination of metrics. It is worth noting that the approach that adjusts the BPA values prior to the fusion process using the FCM (i.e. *FCM01*) produces the highest DR in most of the cases. However, the maximum difference with the rest of DR results is only ~2%. One undesirable phenomenon that is shown in Figure 9 is that the DR decreases as the number of fused metrics increases, which is in contrast to what is expected from cross-layer IDSs. In our experiments, this phenomenon is caused by the automatic BPA methodology and the way the SW slides. When multiple metrics are used, the reference of normality in the BPA methodology becomes wider over time. Hence, the IDS becomes less sensitive and more malicious instances are misclassified as non-malicious. Nonetheless, as the OSR results show in Figure 11, this phenomenon also leads to an increase in the number of non-malicious instances correctly classified.

The FPr results of our IDS with and without the use of an FCM are compared in Figure 10. Again, the metric used to construct the FCM for these results was the THR. In contrast to the DR results, we can see that the use of FCM actually outperforms the FPr results produced by the IDS alone, for all the evaluated approaches. Among the three FCM approaches, *FCM01* is the one that always produces the lowest FPr, when two or more metrics are combined. Focusing upon the evaluations of the two approaches, *FCM01* and *No FCM*, for the set #3 (THR), the difference between the two approaches is over 35%. The largest difference for all the sets that combine two metrics is obtained in #10 (COM-THR), where the difference is 27.82%. Among the sets that combine three metrics, the largest FPr difference is obtained in #14 (COM-THR-SPD), where the difference is 17.15%. When all the metrics are combined, the difference between the two approaches is over 9.68%. This clear improvement is constant for all the combinations of metrics. Also, the set of metrics #15 is the one that produces the best FPr (i.e. the lowest FPr) results, only 6.33%. With respect to the three approaches that use an FCM, *FCM01* outperforms the FPr results generated by the other two approaches in ~5% for all the combination of metrics; and a peak improvement of up to 8.05%, for the set #10 (COM-THR).

The final performance metric that we have used is the OSR, which represents all the instances that have been correctly classified, regardless of whether these are malicious or not. Figure 11 presents the OSR results comparison between all the approaches. Similar to the FPr, the use of FCM in conjunction with the IDS outperforms the OSR results produced by the IDS without FCM, for all the evaluated approaches. Additionally, once again, *FCM01* is the one that always produces the best results among all the approaches. Focusing upon the evaluation

of the two approaches, *FCM01* and *No FCM*, for the set #3 (THR) the improvement in the OSR between the two methods is 35.64%. The largest improvement in all the sets that combine two metrics is obtained in #10 (COM-THR), where the difference between the two approaches is 27.38%. Among the sets that combine three metrics, the largest OSR improvement is obtained in #14 (COM-THR-SPD), where the difference is 17.15%. And finally, when all the metrics are combined, the difference between the two approaches is over 9.68% of improvement. This improvement is constant for all the combinations of metrics, and shows once more that the use of contextual information improves the detection capabilities of our anomaly-based IDS. Again, the set of metrics #15 is the one that produces the best OSR (i.e. the highest OSR) results, 93.19%. The results show that, although less malicious instances are correctly classified, more normal instances are correctly classified as normal as more metrics are combined. With respect to the three approaches that use an FCM, once again, *FCM01* outperforms the OSR results generated by the other two approaches. The average improvement is ~6% for all the combination of metrics; and a peak improvement of up to 8.06%, for the set #10 (COM-THR).

These results indicate that by utilising only measurable information from the network without considering the available contextual information, the IDS may reach a wrong conclusion, leading to an overall low accuracy. Also, from the presented results, we can infer that the most efficient approach is to adjust the BPA values prior to the data fusion process. This is because the approach *FCM01* adjusts all of the considered metrics individually. Hence, the contribution of the contextual information adapts according to the BPA values given by the IDS for each individual metric, and would impact each of the metrics differently. Also, the contribution of the contextual information through the approach that constructs an additional metric, *FCM02*, decreases as the number of metrics being fused increases. This is because generally, after a number of consecutive D-S fusions, the BPA value given to one of the hypotheses will be largely higher than the rest of the BPAs. Therefore, the fusion of the metric computed from the FCM may not reverse the decision of the IDS. Only in cases in which the BPA values of both hypotheses, *Normal* and *Attack*, are close to each other, could the addition of the new metric have an evident effect on the final IDS decision. In the case of the approach that adjusts the BPA values after the data fusion process, *FCM03*, is prone to dominate the entire decision. On the one hand, in cases in which the BPA values of both hypotheses, *Normal* and *Attack*, are close to each other, the addition of the contextual information could greatly influence the final IDS decision. On the other hand, even if one of the hypotheses receives a largely higher BPA value than the rest, the addition of the contextual information could overturn the final IDS decision if the outcome of the FCM is larger than the resulting BPA values given by the IDS.

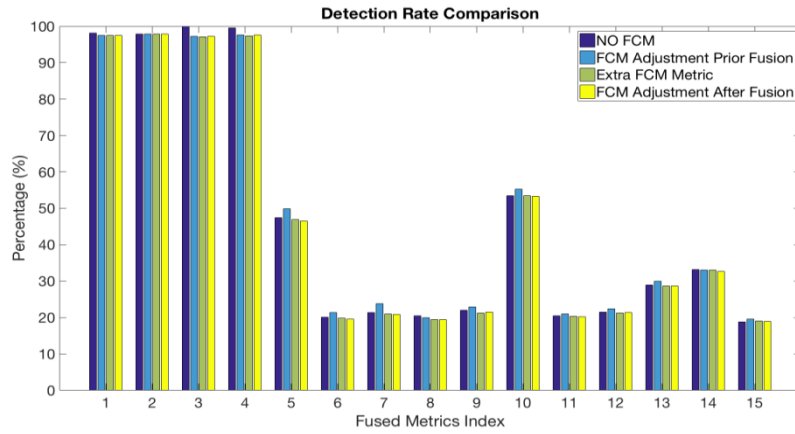


Figure 9 DR comparison: Three approaches that use an FCM (designed based on the THR) in conjunction with IDS, and the IDS without FCM

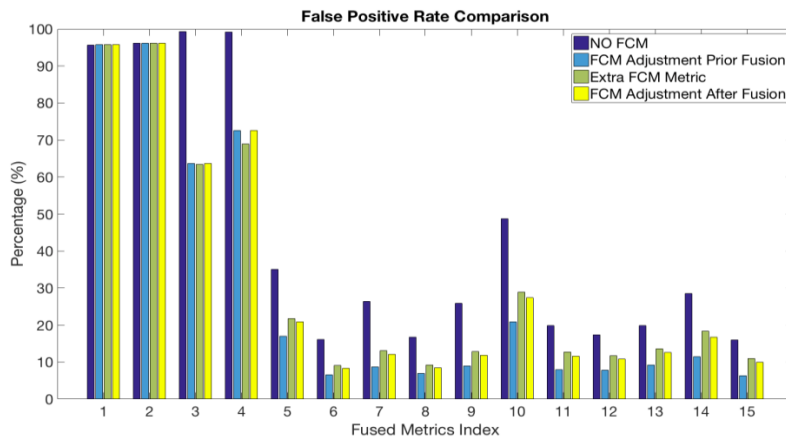


Figure 10 FPr comparison: Three approaches that use an FCM (designed based on the THR) in conjunction with IDS, and the IDS without FCM

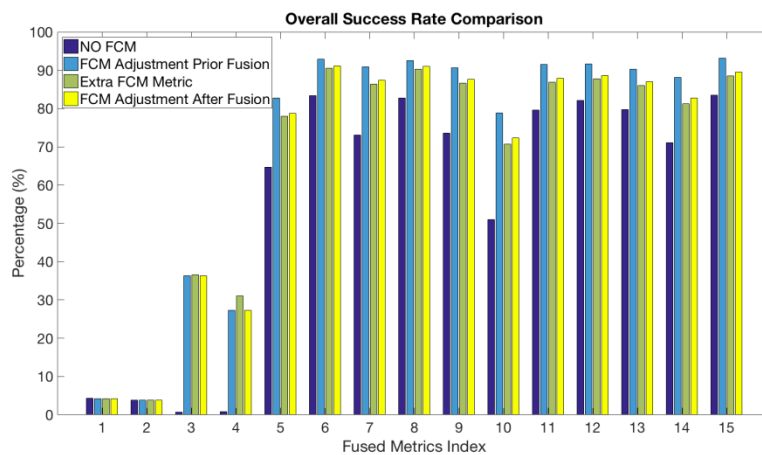


Figure 11 OSR comparison: Three approaches that use an FCM (designed based on the THR) in conjunction with IDS, and the IDS without FCM

We have also compared the detection results generated by our IDS when each of the considered metrics are used to design the modelled FCM, as well as the results of the IDS without an FCM. Since the most efficient approach of the three proposed is *FCM01*, only this approach is considered in the results presented in Figure 9-Figure 14. The DR results of the IDS are compared in Figure 12. The most noticeable characteristic that we can see in the results is the drastic improvement provided by the use of the metrics COM and DPD in the design of the FCMs. For almost all the possible combination of metrics, both approaches provide over 99% of DR. In particular, for the set #15 (COM-THR-SPD- DPD) the DR reaches 99.76%, which improves the DR results provided by the IDS in 80.94% without the use of an FCM. Also, in contrast to the results generated when the THR is used, the DR does not decrease as the number of fused metrics increases. This phenomenon manifests that the contribution of the contextual information tends to dominate the detection.

The FPr results of our IDS are compared in Figure 13. In contrast to the DR results, we can see that the use of the metrics COM and DPD to design the FCMs produces a slightly higher number of false alarms, in comparison with the use of the THR. For the set #15 (COM-THR-SPD-DPD) the FPr reaches 26.42% and 25.42% for the COM and DPD, respectively. This represents an increase in the number of false alarms of approximately 20% (i.e. ~140800 normal data instances misclassified). In comparison with not using an FCM, the increase in the number of false alarms reaches approximately 10% (i.e. ~73000 normal data instances misclassified). As these results suggest, the use of the metric THR to construct the FCM produces the best detection results overall in terms of FPr. Also, similarly to the DR results presented in Figure 12, the FPr does not decrease as the number of fused metrics increases.

Figure 14 presents the OSR results comparison of our IDS. Similar to the DR and FPr results, the OSR results generated when the metrics COM and DPD are used to construct the FCM remain almost unchanged regardless of whether the number of fused metrics increases or not. As in the previous two cases, this phenomenon manifests that the contribution of the FCM tends to dominate the intrusion detection process. Considering the evaluation of the other results, the design of the FCM based on the metrics COM and DPD produces less effective detection results overall than the use of the THR for almost all the combinations of metrics. For the set #15 (COM- THR-SPD-DPD), which is the set index expected to produce the best results overall, the OSR reaches 73.58% and 74.58% for the COM and DPD, respectively. This represents a decrease of approximately 20% of OSR with respect to the use of THR, and a decrease of approximately 10% of OSR with respect to the IDS without an FCM. As these results suggest, once again, the use of the metric THR to construct the FCM produces the best detection results overall.

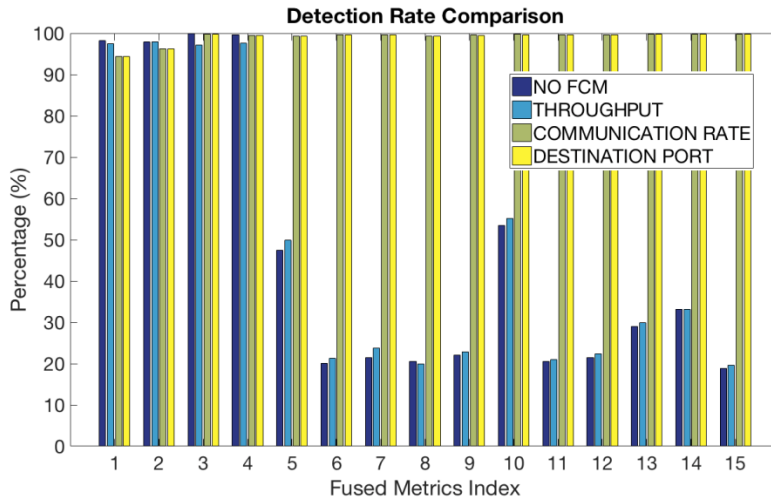


Figure 12 DR comparison: Adjustment of BPAs prior to the fusion process; FCM designed based on the THR, COM or DPD, and the IDS without FCM.

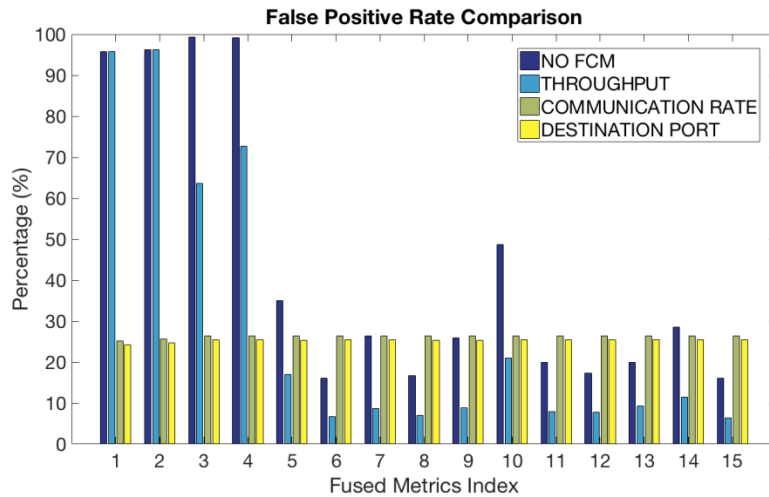


Figure 13 FPr comparison: Adjustment of BPAs prior to the fusion process; FCM designed based on the THR, COM or DPD, and the IDS without FCM

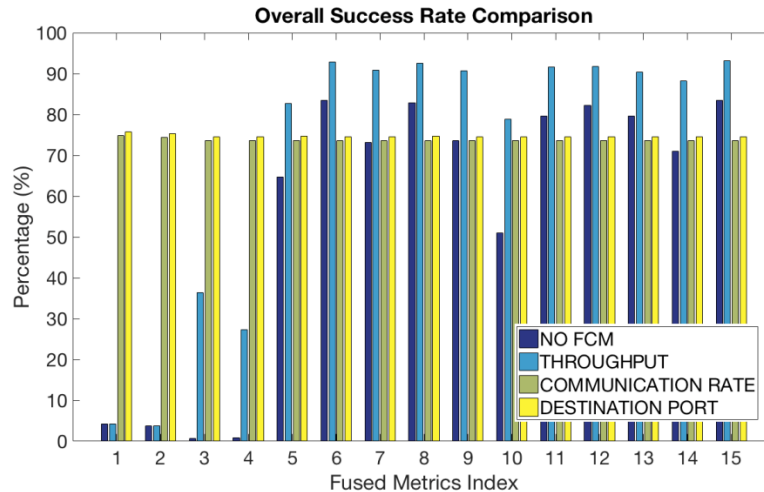


Figure 14 OSR comparison: Adjustment of BPAs prior to the fusion process; FCM designed based on the THR, COM or DPD, and the IDS without FCM

Different conclusions could be extracted from the presented results. First, these results empirically confirm that the use of the FCM provides improvement to the effectiveness of the IDS. Also, the presented results ratify that adjusting the BPAs prior to the data fusion provides the best use of the PoL in the detection process. However, the number of false alarms may not be low enough to be acceptable and make the IDS usable in practice in multiple scenarios. Additionally, it is clear the important role played by the metric selection to design the modelled FCM (i.e. THR, COM and DPD) in the effectiveness of the IDS. Based on the 99% of DR obtained when either the metric COM or DPD is used in the design of the FCM, we might incorrectly assume that these are the best selection of metrics. An IDS that triggers ~140800 false alarms during the 9 days that the experiment lasted would make the network administrator ignore the generated alarms. A tradeoff between the DR and the false alarms should be found, based on the needs of the protected network. The metric selection should be based on whether we prioritise a system that detects most of the attacks regardless of the number of false alarms, or whether we prioritise reducing the number of misclassifications.

Man-in-the-Middle Proxy

We have also implemented a Man-in-the-Middle (MitM) proxy to intercept the network traffic generated by WiFi devices. We designed the WiFi monitoring platform for the interception, decryption and analysis of encrypted network traffic communications. The MitM proxy has been set up using the software tools Mallory (Bitbucket, 2016) and mitmproxy (Cortesi, 2016), which intercept and decrypt the communication in a transparent manner to the network users. The experimental WiFi, depicted in Figure 15, includes one Access Point (AP) connected to the Internet, one laptop acting as the MitM monitoring machine running the MitM proxy and a rogue AP tool, and various WiFi devices acting as clients. The MitM monitoring machine is connected wirelessly to the AP, and provides access to the Internet to all associated devices through a rogue AP service. One of the crucial steps

during our experiments was to provide access to the Internet to the wireless clients, through the MitM monitoring machine, in a transparent manner to them. The monitoring machine can create its own rogue AP by using several publicly available softwares, such as HostAPd (Malinen, 2016) and Airbase-ng (Aircrack, 2016). Airbase-ng and HostAPd are tools for turning a Linux wireless NIC into an AP. Another essential step was to consider the selection of the MitM proxy. Mallory allows the implementation of an extensible TCP/UDP MitM proxy that is designed to run as a communication gateway, and can listen to SSL/TLS encrypted network traffic from/to the WiFi devices. Unfortunately, Mallory was discarded at a later stage because it was unable to unencrypt correctly the SSL/TLS intercepted network traffic in our bespoke setup. It was also necessary to run the DHCP server and assign firewall rules using the iptables tool. There was also the need for port redirection and port masquerading while running mitmproxy. By default, mitmproxy listens on TCP port 8080, and, in order to permit interception of HTTP and HTTPS, ports 80 and 443 had to be forwarded to port 8080.

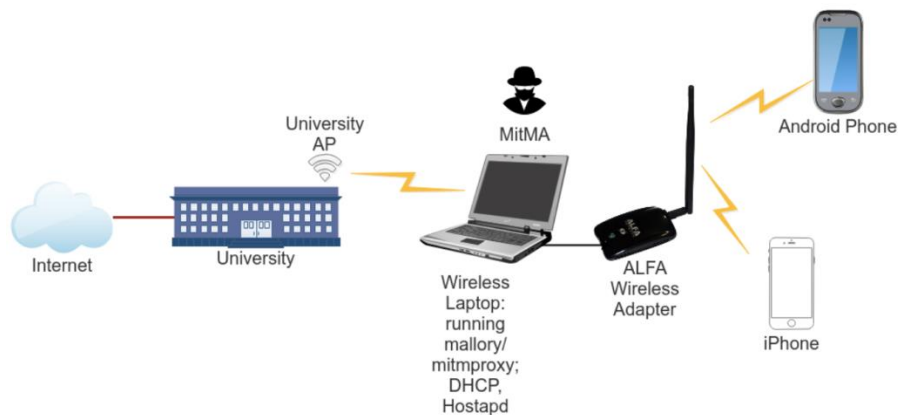


Figure 15 Schematic design of the IEEE 802.11 network used for monitoring and interception of the encrypted network traffic communications generated by the WiFi devices.

The technical advancement that we have conducted on setting up the active monitoring platform has allowed us to be able to implement MitM attacks in a WiFi network. As for future work, we wish to use this platform to enhance our understanding of MitM attacks and thereby assess the possibility of extending and complementing this type of attack with injection capabilities, and to develop a detection mechanism that would accurately identify the presence of these attacks.

One-Class and Two-Class Support Vector Machine Comparison

We have also conducted a comparison study between a two-class Support Vector Machine (SVM) and a one-class SVM as classification techniques for intrusion detection in a WiFi network environment. The comparison study is based on the efficiency of the classification techniques, as well as the processing time required to conduct the training and classification.

These techniques have been tested on a number of network traffic datasets gathered from a live operational IEEE 802.11 network testbed at Loughborough University, comprising two different types of injection attacks.

The two-class SVM is a supervised machine learning technique which uses two different types or classes of samples to construct an accurate classification model during the training process. On the other hand, one-class SVM is a semi-supervised technique that constructs the classification model of normal behaviour during the training process using only one class of samples. Unfortunately, collecting labelled network training datasets is highly complicated, and in many cases, impossible. Training datasets are currently generated by implementing a previous off-line forensic analysis. The aim of this comparison analysis is to evaluate if we are able to generate a robust one-class SVM as classification technique that outperforms a two-class SVM. In that case, we would reduce the need for a thorough off-line dataset labelling process. Only a training dataset containing non-malicious data would be required.

6.2.3 Anomaly Detection in Video (Sub-task 1.1-1 and 1.1-3)

During last year, the novel framework for complex human activity recognition and anomaly detection in heterogeneous streams was enhanced and finalised.

As part of our framework the temporal hierarchy model (THIM) was developed to represent complex activities. THIM is a hierarchical probabilistic state model capable of encoding both short- and long-term temporal dependencies between an activity’s constituent actions. An efficient parameter learning algorithm for THIM based on sampling from the Dirichlet distribution was also proposed. THIM is capable of learning directly unobservable transitions between actions in the training set. This property enables THIM to work efficiently with noisy and incomplete data.

THIM’s inference time complexity is less than that of previous hierarchical models as shown in Figure 16 and equal to that of non-hierarchical models (Kaloskampis & Hicks, 2017).

Model	Inference complexity
THIM (proposed)	$\mathcal{O}(\lambda)$
HMM (Viterbi)	$\mathcal{O}(\lambda M^2)$
HMM (state sequence likelihood)	$\mathcal{O}(\lambda)$
HHMM accurate	$\mathcal{O}(\lambda^3 M)$
HHMM heuristic	$\mathcal{O}(\lambda^2 M)$
SCFG	$\mathcal{O}(\lambda^3 G^3)$

Figure 16 Comparison of inference complexity for different models. λ is the length of the input action sequence and M is the number of the model’s states. In the case of SCFG, G is the number of non-terminal symbols of the normal grammar.

The proposed framework was tested with the state-of-the-art improved dense trajectory features (Wang and Schmid, 2013), using the Breakfast dataset (Kuehne et al., 2014).

A mid-level representation discovers underlying patterns within the extracted features and usually results in representations with enhanced discriminative properties compared to the original extracted features. For this reason, the state-of-the-art Fisher vector mid-level representation was integrated into the framework (Kaloskampis & Hicks, 2017).

The framework is also suitable for work on large datasets (>1500 videos), where the localisation and recognition of primitive actions is hard and there is a large number of missing, unrecognised or incorrectly recognised actions as shown by applying the framework to the breakfast dataset, where state-of-the-art results in activity recognition were demonstrated.

Experimental results – anomaly detection and activity recognition

Bridge design dataset: To demonstrate the efficiency of the proposed framework in anomaly detection, its performance is estimated for the bridge design dataset (Kaloskamps et al., IMA 2014). This dataset features 3 classes of correctly executed activities and 3 classes of erroneously executed activities which are considered as anomalies. The framework’s performance is compared to that of several methods, such as the flat HMM (popular in activity analysis), RF, HHMM and Suffix Trees. The following algorithm combinations are also tested: RF+HMM, HHMM+SVM, RF+HHMM, KAD+HHMM and DeRFHHMM. The results are presented in Figure 17, where it is shown that our framework exhibits higher or equal accuracy in activity recognition and anomaly detection than the other tested methods. The low scores of non-parametric approaches (e.g. RF) in certain activities are attributed to the fact that they do not encode temporal dependencies. On the other hand, models following Markovian properties (e.g. HHMM) face difficulties in representing long term temporal relations accurately. Similarly, Suffix Trees encode neighbouring temporal dependencies but, as they do not encode long-term temporal dependencies explicitly, there are a few cases in which they encounter adversities.

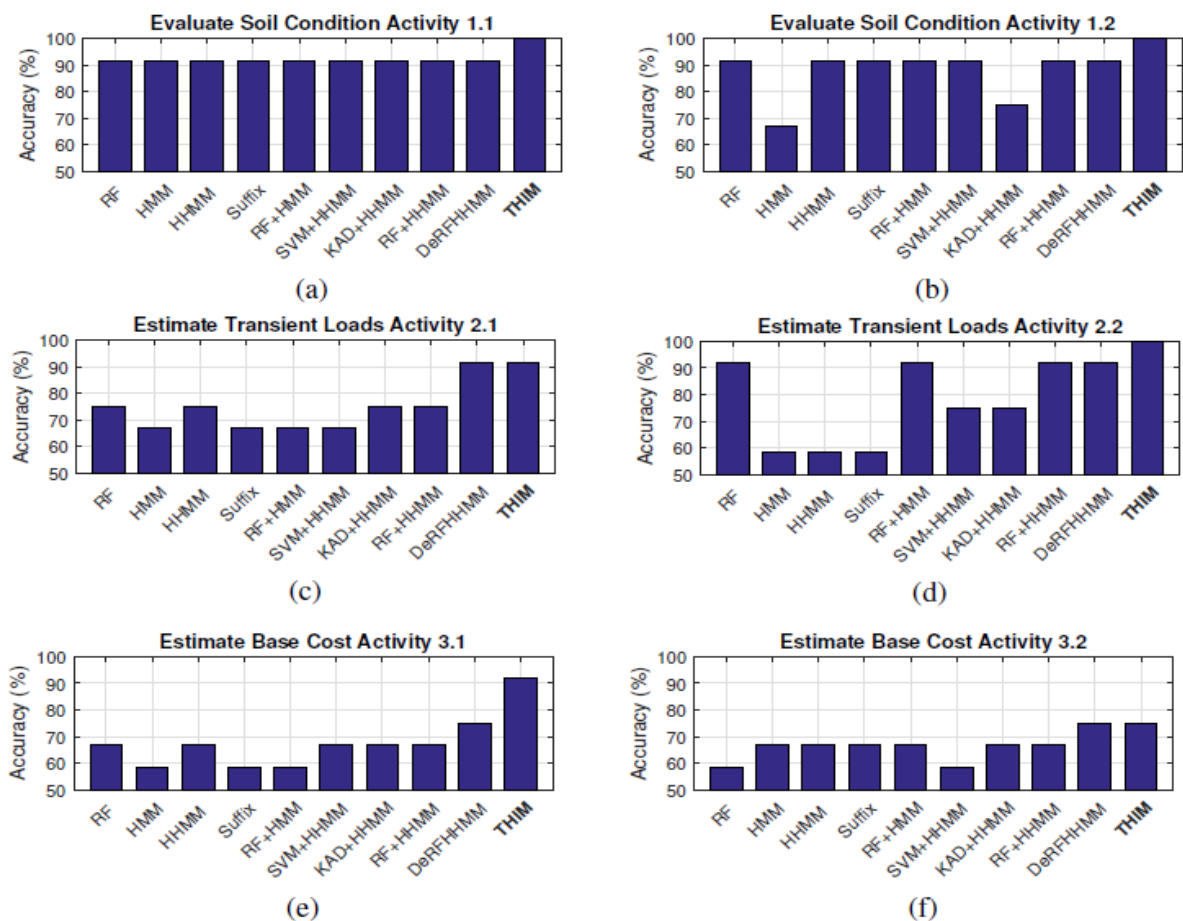


Figure 17 Comparative performance of the proposed framework (THIM) for the six activities of the bridge design dataset. Activities 1.1, 2.1, 3.1 illustrate normal behaviours and activities 1.2, 2.2, 3.2 illustrate anomalous behaviours.

Breakfast dataset

The Breakfast dataset is currently the largest activity recognition dataset, consisting of ~1700 videos of everyday activities. These activities do not fall in the category of composite prolonged activities as the number of each activity's constituent actions is small.

The framework's strength is in the analysis of long sequences. For shorter sequences it may not always offer a performance increase in terms of classification accuracy as simpler models are often adequate for such tasks. Nevertheless, the breakfast dataset presents several important challenges: it consists of a large number of videos recorded in real-world environments from multiple viewing angles, rendering the tasks of action localisation and recognition hard.

For this dataset low-level features with improved dense trajectories (iDTFs) were extracted. Their size was reduced to half (from 426 to 213 elements) with PCA. Then the reduced size features were converted to Fisher vectors, as follows: first, 260000 features were selected at random from the training dataset and clustered to 16 clusters using the GMM algorithm. using these clusters, all reduced-size features were encoded to Fisher vectors; finally, L2 and power normalisations were applied to the resulting vectors. The resulting Fisher vectors are of size $2 \cdot K \cdot D$, where K is the number of clusters of the GMM and D the dimensions of the reduced size iDTF descriptor; in this case, for $K = 16$ and $D = 213$ the size of each Fisher vector is 6816 dimensions. This size was reduced to 64 dimensions with a second PCA. Having obtained the reduced Fisher vectors, the actions in the dataset were recognised with the HTK toolkit. The resulting action sequences are then passed to the framework. The framework achieved an accuracy of 76.2% in activity recognition. The obtained result is compared to that of the state-of-the-art framework from (Kuehne et al., 2016). The reported performance in (Kuehne et al., 2016) is 75.4% accuracy in activity recognition. For fair comparison, this algorithm was implemented. An accuracy of 73.4% was achieved after many trials, which is below the accuracy the proposed framework algorithm achieves. Figure 18 shows the results of several algorithms for this dataset.

Method	Year	Accuracy (%)
THIM (this work)	2017	76.2
Kuehne et al.	2016	75.4 / 73.4
Alexiou et al.	2015	52.0
Kuehne et al.	2014	40.5

Figure 18 Breakfast dataset, accuracy in activity identification. For the method from (Kuehne et al., 2016) we also report in italics the result we obtained when testing this method with the same action sequences we used to acquire our method's result.

7 Future Work

The plans for future work can be summarized as follows:

- The generic domain anomaly detection framework will be demonstrated on anomaly detection in videos in collaboration between Surrey and Cardiff Universities.

- Example scenarios which resemble pattern of life exhibited by agents in the Wright-Patterson dataset will be identified in the maritime AIS dataset, and the AIS anomaly detection system developed to date will be adapted to detect any pattern of life anomalies as a precursor to detecting anomalies in the WASABI data set.
- As for future work in network anomaly, we will investigate the efficiency of our anomaly-based IDS detecting multi-stage attacks. This process will require the implementation of realistic multi-stage attacks that could be replicated in our experimental testbed. The network traffic that we may be able to generate will allow us to identify metrics that would help manifest the presence of this type of attacks. We will also focus our work on the complementing our IDS with machine learning and data mining techniques to improve the overall efficiency of the system.
- Further work will utilise the technical advancement that we have conducted on setting up the active MitM attacks in a WiFi network. We wish to use this platform to enhance our understanding of MitM attacks and thereby assess the possibility of extending and complementing this type of attack with injection capabilities, and to develop a detection mechanism that would accurately identify the presence of these attacks.
- We will continue with the development, in the C programming language, of the advanced detection system throughout the project duration. A single piece of software is being built as new functionalities are proposed and evaluated.
- In the area of anomaly detection in surveillance videos and heterogeneous spatio-temporal data, the work will focus on anomaly detection and activity recognition in multi-camera scenarios and quality assessment of video streams.
- The framework for activity recognition and anomaly detection accuracies will be improved with the integration of deep learning techniques for action recognition.
- Regarding the collaboration between Cardiff and Surrey, work will focus on applying the incongruence measures proposed by Surrey on the video data processed by Cardiff.
- The work on application of the anomaly detection framework to the Wright-Patterson dataset supplied by DSTL will continue and will be switched to the WASABI dataset once the problems identified with this dataset are resolved.

8 Publications

- M. Ponti, J. Kittler, M. Riva, T. de Campos and C. Zor, “A decision cognizant Kullback–Leibler divergence”, *Pattern Recognition*, 61: 470-478, 2017.
- C. Zor and J. Kittler, “Maritime anomaly detection in ferry tracks”, *IEEE International Conference on Acoustics, Speech and Signal Processing*, 2017, accepted.
- J. Kittler, C. Zor and W. Wang, “Error sensitivity analysis of Delta divergence – a novel measure for classifier incongruence detection”, *Pattern Recognition*, 2017, submitted.
- C. Zor, B. Yanikoglu, E. Merdivan, T. Windeatt, J. Kittler and E. Alpaydin, “BeamECOC: a local search for the optimization of the ECOC matrix”, *International Conference on Pattern Recognition*, 2016.
- M. Ponti, T.S. Nazare and J. Kittler, “Optical-flow features empirical mode decomposition for motion anomaly detection”, *IEEE International Conference on Acoustics, Speech and Signal Processing*, 2017, accepted.

S.R. Arashloo and J. Kittler, "An anomaly detection approach to face spoofing detection: A formulation and evaluation protocol", *IEEE Trans on Information Forensics and Security* (submitted).

K. Ghanem, F.J. Aparicio-Navarro, K.G. Kyriakopoulos, S.Lambotharan, and J.A. Chambers, "Comparison of One-Class and Two-Class SVM for Anomaly-based IDSs in Wireless Networks," in *Proc. of the ACM Conference on Security and Privacy in Wireless and Mobile Networks (WiSec)*, 2017, (to be submitted).

F.J. Aparicio-Navarro, K.G. Kyriakopoulos, D.J. Parish, and J.A. Chambers, "Using Pattern-of-Life as Contextual Information for Anomaly-based Intrusion Detection Systems," in *IEEE/ACM Transactions on Networking*; (submitted).

F.J. Aparicio-Navarro, J.A. Chambers, K.G. Kyriakopoulos, Y. Gong, and D.J. Parish, "Using the pattern-of-life in networks to improve the effectiveness of intrusion detection systems," in *Proc. of the IEEE International Conference on Communications (ICC)*, 2017; accepted for publication.

F.J. Aparicio-Navarro, K.G. Kyriakopoulos, D.J. Parish, and J.A. Chambers, "Adding contextual information to intrusion detection systems using fuzzy cognitive maps," in *Proc. of the IEEE International Multi-Disciplinary Conference on Cognitive Methods in Situation Awareness and Decision Support (CogSIMA)*, 2016, pp. 187-193.

D. Santoro, G. Escudero-Andreu, K. G. Kyriakopoulos, F.J. Aparicio-Navarro, D.J. Parish, and M. Vadursi, "A Hybrid Intrusion Detection System for Virtual Jamming Attacks on Wireless Networks," in *Elsevier Measurement*; (submitted).

I. Kaloskamps and Y. Hicks, "Activity Recognition in Concurrent Multimedia Streams with the Temporal Hierarchy Model", *IEEE Transactions on Multimedia*, submitted.

I. Kaloskamps and Y. Hicks, "Human activity recognition by combining discriminative and generative classifiers", 11th IMA International Conference on Mathematics in Signal Processing, Birmingham, December 2016.

I. Kaloskamps, M. Mohammad and Y. Hicks, "Video-based Road Detection Using Evolving GMMs and Region Enhancement", 11th IMA International Conference on Mathematics in Signal Processing, Birmingham, December 2016.

References

Aeroflex website. Available: <http://www.aeroflex.com> (Access date: 27 Feb, 2017).

Aircrack, "Airbase-ng description" Available: <http://www.aircrack-ng.org/doku.php?id=airbase-ng> (Access Date: 29 Nov, 2016).

Aparicio-Navarro, F. J., Kyriakopoulos, K. G., Parish, D. J., & Chambers, J. A. (2016, March). Adding Contextual Information to Intrusion Detection Systems Using Fuzzy Cognitive Maps. In *Cognitive Methods in Situation Awareness and Decision Support (CogSIMA)*, 2016 IEEE International Multi-Disciplinary Conference on (pp. 180-186). IEEE.

Bitbucket, A., "Mallory Wiki home page," Available: <https://bitbucket.org/IntrepidusGroup/mallory/wiki/Home> (Access Date: 29 Nov, 2016).

Cortesi, A., Hils, M., and Kriechbaumer, T., "mitmproxy Project," Available: <https://mitmproxy.org/index.html> (Access Date: 29 Nov, 2016).

Jacobson, V., Leres, C., and McCanne, S., "Tcpdump/libpcap", 1987. Available: <http://www.tcpdump.org> (Access date: 23 Jun, 2016).

Kyriakopoulos, K. G., Aparicio-Navarro, F. J., & Parish, D. J. (2014). Manual and Automatic assigned thresholds in multi-layer data fusion intrusion detection system for 802.11 attacks. *IET Information Security*, 8(1), 42-50.

Lyon G., "Nmap: The network mapper – Free security scanner," Available: <http://nmap.org/> (Access Date: 21 Jun, 2016).

Malinen, J., "Hostapd: IEEE802.11AP, IEEE802.1X/WPA/WPA2/EAP/RADIUS Authenticator," Available: <http://w1.fi/hostapd/> (Access Date: 29 Nov, 2016).

I. Kaloskampis and Y. Hicks, "Estimating adaptive coefficients of evolving GMMs for online video segmentation", 6th IEEE International Symposium on Communications, Control and Signal Processing (ISCCSP), Athens, Greece, 21-23 May 2014, pp. 513-516.

I. Kaloskampis, Y. Hicks and D. Marshall, "Complex activity recognition and anomaly detection in multimedia streams", 10th IMA International Conference on Mathematics in Signal Processing, Birmingham, December 2014.

H. Kuehne, A. Arslan and T. Serre, "The Language of Actions: Recovering the Syntax and Semantics of Goal-Directed Human Activities," IEEE Conference on Computer Vision and Pattern Recognition, Columbus, OH, 2014, pp. 780-787.

M. Mohammad, I. Kaloskampis, Y. Hicks and R. Setchi, "Ontology-based framework for risk assessment in road scenes using videos", 19th Annual Conference on Knowledge-Based and Intelligent Information & Engineering Systems (KES-2015), Singapore, 7-9 September 2015, pp. 1532-1541.

H. Kuehne, J. Gall and T. Serre, "An end-to-end generative framework for video segmentation and recognition," IEEE Winter Conference on Applications of Computer Vision (WACV), Lake Placid, NY, 2016, pp. 1-8.

L_WP2 (HU) Handling uncertainty and incorporating domain knowledge

1. Staffing

Work Package Leaders: Prof. Lambotharan (EESE, LU) and Prof. Wen-Hua Chen (AAE, LU)

Research Associates: Dr. Tasos Deligiannis (EEE, LU), Dr. Miao Yu (AAE, LU)

Affiliated PhD Students: Mr. Abdullahi Daniyan, Ms. Gaia Rossetti and Mr. Michael Hutchinson.

Lead Project Partner: Prof. Malcolm Macleod (QinetiQ)

Dstl contact: Dr. Jordi Barr (Sensors & Countermeasures Department).

2. Aims and the lists of the original L_WP2 in the case for support:

Aims: To develop a generic learning framework for handling uncertainties in the measurements acquired in the networked battlespace environment. Links to WP1 through domain knowledge; and WP3 & WP4 in handling incomplete sensor information & achieving robustness to jamming. (T3,T5)

This WP exploits the world model of the networked battlespace to improve performance and confidence and to reduce uncertainty to an unprecedented level. Due to the abundance of previously collected information of a battlespace and increasing availability of mobile communication and storage, rich information may be available for sensor platforms when performing signal processing as they operate in a **networked** battlespace. Examples for such information are digital maps about terrain and layout of the field, historical data about the site, geometric relations between platforms, and operational conditions such as weather (e.g. the influence of shadowing on optical sensors).

WP2.1 Reducing uncertainty by incorporating domain knowledge using Bayesian inference, adaptive signal processing and sparse sampling [PDRA2]

We will consider how to quantify the information in the world model and express it in a probabilistic statement; for example, how to synthesize the information in the *prior* of the world model (e.g. geometric constraints) with the *prior* of the state variables obtained in the previous time steps to form a combined prior probability function, and how to pool different sources of information measured via different types of sensors or provided by other resources (e.g. digital maps) for statistical inference. New signal processing algorithms offering adaptivity to operational environments will also be developed by exploiting the domain knowledge. Various parameters in these algorithms (e.g. the threshold for detection) or different types of signal processing models/algorithms will be selected based on the domain information (e.g. the change of the operation conditions when the sensor platforms move, or what decisions follow from the signal processing results and their consequence). Historical data will be used to build up the *priors* in Bayesian inference for different objects of interest and different scenarios, which will reduce the reliance on real-time measurements in the battlespace. New sparse sampling measurements will be not only used to update the priors but also to confirm or reject the previous priors selected for the Bayesian learning (hypothesis tests) with the help of domain knowledge (e.g. how likely it could be that an object of interest occurs based on domain knowledge). The Bayesian inference framework will also be extended from a single to multiple sensor platforms operating in a networked environment, by fusing all the information, including the sensory capabilities and constraints (e.g. angle of field view) and geometric relationships between different sensor platforms. One research

challenge here is to create a joint model for multiple sensor platforms with heterogenous attributes to gather intelligence of an object of interest (e.g. a threat), where information synthesis is of particular importance.

WP2.2: Robust signal processing techniques under uncertainty, modelling uncertainty with stochastic dynamic processes, and characterization of uncertainty with a game theoretic framework [PDRA3]

Robust signal processing techniques based on convex optimizations will be developed to tackle uncertainty. Mathematical models and approximation techniques will be developed to model an uncertainty region as a convex hull so that low complexity algorithms can be developed. Robust techniques based on both a probabilistic approach and worst case optimizations will be developed. The application scenario will include distributed/networked beamformer design under manifold uncertainty, imperfect sensor measurements and radar clutters. Instead of treating uncertainty as caused by a static collection of events and associated relationship, the uncertainty will be investigated within the framework of dynamically evolving phenomena. In this framework, uncertainty will be considered as caused by dynamic entities having states and transitions from one state to another resulting from actions in the battlespace. Both hidden Markov model and Bayesian networks will be used to characterise uncertainty. To enhance characterization of uncertainty and to understand the underlying mechanisms further, this WP will consider uncertainty as caused by dynamically varying actions created by various players in the battlespace, e.g. coalitional forces and enemies. Hence a game theoretical framework will be developed. The work will start with a non-cooperative game theoretical framework and will be extended to Bayesian games to account for incomplete information. The framework will then be extended to stochastic games (Markov games) to model dynamically changing actions and evolution of uncertainty. The possible battlespace scenarios that will be considered within this framework will include air formation to ground attack-defence system, defence against jamming in radars (linked to WP 4.1) and counteracting uncertainty created by deception by enemies, for example fake RF signal injection.

3. Progress made in the fourth year in addressing the original objectives

3.1 Overview

The original aim of this work package is “to develop a generic learning framework for handling uncertainties in the measurements acquired in the networked battlespace environment”. There has not been any significant change on this stated aim, and the focus remains on the development of signal processing algorithms for handling uncertainties by incorporating domain knowledge, convex optimizations and game-theoretical methods. Two postdoctoral research associates and three PhD students work on this work package.

3.2 Engagement with partners

The leading industrial contact for this work package is Prof. Malcolm Macleod from QinetiQ. We have also discussed with Paul Westoby and his colleague in Dstl on how to exploit the prior information for more efficient hazardous source term estimation and Alasdair Hunter on the application of the developed particle filtering algorithms for the software demonstration.

The current technical contact for WP2.1 and WP2.2 is Dr. Jordi Barr from the Sensors & Countermeasures Department in Dstl. Dr. Barr is an experienced signal processing expert and has provided a number of very insightful comments and suggestions to this work package.

3.3 Overview of progress

A number of achievements have been made for WP2 in the fourth year.

1. Ballistic missile tracking (highlighted technical output, related to Tasks 2.1-1 World modelling, 2.1-3 New adaptive algorithms and 2.1-4 Bayesian inference)

We have proposed a new method for ballistic missile tracking. Firstly, state dependent hybrid modelling is used to reflect the realistic missile movement where multiple models are applied for three different flight phases (boost, coast and re-entry). In particular, the transition probabilities between models are defined in a state dependent way according to the domain knowledge of flight phases' dependence on the altitude. We consider a more realistic scenario by considering both miss detection and false alarms in the measurements, which are modelled by the random finite set (RFS). Based on the state dependent multiple modelling and RFS measurement model, a generalized state dependent interactive multiple model particle filtering (G-SD-IMMPF) has been developed for the missile state estimation.

2. Chemical, Biological and Radiological (CBR) dispersion source estimation (highlighted technical output, related to Tasks 2.1-1 World modelling, 2.1-3 New adaptive algorithms and 2.1-4 Bayesian inference)

A new strategy for performing an efficient autonomous search has been proposed to find a source of unknown strength, releasing particles into the atmosphere. The proposed search strategy, which we have named 'Entrotaxis', is based on maximum entropy sampling principles. Bayesian inference is used to update approximate posterior probability distributions of the source location and strength. Posterior sampling is used to approximate a reward function for searching. We compared the performance and search behaviour of Entrotaxis with the state of the art in the literature, for searching in sparse and turbulent conditions. Whilst outperforming previous methods in most scenarios by achieving a faster mean search time, the strategy is also more computationally efficient during the decision-making process. The current work focused on the search for a weak emitting source undergoing turbulent atmospheric transport, it is envisaged that the strategy would be more effective in search scenarios where a model incorporating more comprehensive information can be provided.

3. Particle filtering tracking in videos (related to 2.1-3 New adaptive algorithms and 2.1-4 Bayesian inference)

The developed particle filtering algorithm is tested on the tracking application for real data. Video sequences have been recorded by a moving camera mounted on an unmanned aerial vehicle (UAV). We target to design tracking approaches for tracking vehicles in the recording. To achieve it, a dynamic model is used to represent the vehicle movement in the image while colour and gradient information is extracted to construct the measurement model. Based on the dynamic/measurement models, a particle filtering approach is developed for the vehicles tracking. This work will be a potential *software demonstration* for the application of the developed particle filtering algorithm in the real dataset.

4. Game Theory for Distributed Optimizations and Tracking (contributes to Tasks, 2.2-1 Convex optimisation and robust SP, 2.1-3 New adaptive algorithms, 2.2-2 Radar and sensor applications and 2.2-4 Game Theory, highlighted technical output relates to 2.2-5 Bayesian Games)

We have proposed and analysed game theoretic optimization techniques for a wide range of problems including waveform design, power allocation, beamforming and electronic countermeasures within the context of multi-static radars [10-12, 15, 18]. This work is significant due to completion of rigorous mathematical analyses for establishing existence and uniqueness of the Nash equilibrium for various classes of game theoretic methods [10-12]. Particularly, for power allocation in a multi-static radar setup, we demonstrated through Nash equilibrium analysis and Karush–Kuhn–Tucker (KKT) conditions that certain radars may opt to be inactive, but use illuminations of other radars as the signals of opportunity [12]. Distributed beamformer design techniques using non cooperative games and interference mitigation methods for the co-existence of a surveillance radar with tracking radars using a Stackelberg game were also developed [11]. Power allocation techniques in the presence of uncertainty have been developed using Bayesian game theoretic framework in [18]. We have also developed a correlated equilibria based data association techniques for multiple target tracking which outperforms the probabilistic data association (PDA) technique and joint-PDA [14, 17].

5. Robust waveform design for cognitive radars (highlighted technical output relates to Tasks, 2.2-1 Convex optimisation and robust, 2.1-3 New adaptive algorithms, 2.2-2 Radar and sensor applications)

Convex optimization techniques for designing optimal waveforms within the context of multistatic cognitive radars have been proposed [16, 19]. The method aims to maximise signal to interference plus noise ratio (SINR) of principal radar while satisfying constraints on the transmission power, orthogonality between waveforms and minimum required SINR for secondary radars. The method assumed certain second order statistics of the clutter return. As the estimate of the clutter statistics may have errors, the convex optimization method was extended to consider uncertainty on the clutter parameters. Worst case robust optimization and stochastic robust optimisation techniques have proposed that assumed error in the covariance matrix of the clutter return. Finally, a stochastic optimization that considers uncertainty directly on the clutter radar cross section and clutter Doppler was proposed using Taylor series approximation and convex optimizations. The robust methods are able to achieve the SINR target with a specific outage probability [20].

6. New Algorithms for Multi-target Tracking and Extended Target Tracking (highlighted technical output relates to Tasks, 2.1-3 New adaptive algorithms, 2.1-4 Bayesian inference, 2.2-2 Radar and sensor applications)

A new Kalman-gain aided particle probability hypothesis density (PHD) filter for multi-target tracking has been proposed [13]. The method aims to apply particle state correction/improvement using the Kalman-gain to guide validated particles in the sequential Monte Carlo PHD (SMC-PHD) filter to the region of higher likelihood to better approximate the posterior at each time step. The proposed method outperforms the Gaussian mixture (GM) PHD filter, the GM-unscented-SMC-PHD filter and the auxiliary particle (AP) PHD filter in terms of high track continuity and optimal sub-pattern assignment (OSPA) distance. For

extended target tracking, a new MCMC variational Bayesian (VB) approach has been proposed to estimate the measurement rates and number of measurements per rate for multiple extended targets having Poisson distributed measurements. The proposed approach offers efficient clustering of multiple extended target measurements in the case of large measurement sets. It provides improved performance and accuracy in jointly estimating both measurement rates and number of measurements for multiple extended targets [21].

4. Technical details

4.1 Work package 2.1

4.1.1. Ballistic missile tracking

We have proposed a new method for tracking the entire trajectory of a ballistic missile from launch to impact on the ground. A state dependent hybrid modelling system is proposed where multiple state models are used to represent the different ballistic missile dynamics in different flight phases: boost, coast and reentry. In particular, the transition probabilities between state models (i.e. flight phases) are represented in a *state dependent* way by exploiting domain knowledge (e.g. the correlation between the flight phase and the missile altitude). Both the miss detection and false alarms are considered for a realistic scenario. Random finite set (RFS) is applied to model miss detections/false alarm and a generalized measurement likelihood function is constructed through the RFS theory. Based on the hybrid modelling system and generalized measurement function, a generalized state-dependent interactive multiple model based particle filtering (G-SD-IMMPF) approach is developed to accurately estimate the ballistic missile information such as the flight phase, position and velocity.

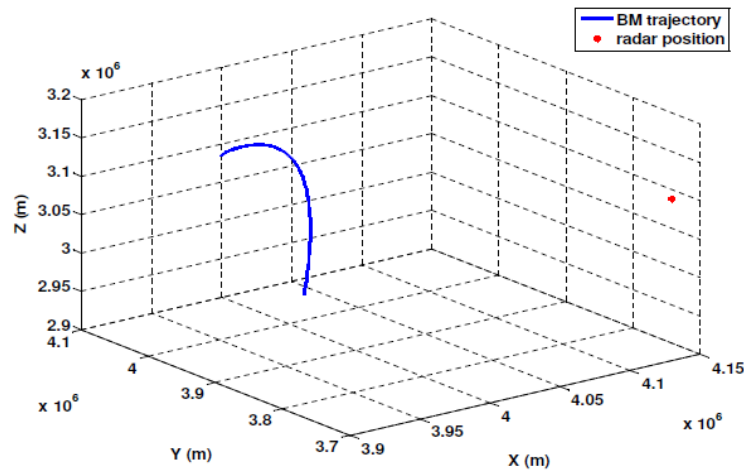


Fig. 1 Simulated BM trajectory and radar position in the ECEF coordinate system

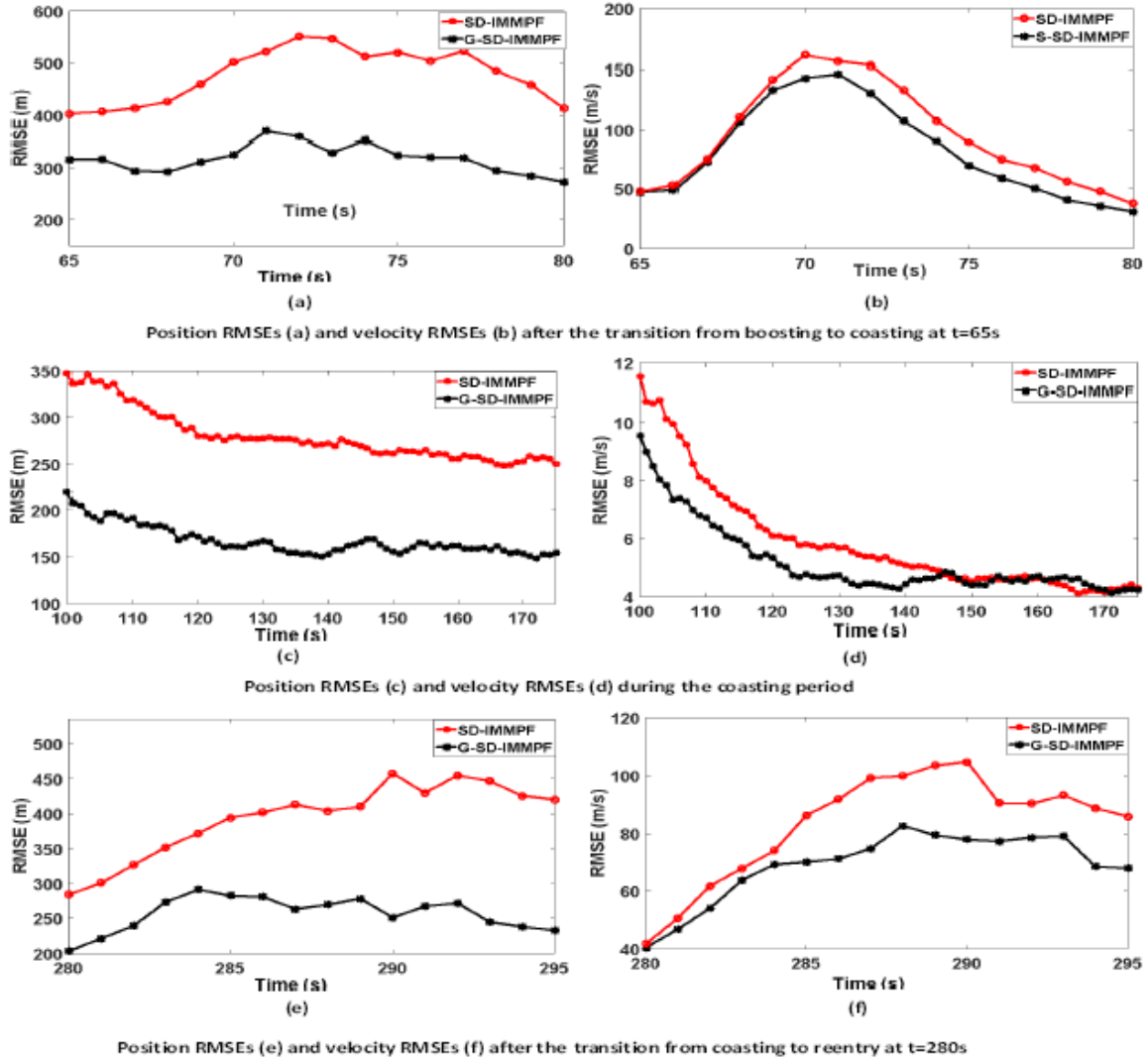


Fig. 2 Position/velocity RMSEs comparisons for different methods

Comprehensive numerical comparisons are made between the proposed method and traditional approaches for a simulated scenario as in Fig. 1. 100 Monte Carlo simulations are made and the comparison results on the averaged root mean square errors (RMSEs) for both the position and velocity are shown in Fig. 2, from which we can see that the proposed method achieves much better performance than the traditional SD-IMMPF one [1], during different BM fight phases. The reason behind it is that for the proposed method, the miss detection, object measurement and false alarms are comprehensively considered and modelled in a theoretical way by the RFS theory. However, in the traditional SD-IMMPF method, only one measurement is chosen for updating in an empirical way. When the object is not detected, some false alarm may be chosen for updating, which may lead to poor estimation results.

The mode estimation comparisons of different methods (including the proposed method using a state dependent transition probabilities (SDPT) model and traditional ones adopting constant transition probabilities (CTP) model ([2] and [3])) are shown in Fig. 3. It is shown that the mode estimation results better coincide with the ground truth ones by the SDPT Model approach thanks to the domain knowledge aided transition probabilities.

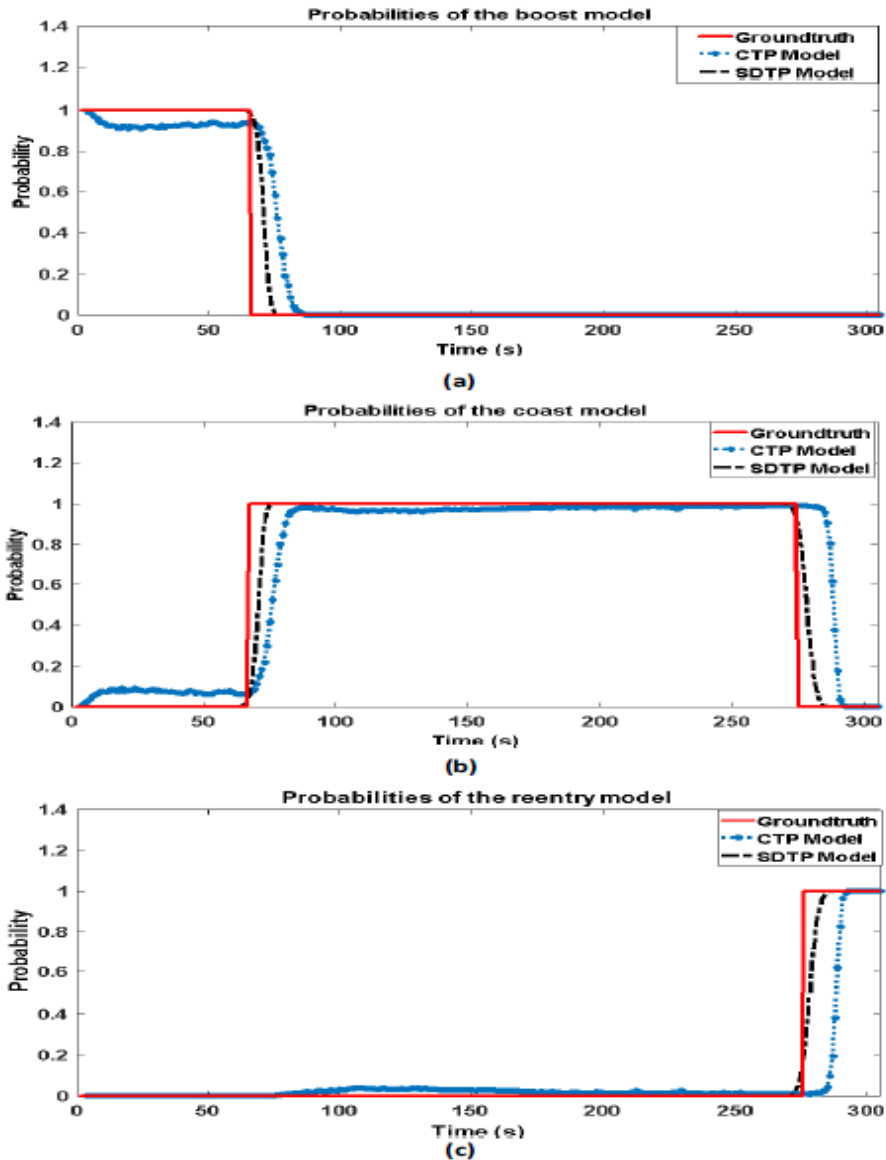


Fig. 3 Flight mode probabilities estimation by different modelling approaches

4.1.2. Chemical, Biological and Radiological (CBR) dispersion source estimation

A new strategy for performing an efficient autonomous search has been proposed to find a source of sporadic cues of noisy information. We focused on the search for a source of unknown strength, releasing particles into the atmosphere where turbulence can cause irregular gradients and intermittent patches of sensory cues. We proposed a new information theoretic search strategy (otherwise known as cognitive search), which we have named 'Entrotaxis'. The approach is based on maximum entropy sampling principles. Bayesian inference, implemented via the sequential Monte Carlo method using a particle filter, is used to update approximate posterior probability distributions of the source location and strength. The posterior is updated recursively, in response to the stochastic process of particle encounters with a sensor. A Markov Chain Monte Carlo move step is used to avoid particle degeneracy. The reward function, which is defined as the entropy of the predictive measurement distribution, is approximated by the samples representing the Posterior distribution and used for searching. We compare the performance and search behaviour of Entrotaxis with the popular Infotaxis algorithm [4], for searching in sparse and turbulent

conditions where typical gradient based approaches become inefficient or fail. The algorithms are assessed via Monte Carlo simulations with simulated data and an experimental dataset.

A typical run of the Entrotaxis algorithm using the experimental dataset is shown in the Figures below. The source, located at $[x_s \ y_s] = [2:935 \ 2:935]$, is represented by a large black dot (a). Green dots represent the random samples of the particle filter, the lines in (b) and (c) indicate the estimated trajectories for searching, while red dots denote zero sensor measurements and black crosses non-zero measurements. The greyscale shading depicts the instantaneous concentration field at the current time step k . The histogram in Fig. d displays the posterior distribution of the source release rate at the end of the search. Although true release rate was unknown, the result was consistent with others in the literature.

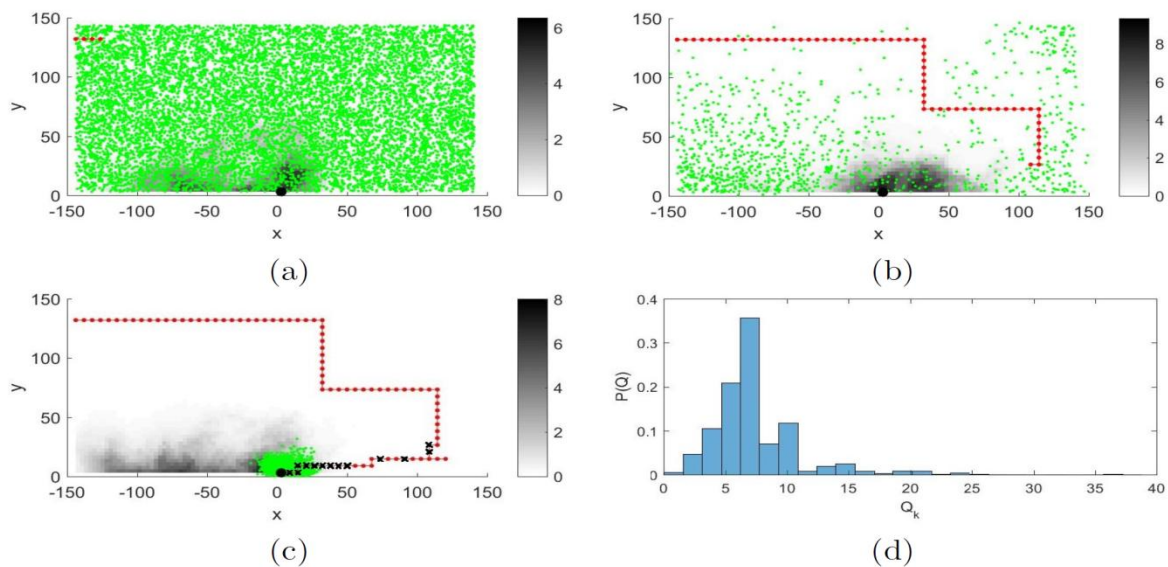


Fig. 4 Searching trajectory and posterior estimation by the Entrotaxis algorithm

Quantitative results of our approach (Entrotaxis) compared to the current state of the art (Infotaxis) using the experimental dataset are given in the Table below. We compare the effect of different priors (the first line in the Table) on the source release rate on the search performance. Throughout the simulations, the Entrotaxis algorithm achieved a higher success rate. With regards to search time, the Infotaxis algorithm was slightly more robust, however, with less prior information, the Entrotaxis approach showed significant improvements in the mean search time (as in the last column). Future works will relax assumptions made about the quality of meteorological information considering an urban domain, and extend the approach to a multi vehicle collaborative search.

Table Comparison of the search performance under different priors

Monte Carlo results using the experimental dataset after 200 runs with various prior distributions for the release rate. (SR = success rate; MST = mean search time)

Method	$\mathcal{L}(1, 1.2)$	$\mathcal{L}(1.3, 1)$	$\mathcal{L}(1.5, 1)$	$\mathcal{U}(0, 20)$	$\mathcal{N}(7, 2)$
Entrotaxis					
SR [%]	100	100	100	100	100
MST	109	101	85	75	71
Infotaxis					
SR [%]	99	98.5	100	99	98.5
MST	107	106	106	103	91

4.1.3. Particle filter tracking in videos

We developed the particle filtering tracking approach for vehicles tracking in the video sequence for a potential *software demonstration*. In this work, real video recordings are taken from a moving camera mounted on a UAV platform. We apply the Brownian motion model to represent the vehicle movement in the 2-D image. Both the gradient and colour histogram information are extracted, which is combined to construct the measurement model to evaluate the likelihood that a patch in the image is the object of interest. Based on the dynamic model and colour measurements, particle filtering is developed for tracking. Selective tracking results are shown in the following figure.



Fig. 5 Vehicle tracking results in selective frames

4.2. Work package 2.2

4.2.1. Bayesian Game Theoretic Resource Allocation for Multistatic Radars

We have proposed a Bayesian game-theoretic power allocation technique based on SINR maximization for multistatic tracking radars. The primary goal of each radar is to maximize its signal to interference plus noise ratio (SINR), within the constraint of its maximum transmission power and in the presence of uncertainty of other radar's channel parameters. There is no communication presumed between the radars, hence we utilize a noncooperative game-theoretic approach. The channel gain between a radar and the target is assumed to be private information to the corresponding radar. However the other radars do not have this private information but they know its probability distribution, which characterizes the type of the player (i.e. radar). The radars aim to allocate power to maximise SINR knowing their own private information and with only the probability of type of the other radars. We have examined and proven the existence and the uniqueness of the Bayesian Nash equilibrium (BNE) for the aforementioned game by exploiting geometric programming techniques.

To demonstrate the convergence of the algorithm to the unique solution, we considered a bistatic tracking radar network consisting of two radars. We assumed that a particular radar knows only the probability of the type of the other radar, i.e. the other radar could induce two possible cross-channel interference states namely $g_- = 1$ and $g_+ = 4$, whose probability distribution is known (in our case we assumed Bernoulli distribution with equal probabilities). Fig.6 shows the allocated power for each radar for two different initializations (i.e. subplot 1

and 2 respectively). For both the initialisations, the power allocations converge to a unique solution.

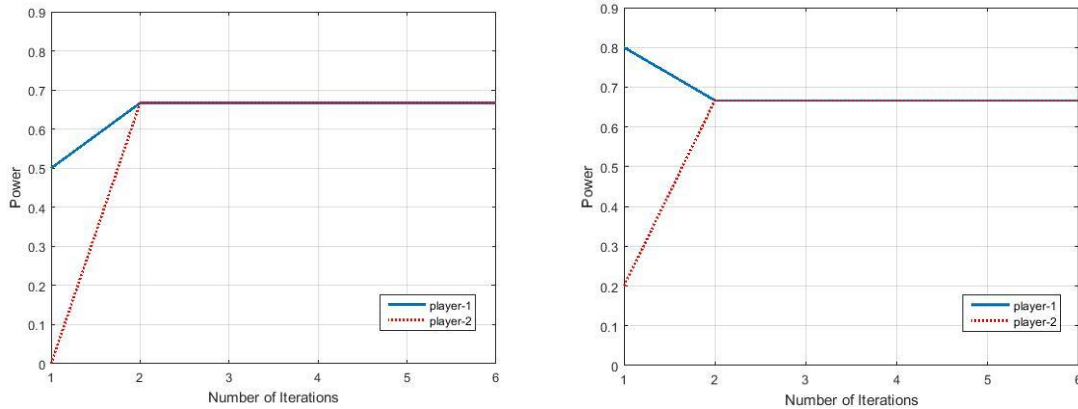
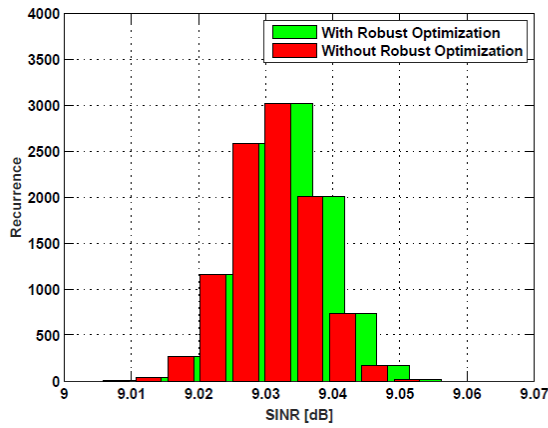


Fig. 6: Convergence of the power allocation for two different initialisations.

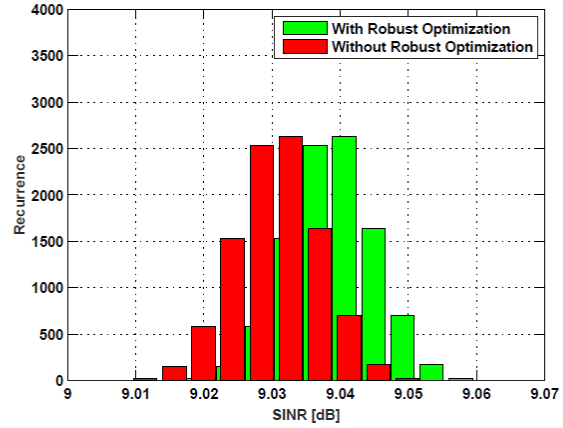
4.2.2. Robust Waveform Design for Multistatic Cognitive Radars

We have developed robust waveform techniques for multistatic cognitive radars in a signal-dependent clutter environment. In cognitive radar design, certain second order statistics such as the covariance matrix of the clutter, are assumed to be known. However, exact knowledge of the clutter parameters is difficult to obtain in practical scenarios. Hence we considered the case of waveform design in the presence of uncertainty on the knowledge of the clutter environment and developed both the worst-case and the probabilistic robust waveform design techniques. As existing methods in the literature appeared to be over conservative and generic, we proposed a new approach where we assumed uncertainty directly on the radar cross-section and Doppler parameters of the clutters. Using Taylor series approximation, we developed a clutter-specific stochastic optimization that, while maximising the SINR of particular radar, is able to ensure the other radars in the network achieve a desired SINR with certain probability.

Performance of all three optimization techniques was evaluated for the case of two radars. For the worst case robust optimization, we aimed to maximise the SINR of the first radar while ensuring a desired SINR is achieved for the second radar for all possible errors in the clutter covariance matrix. As expected, non-robust optimization method was unable to achieve the required SINR all the time. On the other hand, the worst-case robust optimization achieved the goal SINR; however, with a value considerably higher than the desired SINR, hence this method is over-conservative. For the stochastic optimizations, the aim is to maximise the SINR of the first radar while ensuring the goal SINR (9.03dB in our simulation) of the second radar is achieved with a specific probability. We evaluated the performance in the presence of uncertainty on the clutter covariance matrix for two different success probabilities of 70% and 90%. As seen in Figure 7, the non-robust scheme achieved the goal SINR only 50% of the time while stochastic robust optimization is able to achieve the goal SINR with the required probabilities. Finally, we considered uncertainty directly on the clutter parameter such as radar cross section and Doppler and compared the performance with the ordinary stochastic optimization scheme that assumes uncertainty on the clutter covariance matrix. The proposed method outperforms the ordinary stochastic optimization for the same amount of uncertainty as shown in Figure 8.

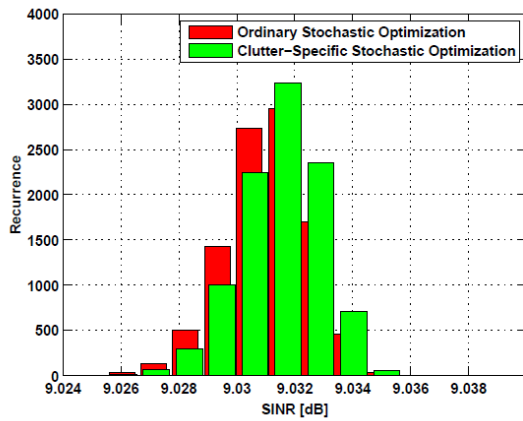


(a) Success Rate - 70%

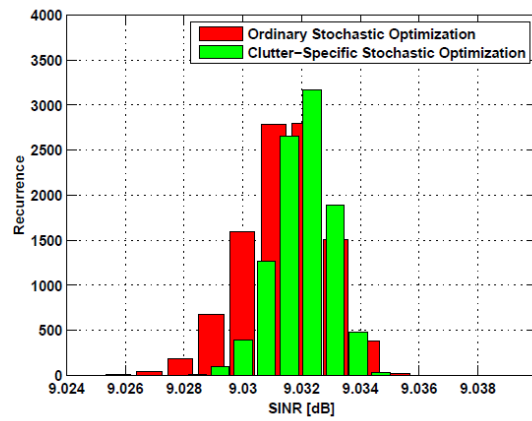


(b) Success Rate - 90%

Fig. 7: Comparison between the stochastic (robust) optimization and the non-robust optimization. The required SINR of 9.03 dB was achieved with the desired probabilities for the stochastic optimization but with only 50% success rate for the non-robust optimization.



(a) Success Rate - 70%



(b) Success Rate - 90%

Fig. 8: Comparison between ordinary stochastic optimization and clutter-specific stochastic optimization. The required success rate was achieved with approximately 1% error due to Taylor series approximations for the case of clutter-specific optimization. However, for the same amount of uncertainty, the ordinary stochastic optimization resulted in poor performance in terms of achieving the success rate.

4.2.1. Bayesian Multiple Extended Target Tracking

In target tracking, it is a common assumption that one target produces one measurement per time step. Tracking more than one of such target is known as point multi-target tracking. Due to high resolution sensors etc., a target can occupy more than one resolution cells and this could be modelled by a cluster of points giving rise to an extended target (ET) scenario. We have developed multiple-extended-target tracking (METT) algorithms for tracking more than

one of such targets. We modelled measurements as an inhomogeneous Poisson distribution and applied a joint Markov Chain Monte Carlo (MCMC) and Poisson mixture variational Bayesian (PMVB) technique to estimate extended target measurement rates and the number of measurements. In order to extract information about the target such as shape, size, orientation etc, we proposed a B-spline approach that can characterise any arbitrary geometrical, numerical or statistical function.

The proposed algorithm is based on MCMC-PMVB, B-spline and a newly introduced generalized labelled multi-Bernoulli (GLMB) filter. The GLMB filter has the advantage of creating and maintaining target labels during tracking hence avoiding the need for any post processing to achieve data association. Fig. 9 confirms that the proposed technique gives a better estimate when compared to the Bayesian rate estimator (BRE) even for a large window length for the forgetting factor. As seen in Figure 9, BRE gives poor estimate for both the targets in the first few time steps. Figure 10 demonstrates that the proposed MCMC-PMVB technique is able to estimate the number of measurements for two different measurement rates. The estimation results improve as the time progresses. This is because more samples are available for the VB clustering. Figure 11 shows that incorporating the MCMC-PMVB technique and the B-spline approach in the existing ET-GLMB filter offers an improved performance in terms of a lower optimal sub pattern assignment (OSPA) distance.

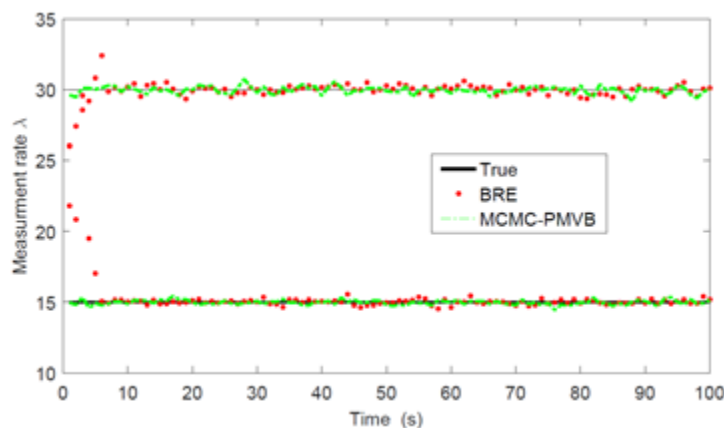


Fig. 9 Estimation results for two different true fixed measures $\lambda = 15$ and 30 using both BRE (window length=100) and the MCMC-PMVB methods.

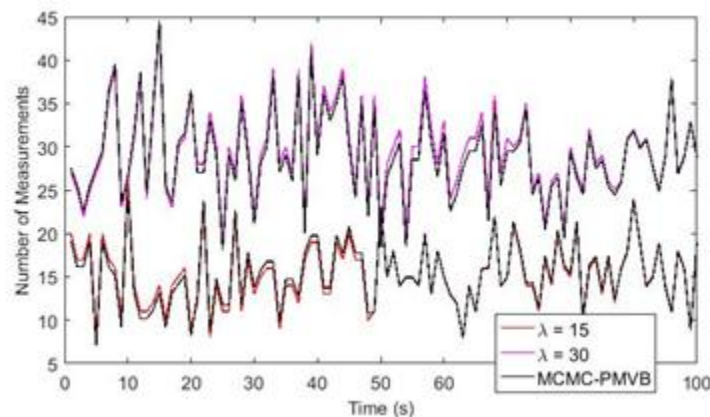


Fig. 10 True number of measurements for two distinct rate parameters and the estimate of this by MCMC-PMVB.

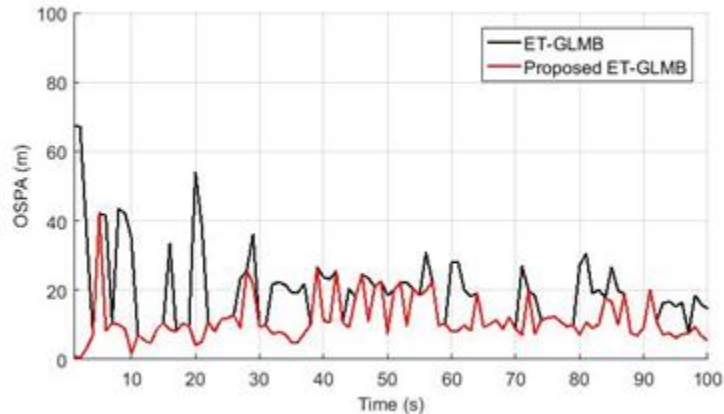


Fig. 11 OSPA distance plot of the proposed ET-GLMB and the ET-GLMB

5. Plan for the next year

For WP2.1, the focus is on:

1. Extending our current ballistic missile tracking work to the areas of joint tracking and missile types identification, as well as missile trajectory prediction;
2. Chemical, Biological and Radiological (CBR) dispersion source estimation with the aid of local domain knowledge.
3. Software demonstration of the proposed particle filtering approaches

For WP2.2, the focus is on:

1. Extension of Bayesian game theoretic framework for the inclusion of uncertainty on clutter parameters.
2. Convex optimisation based resource allocation for communication radars in the presence of eavesdroppers.
3. Developing a Bayesian framework for multiple target tracking, possibly incorporating cognitive radar environment.

6. Outputs during the last year:

1. M. Yu, C. Liu, WH. Chen and B. Li, “An enhanced particle filtering method for GMTI radar tracking”, *IEEE Transactions on Aerospace and Electronic Systems*, Vol. 52, No. 3, pp. 1408-1420, 2016.
2. M. Yu, H. Oh, WH. Chen and J. A. Chambers. “An improved multiple model particle filtering approach for manoeuvring target tracking using airborne GMTI with geographic information”, *Aerospace Science and Technology*, vol. 52, pp.62—69,2016.
3. M. Yu, Y. Xue, R. Ding, H. Oh, WH. Chen and J. A. Chambers. “New environmental dependent modelling with Gaussian particle filtering based implementation for ground vehicle tracking”, *Sensor Signal Processing for Defense*, Edinburgh, UK, 2016.
4. M. Yu, WH. Chen and J. A. Chambers, “State Dependent Multiple Model-Based Particle Filtering for Ballistic Missile Tracking in a Low-Observable Environment”, submitted to *Aerospace Science and Technology*, major revision.

5. M. Yu, H. Oh, WH. Chen and J. A. Chambers, "Multiple Model Ballistic Missile Tracking with State-Dependent Transitions and Gaussian Particle Filtering", submitted to *IEEE Transactions on Aerospace and Electronic Systems*, major revision.
6. R. Ding, M. Yu, H. Oh and WH Chen, "New Multiple Target Tracking Strategy Using Contextual Information and Optimization", *IEEE Transactions on Systems, Man and Cybernetics: Systems*. DOI:10.1109/TSMC.2016.2615188.
7. Hutchinson, M., Oh, H. and Chen, W.H., 2017. A review of source term estimation methods for atmospheric dispersion events using static or mobile sensors. *Information Fusion*, Vol.36, pp.130-148.
8. Hutchinson, M., Oh, H., and Chen, W., 2017. Adaptive Bayesian Sensor Motion Planning for Hazardous Source Term Reconstruction. The 20th World Congress of the International Federation of Automatic Control, 9-14 July 2017, (under review).
9. Hutchinson, M., Oh, H., and Chen, W., 2017. Entrotaxis as a strategy for autonomous search and source reconstruction in turbulent conditions, (to be submitted to *Information Fusion*).
10. A. Panoui, S. Lambbotharan and J.A. Chambers, "Game Theoretic Distributed Waveform Design for Multistatic Radar Networks," *IEEE Transactions on Aerospace and Electronic Systems*, vol. 52(4), pp. 1855 – 1865, Nov. 2016.
11. A. Deligiannis, S. Lambbotharan, and J.A. Chambers, "Game Theoretic Analysis for MIMO Radars with Multiple Targets," *IEEE Transactions on Aerospace and Electronic Systems*, , vol. 52(6), pp. 2760 - 2774, February 2017.
12. A. Deligiannis, A. Panoui, S. Lambbotharan, and J.A. Chambers, "Game Theoretic Power Allocation and the Nash Equilibrium Analysis for a Multistatic MIMO Radar Network," *IEEE Transactions on Signal Processing*, submitted, February 2017.
13. A. Daniyan, Y. Gong, P. Feng, J.A. Chambers, and S. Lambbotharan, "Kalman-Gain Aided Particle PHD Filter for Multitarget Tracking," *IEEE Transactions on Aerospace and Electronic Systems*, under second review, Nov 2016.
14. A. Daniyan and S. Lambbotharan "Game Theoretic Data Association for Multi-target Tracking with Varying Number of Targets," *IEEE Radar Conference*, Philadelphia, May 2016.
15. A. Deligiannis, G. Rossetti, A. Panoui and S. Lambbotharan, and J.A. Chambers, "Power Allocation Game Between a Radar Network and Multiple Jammers," *IEEE Radar Conference*, Philadelphia, May 2016.
16. G. Rossetti, A. Deligiannis and S. Lambbotharan, "Waveform Design and Receiver Filter Optimization for Multistatic Cognitive Radar," *IEEE Radar Conference*, Philadelphia, May 2016.
17. A. Daniyan, S. Lambbotharan, "Data Association Using Game Theory for Multi-Target Tracking in Passive Bistatic Radar", *IEEE Radar Conference*, Seattle, May 2017.
18. A. Deligiannis and S. Lambbotharan, "A Bayesian Game Theoretic Framework for Resource Allocation in Multistatic Radar Networks", *IEEE Radar Conference*, Seattle, May 2017.
19. G. Rossetti and S. Lambbotharan, "Coordinated Waveform Design and Receiver Filter Optimization for Cognitive Radar Networks," *IEEE Sensor Array and Multichannel Signal Processing Workshop (SAM)*, Rio de Janeiro, July 2016.
20. G. Rossetti and S. Lambbotharan, "Robust Waveform Design for Multistatic Cognitive Radars," *IEEE Transactions on Aerospace and Electronic Systems*, April 2017.
21. A. Daniyan, S. Lambbotharan, " Bayesian Multiple Extended Target Tracking Using

Labelled Random Finite Sets and Splines", to be submitted to IEEE Transactions on Signal Processing, April 2017.

7. List of affiliated PhD students

WP2.1:

Affiliated PhD student: Mr. Michael Hutchinson

PhD title: Autonomous search and source term reconstruction of hazardous, atmospheric releases using unmanned aerial vehicles.

WP2.2:

Affiliated PhD students:

Mr. Abdullahi Daniyan, PhD title: Multiple target tracking.

Ms. Gaia Rossetti, PhD title: Convex optimization techniques for cognitive radar networks.

References:

[1] H. Blom and E. Bloem, "Exact Bayesian and particle filtering of stochastic hybrid systems", *IEEE Transactions on Aerospace and Electronic Systems*, Vol. 43, no.1, pp. 55–70, 2007.

[2] W. Farrell. "Tracking of a ballistic missile with a-priori information", *IEEE Transactions on Aerospace and Electronic Systems*, Vol. 44, no. 2, pp.418–426, 2008.

[3]. H. Song and Y. Han, "Comparison of space launch vehicle tracking using different types of multiple models", *19th International Conference on Information Fusion (FUSION)*, Heidelberg, Germany, 2016.

[4]. B. Ristic, A. Skvortsov and A. Gunatilaka, "A study of cognitive strategies for an autonomous search", Vol. 28, pp. 1–9, 2016.

L_WP3: (SS) Signal Separation and Broadband Distributed Beamforming

3.1 Staffing

Work Package Leaders: Dr Wenwu Wang (SU) and Prof John McWhirter (CU)

Other Academics Involved: Prof. Ian Proudler, Prof. Jonathon Chambers, Dr. Philip Jackson, Prof. Josef Kittler, Dr. Stephan Weiss, Dr. Yulia Hicks, and Dr Syed Mohsen Naqvi

Research Associates: Dr Mark Barnard

Research students: Mr Luca Remaggi (SU), Miss Jing Dong (SU), Mr Zeliang Wang (CU), Waqas Rafique (NU), Pengming Feng (NU), Mingyang Chen (SU)

Lead Project Partner: Macleod Malcolm (QinetiQ), and Richard Brind (Atlas Elektronik)

Dstl contact: Julian Deeks (Naval Systems Dept), Nick Goddard (Naval Systems Dept), and Alan Johnson (Sensors & Countermeasures Dept)

3.2 Aims and Introduction

This work package is concerned with the development of low-complexity robust algorithms for underdetermined and convolutive signal separation, broadband distributed beamforming, facilitated by low-rank and sparse representations, and their fast implementations, and the application of these techniques to defence related problems, especially for processing underwater acoustic and sonar data, such as for signal denoising, source localisation, separation, extraction and tracking.

We aim at proposing novel methods to address the challenges in source separation in dense signal environments. This includes extracting signals of interest and suppression of interference from corrupted sensor measurements, e.g. for the problems of convolutive mixing (i.e. multipath signal propagation), underdetermined mixing (i.e. more sources than sensors), and unknown number of target signals. This work package links to L_WP1 in weak signal detection; L_WP2 in unknown number of targets and order selection; L_WP4 in MIMO signal detection; and L_WP5 in data reduction.

L_WP3.1 is devoted to the problem of multichannel convolutive source separation and broadband distributed beamforming, with a focus on polynomial matrix decomposition techniques and their variants. L_WP3.2 focuses on reverberant, underdetermined and noisy source separation, with particular techniques such as robust statistics and bootstrapping, time-frequency masking, sparse representation, and Bayesian estimation. Both L_WP3.1 and L_WP3.2 have focussed on the underwater acoustic data e.g. the Portland 3 sonar datasets, with additional data including SAR image data and video datasets.

3.3 Available Datasets

Currently we have access to the following datasets:

- Portland 3 dataset
- An underwater acoustic channel simulator
- Surrey's BRIR datasets
- Surrey's RIR datasets
- CAVIAR datasets
- PETS2009 datasets
- TUD datasets

3.4 Overview of Technical Progress

We have made a number of advancements in the past year, which are summarized as follows.

- We have developed a new method for controlling the order growth of polynomial matrices in the multiple shift second order sequential best rotation (MS-SBR2) algorithm and used it for calculating the polynomial eigenvalue decomposition (PEVD) for para-Hermitian matrices. In the proposed method, we introduced a new elementary delay strategy to keep all the row (column) shifts in the same direction in each iteration. This gives us the flexibility to control the polynomial order growth by selecting the shifts that ensure non-zero coefficients are kept closer to the zero-lag coefficient matrix. The details about the methods and results can be found in (Wang et al. 2016).
- We have taken a fresh look at the SBR2 algorithm in terms of its potential for optimising the subband coding gain. It is demonstrated how every iteration of the SBR2 algorithm must lead to an increase in the subband coding gain until it comes arbitrarily close to its maximum possible value. Since the algorithm achieves both strong decorrelation and optimal subband coding, it follows that it must also produce spectral majorisation. A new quantity associated with the coding gain optimization is introduced, and its monotonic behaviour brings a new insight to the convergence of the SBR2 algorithm, leading to a first proof that it must also achieve spectral majorization. A detailed account of this proof can be found in (McWhirter and Wang, 2016).
- We have performed an investigation into sparse sensor configurations in hydrophone arrays. We use Compressive sensing (CS) for the design of sparse arrays by trying to match the response of the array to a desired/reference response for a given direction of arrival (DOA) angle. This is achieved by minimizing the ℓ_0 norm, or relaxed as the ℓ_1 norm of the weighting coefficients, subject to the error between the desired and designed responses being below a predefined level. We have also shown that it is possible to improve the sparseness of a solution by considering a re-weighted ℓ_1 minimization problem. The aim of these methods is to bring the minimization of the ℓ_1 norm of the weight coefficients closer to that of the minimization of the ℓ_0 norm, by solving a series of re-weighted ℓ_1 minimizations, where locations with small weight coefficients are more heavily penalized than locations with large weight coefficients. The details of this work were summarised in an internal report (shared with both Dstl and the industrial partner Atlas).
- We have also investigated a related problem to sparse array optimisation in the context of dealing with sensor failures in the array. To this end, we take a given array configuration with missing sensors and then optimise the response for this configuration. Sensor arrays operating in difficult environments can suffer from high failure rates of components or blocks of components. It can also be very difficult and expensive to replace those damaged sensors. Therefore a method of improving the robustness of these arrays to sensor failure by optimising the weighting on each sensor to give the best possible response given the missing sensors would be valuable. A conference draft was written based on this work (Barnard et al., 2017).
- We have proposed a method of joint optimisation of sparse array and spatial sparsity, to achieve source detection in a subset of space with as few sensors as possible. The method is operated in a two-step iterative process, where the first step is to find the

minimum number of sensors to be used in the array and the second step is to perform source localisation based on the least absolute shrinkage and selection operator (LASSO) algorithm with the selected sensors. This method is potentially useful for joint source localisation and sensor selection. The details about this method can be found in (Chen et al., 2016).

- We have developed a new method for detecting acoustic reflectors/boundaries from acoustic impulse response, using a multistage method including epoch detector, image source reversion, and a times of arrival (TOAs) estimator. This method has been evaluated using several room impulse responses (RIRs) datasets. The details and the results can be found in (Remaggi et al., 2017). The acoustic reflector has also been incorporated into a blind source separation as side information for further improving the performance of source separation in a reverberant environment.
- We proposed a novel method to address the challenges within the prediction stage of Bayesian filtering algorithm based on probability hypothesis density (PHD) filtering with a Markov chain Monte Carlo (MCMC) implementation. More specifically, a novel social force model (SFM) for describing the interaction between the targets is used to calculate the likelihood within the MCMC resampling step in the prediction step of the PHD filter, and a one class support vector machine (OCSVM) is then used in the update step to mitigate the noise in the measurements, where the SVM is trained with features from both colour and oriented gradient histograms. The details about the methods and results can be found in (Feng et al. 2016).
- In order to achieve more observable measurements, we employed a forward-backward filtering algorithm in the framework of particle PHD filtering, which provides backward estimation from the aid of delayed measurement set. Moreover, the forward and backward processes were combined with an adaptive weight which is calculated by the similarity of the observed measurement from forward and backward process (Feng et al. 2016).
- We studied and proposed new methods to improve the separation performance of the independent vector analysis (IVA) algorithms, especially on how to better preserve the inter-frequency dependency. We have introduced a new mixed source prior to be used in both the IVA and the fast fixed point IVA (FastIVA) algorithm, based on a mixture of multivariate Student's t and the super Gaussian distribution. In order to further enhance separation performance of the mixed multivariate source prior, the ratio of the Student's t distribution and the super Gaussian source prior were adjusted automatically according to the energy of the source signals. This work is published in (Rafique et al., 2015) and (Rafique et al., 2016). A new Student's t mixture model (SMM) is also proposed and an expectation maximisation algorithm is developed for this new model.

3.5 Technical Details

3.5.1 New MS-SBR2 and SBR2 Algorithms

1) Order-Controlled MS-SBR2 Algorithm for PEVD

One common feature among the existing PEVD algorithms is that the order of polynomial matrices continuously increases with each iteration. This is problematic, as such order growth

will lead to a significant increase in computational cost. During the last year, we have developed a new method for controlling the order growth of polynomial matrices in the multiple shift second order sequential best rotation (MS-SBR2) algorithm which has been used for calculating the polynomial eigenvalue decomposition (PEVD) for para-Hermitian matrices. In effect, the proposed method introduces a new elementary delay strategy which keeps all the row (column) shifts in the same direction in each iteration, which therefore gives us the flexibility to control the polynomial order growth by selecting the shifts that ensure non-zero coefficients are kept closer to the zero-lag coefficient matrix. Simulation results confirm that further order reductions of polynomial matrices can be achieved by using this direction-fixed delay strategy for the MS-SBR2 algorithm.

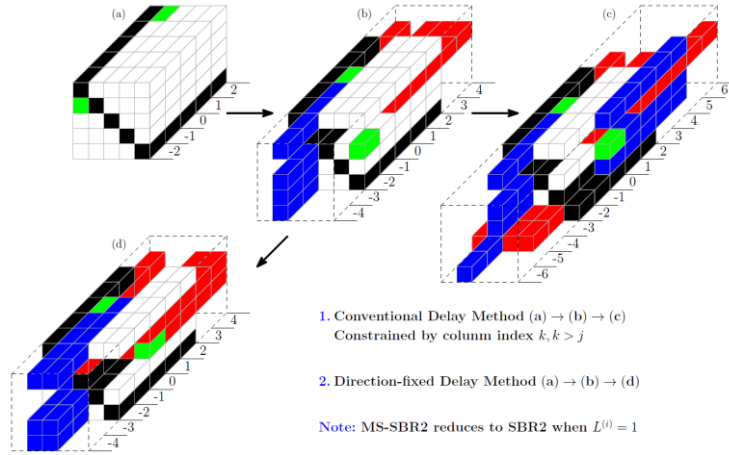


Fig. 3.1. Illustration of the two different elementary delay strategies in the MS-SBR2 algorithm.

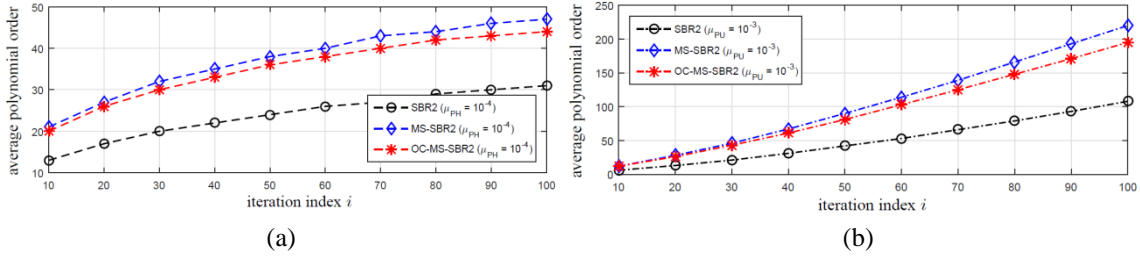


Fig. 3.2. The resulting polynomial order comparison after diagonalising para-Hermitian matrices using different versions of SBR2. Sub-figure (a) shows the average order of the para-Hermitian matrix $R^{(i)}(z)$ at i^{th} iteration with the truncation parameter $\mu_{PH} = 10^{-4}$, and sub-figure (b) shows the average order of the paraunitary matrix $H^{(i)}(z)$ at i^{th} iteration with the truncation parameter $\mu_{PU} = 10^{-3}$.

As shown in Fig. 3.2, the order-controlled MS-SBR2 (OC-MS-SBR2) has produced lower order para-Hermitian and paraunitary matrices than that of the MS-SBR2 algorithm. The reason why the SBR algorithm has been shown to produce much lower order is that within each iteration the SBR2 algorithm can only transfer a single off-diagonal element onto the diagonal, while for the multiple shift versions including MS-SBR2 and OC-MS-SBR2 the number is usually three times for this 6×6 para-Hermitian matrix example. This means that there are more paraunitary transformations involved, which can cause higher polynomial

order. More details about this work can be found in (Wang et al. 2016) that has been published in the 2016 IEEE SAM.

2) A Novel Insight to the SBR2 Algorithm for Diagonalising Para-Hermitian Matrices

Most of the work reported since then has focused on improving the performance or reducing the computational cost of the PEVD algorithms including the SBR2 (McWhirter et al. 2007) and SMD (Redif et al. 2015) algorithm families. The SBR2 algorithm was originally developed for achieving strong decorrelation of convolutively mixed sensor array signals. It was observed that the algorithm always seems to produce spectrally majorised output signals, but this property has not previously been proven. In this work, we have taken a fresh look at the SBR2 algorithm in terms of its potential for optimising the subband coding gain. It is demonstrated how every iteration of the SBR2 algorithm must lead to an increase in the subband coding gain until it comes arbitrarily close to its maximum possible value. Since the algorithm achieves both strong decorrelation and optimal subband coding, it follows that it must also produce spectral majorisation. A new quantity γ associated with the coding gain optimization is introduced, and its monotonic behaviour brings a new insight to the convergence of the SBR2 algorithm.

We have investigated the SBR2 algorithm in terms of optimizing the subband coding gain, leading to a first proof that it must also achieve spectral majorization. In addition, the monotonically increasing behaviour of the coding gain $G^{(i)}$ has been exploited to obtain a more reliable test of convergence for the algorithm. A detailed account of this proof can be found in (McWhirter and Wang, 2016) that has been presented in the 2016 IMA conference.

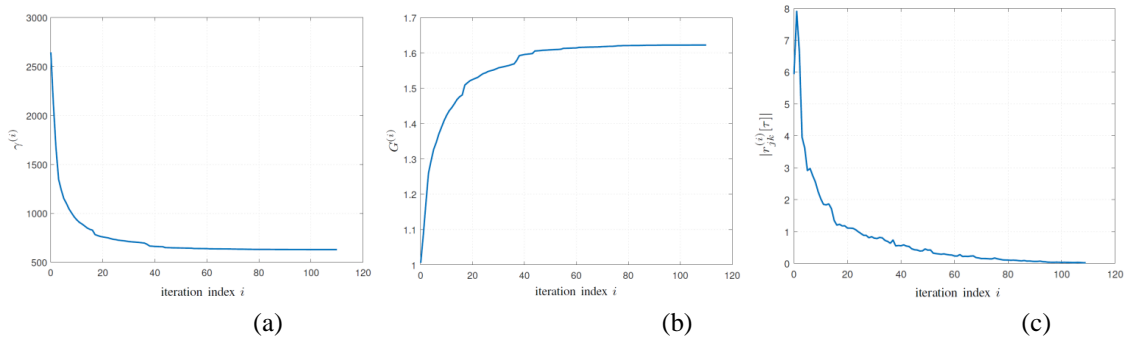


Fig. 3.3. Convergence of the SBR2 algorithm for diagonalising the space-time covariance matrix $R[\tau]$, showing (a) the behaviour of $\gamma^{(i)}$; (b) behaviour of the coding gain $G^{(i)}$; (c) behaviour of the off-diagonal element $|r_{jk}^{(i)}[\tau]|$.

3.5.2 Sparse Array Design

1) Compressed Sensing based Sparse Array Optimisation

We have performed an investigation into sparse sensor configurations in hydrophone arrays. Compressive sensing (CS) has been employed in the design of sparse arrays by trying to

match the response of the array to a desired/reference response for a given direction of arrival (DOA) angle θ . This is achieved by minimizing the ℓ_0 norm, or relaxed as the ℓ_1 norm of the weighting coefficients, subject to the error between the desired and designed responses being below a predefined level. The ℓ_1 norm is defined as the sum of the elements in a vector and for a vector with complex entries, this is the absolute value of the entries. The ℓ_0 norm is defined as the number of non-zero entries in a given vector. Further work has also shown that it is possible to improve the sparseness of a solution by considering a re-weighted ℓ_1 minimization problem. The aim of these methods is to bring the minimization of the ℓ_1 norm of the weight coefficients closer to that of the minimization of the ℓ_0 norm, by solving a series of re-weighted ℓ_1 minimizations, where locations with small weight coefficients are more heavily penalized than locations with large weight coefficients.

In order to create a sparse sensor configuration we employ a weighting vector \mathbf{w} of length M for the sensors in the array. We perform a convex optimisation to ensure a minimum error in the array response whilst ensuring sparsity in \mathbf{w} . This convex optimisation is formulated as follows:

$$\text{minimise } |\mathbf{w}|_1 \text{ subject to } \|\mathbf{p}_r - \mathbf{w}^H \mathbf{A}\|_2 \leq \alpha \quad (3.1)$$

where $|\mathbf{w}|_1$ is the ℓ_1 norm of \mathbf{w} , \mathbf{p}_r is the vector holding the desired beam response at a particular frequency Ω and DOA angle θ , \mathbf{A} is the matrix composed of the steering vectors at the corresponding frequency Ω and DOA and α places a limit on the error between the desired and the designed responses. This minimisation was implemented using the CVX toolbox in Matlab.

We also introduce here the measure of array gain which is the ratio of the overall signal to noise ratio (SNR) of the array and the SNR of an individual hydrophone. The array gain is calculated using the following formula

$$G_a = \frac{SNR_{array}}{SNR_{hydrophone}} = \frac{|\mathbf{w}^H \mathbf{A}|^2}{\mathbf{w}^H \mathbf{R} \mathbf{w}} \quad (3.2)$$

where \mathbf{R} is the $M \times N$ (where $M = N$) noise coherence matrix for a particular frequency Ω . A particular choice of \mathbf{R} is considered here to demonstrate the ability to treat arbitrary noise distributions. More specifically the mn -th entry R_{mn} is given by

$$R_{mn} = 3 \left[\frac{\sin(kd_{mn})}{(kd_{mn})^3} - \frac{\cos(kd_{mn})}{(kd_{mn})^2} \right] \quad (3.3)$$

where k is the wavefront number given by $\frac{\omega}{c}$ (c being the speed of sound in water) and d_{mn} is the distance between the n th and m th microphones. So each entry in \mathbf{R} is the coherence between the n th and m th microphones.

A second measure used in our experiments is the white noise gain (WNG) of the array and this measures the gain in the presence of incoherent noise between sensors. This is a measure of the robustness of the array to factors such as small changes in sensor position. The WNG of the array is given by

$$G_w = \frac{|\mathbf{w}^H \mathbf{A}|^2}{\mathbf{w}^H \mathbf{w}} \quad (3.4)$$

For an unshaded array the WNG is equal to the number of sensors, $G_w = M$.

We initially test the effect of sparse optimisation on an array at a DOA of zero degrees, this corresponds to the direction of the main beam being perpendicular to the array. We then steer the array to -30 and -60 degrees where the array response is tested and array gain is measured for different numbers of elements selected by the sparse optimisation Equation (3.1). Initially we allow different sensor configurations for each different steering angle. We test the array first with the full 100 elements then this is reduced in steps of 10 sensors until we select only 50 sensors (half of the elements in the array).

In the first set of experiments we examine the performance of an unshaded array in which all the weights in \mathbf{w} are set to $\frac{1}{m}$. We also test the Dolph-Chebyshev weighting configuration. This weighting is used to make all sidelobes the same height below the main lobe and in all our experiments the sidelobe level was set to 20dB below the peak of the main lobe. After the optimisation process a threshold of 0.001 on the real component of the weights is applied, thus adding to the sparsity of \mathbf{w} .

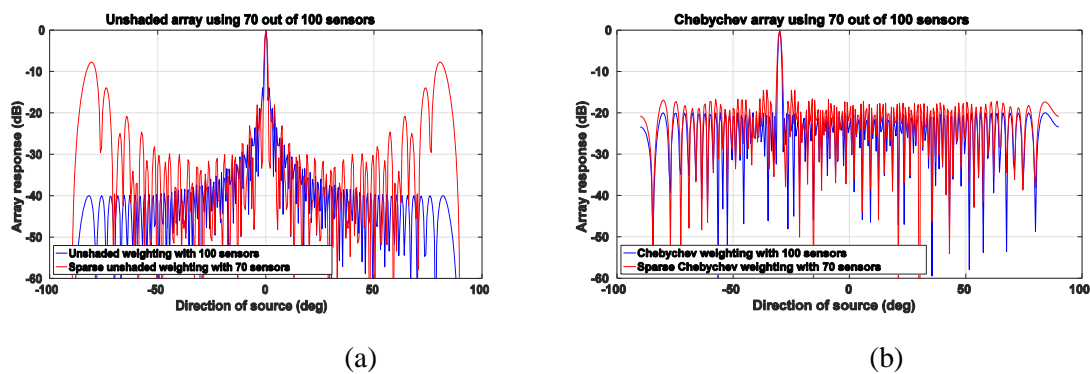


Figure 3.4. Response from an unshaded array (a) at 0 degrees, and from a Dolph-Chebyshev weighted array (b) steered to -30 degrees, both using 70 out of 100 sensors.

It can be observed in Figure 3.4 that while the main beam is still narrow and the side lobes close to the main beam are low, almost immediately large sidelobes form toward -90 and +90 degrees and quickly grow. The weighting pattern for 70 sensors at 0 degrees can be seen in Figure 3.5, which clearly shows that the weights in the centre of the array are maintained at the expense of those at either end of the array. This may be due to the fact that the optimisation in Equation (3.1) is based on minimising the total error between the desired and designed response. As the values of the response are much higher in the centre than at -90 and 90 degrees, the optimisation allows the errors at -90 and 90 degrees to increase whilst a narrow beam width and low sidelobes are maintained in the centre as the number of sensors are decreased.

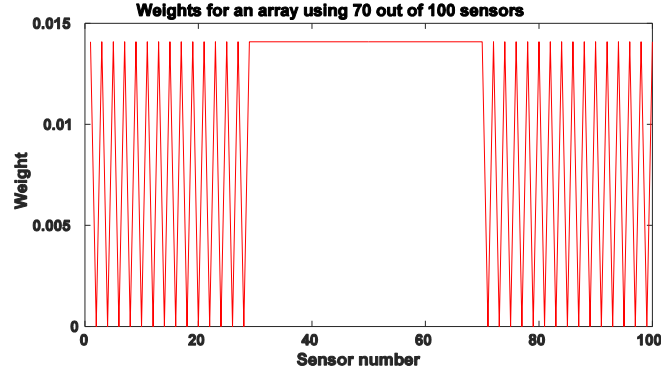


Figure 1.5. Weight configuration for an unshaded array using 70 out of 100 sensors.

Number of sensors	Unshaded array at 0 degrees		Dolph-Chebyshev array at -30 degrees	
	Array gain	WNG	Array gain	WNG
100/100	66.86 (18.25dB)	100.00 (20.00 dB)	53.38 (17.27dB)	70.64 (18.49dB)
90/100	62.80 (17.98dB)	90.00 (19.54dB)	49.64 (16.96dB)	64.54 (18.10dB)
80/100	59.93 (17.78dB)	80.00 (19.03dB)	44.79 (16.51dB)	57.99 (17.63dB)
70/100	58.00 (17.63dB)	70.00 (18.45dB)	39.57 (15.97dB)	50.88 (17.07dB)
60/100	57.95 (17.63dB)	60.00 (17.78db)	34.04 (15.32dB)	43.34 (16.37dB)
50/100	63.39 (18.02dB)	50.00 (16.99dB)	28.31 (14.52dB)	35.55 (15.51dB)

Table 3.1. Array gains for an unshaded array at 0 degrees and for a Dolph-Chebyshev array at -30 degrees.

Tables 3.1 shows respectively the array gain and WNG for an unshaded array with different numbers of sensors for both an unshaded and a Dolph-Chebyshev array. This table shows how both measures, in general, decline as the number of sensors are reduced.

We then look at controlling the size of the sidelobes of the array response. In order to achieve this we introduced additional constraints into Equation (3.1) to enforce a maximum value on the first two sidelobes of the response, as follows

$$\begin{aligned}
 \text{minimise } |\mathbf{w}|_1 \text{ subject to } & \|\mathbf{p}_r - \mathbf{w}^H \mathbf{A}\|_2 \leq \alpha & (3.5) \\
 & \|\mathbf{w}^H \mathbf{a}_{\theta_1}\|_2 \leq \beta \\
 & \|\mathbf{w}^H \mathbf{a}_{\theta_2}\|_2 \leq \beta
 \end{aligned}$$

where a_{θ_1} and a_{θ_2} are steering vectors corresponding to the first two sidelobes on either side of the main beam and β is a threshold placed on the level of these sidelobes. In practice the values of α and β are a trade off between the sidelobe level controlled by β and the amount of overall error in the response of the array controlled by α . In order to incorporate these additional constraints into the minimisation, we need to relax the overall error to obtain a tractable solution. So in the following experiments we set $\alpha = 1$ and $\beta = 0$. The problem of tractability with an increased number of constraints can also be addressed by using more sensors, as this is equivalent to adding parameters to the system.

The results of applying the optimisation to a Chebychev weighted array can be seen in Figure 3.6. It can be observed that the first two side lobes are significantly reduced, by at least 5 dB from the previous sidelobe level. As well as having to increase the error limit on the response, we also noted that with the additional constraints introduced to lower the first pair of sidelobes the array gain is reduced from 16.76 dB to 14.05 dB and the WNG from 15.08 dB to 13.37 dB.

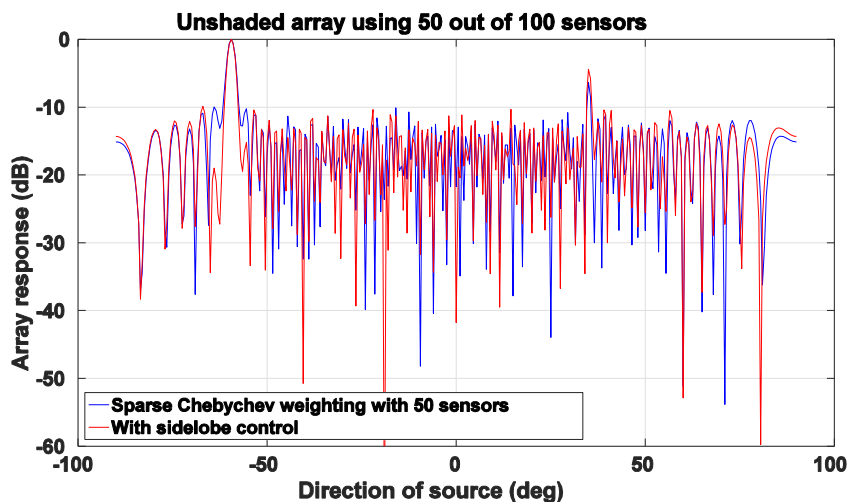


Figure 3.6. Response after imposing additional constraints on sidelobe levels.

2) Dealing with Sensor Failures

We have also proposed to approach the sparse array problem from the opposite direction. Instead of attempting to determine the array configuration that gives the optimal response, we take a given array configuration with missing sensors and then optimise the response for this configuration. Sensor arrays operating in difficult environments can suffer from high failure rates of components or blocks of components. It can also be very difficult and expensive to replace those damaged sensors. This is particularly true in the case of underwater hydrophone arrays, whether mounted on vessels or placed on the sea floor. Therefore a method of improving the robustness of these arrays to sensor failure by optimising the weighting on each sensor to give the best possible response given the missing sensors would be valuable.

We can introduce additional constraints in the convex minimisation. Using additional constraints to Equation (3.1) we can include a specific arbitrary array configuration in the optimisation. This configuration could correspond, for example, to an array with damaged or missing sensors. More specifically the weight of any sensor that is not used is constrained to be zero, so effectively turning that sensor off. This is then used to optimise the array response in the event of sensor failure. We define the set of sensor indices to be $\mathbf{I} = \{1, 2, 3, \dots, M\}$, we then define the subset of failed sensor indices to be $\mathbf{J} \subseteq \mathbf{I}$, where $\mathbf{J} = \{w_{J_1}, w_{J_2}, \dots, w_{J_k}\}$. The optimisation equation with additional constraints is given by:

$$\text{minimise } \|\mathbf{w}\|_1 \text{ subject to } \|\mathbf{p}_r - \mathbf{w}^H \mathbf{A}\|_2 \leq \alpha \quad (3.6)$$

$$\{w_{J_1}, w_{J_2}, \dots, w_{J_k}\} = 0$$

where k is the number of missing or damaged sensors $\{w_{J_1}, w_{J_2}, \dots, w_{J_k}\}$ corresponding to the weights of the sensors that are set to zero.

Losing individual sensors randomly from an array does not necessarily affect the array response. However in practice many sensor array systems, for example hull mounted hydrophone arrays, are modular in design so sensors often fail in blocks not individually. In the following set of experiments we simulate the failure of blocks of sensors in the array and show the response of the damaged array before and after the blocks of sensors are removed. Here we simulate failures in two types of modular array, the first with modules of 5 sensors and the second with modules of 15 sensors. In our first set of experiments, we simulate the failure of two blocks of five sensors and the pattern of this sensor loss is shown in Figure 3.7a (Failure mode 1). In the second set we simulate the failure of two blocks each containing 15 sensors as shown in Figure 3.7b (Failure mode 2).

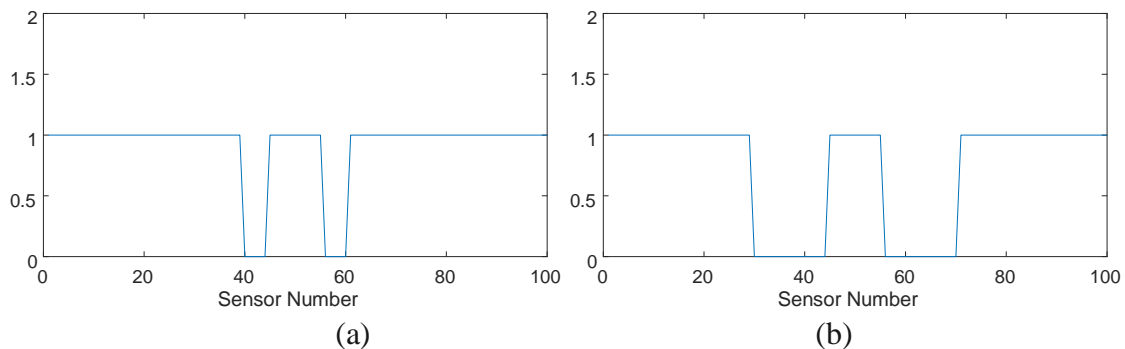


Figure 3.7. Array configuration with (a) modules of five sensors and two modules failed, and (b) 15 sensors and two modules failed.

The result of the first failure mode with 10 missing sensors is shown in Figure 3.8a and 3.8b, it can be seen that for both the unshaded and the Dolph-Chebyshev the optimisation taking into account the damaged array configuration generally improves the response of the array. This improvement is increased when the level of damage to the array is increased.

This can be seen when the number of missing sensors is increased to 30 as shown in Figure 3.9a and 3.9b.

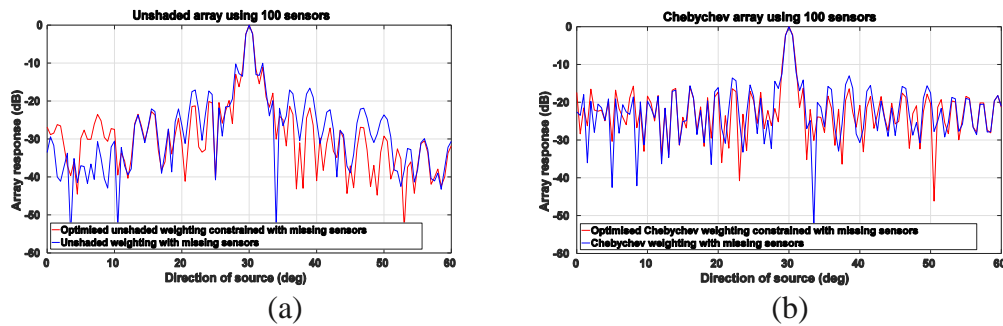


Figure 3.8. Response of unshaded array (a) and Dolph-Chebyshev array (b) in failure mode 1.

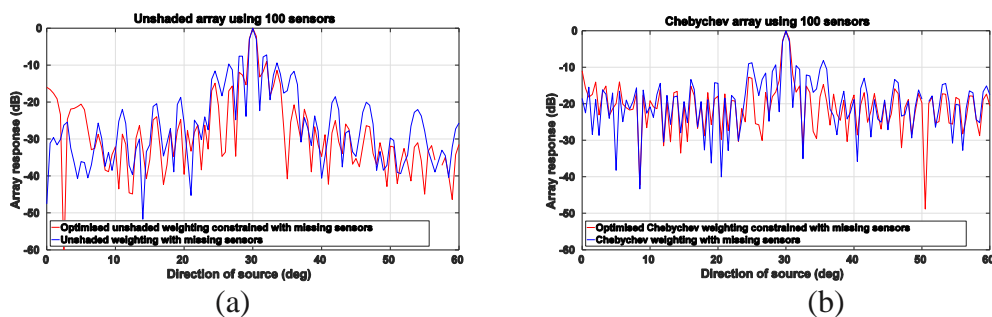


Figure 3.9. Response of unshaded array (a) and Dolph-Chebyshev array (b) in failure mode 2.

It should particularly be noted that in all cases the level of the sidelobes in the damaged array response is significantly increased, in the case of the array missing 30 sensors these rise to more than -10 dB below the main beam. In all cases the optimisation decreases these sidelobe levels to below -10 dB.

In order to quantify the level of sidelobe reduction we measure the relative sidelobe level (RSL) which is the maximum sidelobe level for a given response. We measured this level for steering angles from 0 degrees (beam on to the array) to 60 degrees in 10 degree increments and then took the mean of the levels for both the damaged array and the optimised array for the two failure modes shown in Figures 3.7. Table 3.2 shows the mean and variance of the RSL for failure modes 1 and 2 respectively. It can clearly be seen in these results that optimising the array taking into account the damaged configuration significantly lowers the level of the sidelobes in the responses for both failure modes.

	Damaged array		Optimised array	
	Mode 1	Mode 2	Mode 1	Mode 2
Dolph-Chebyshev	-13.80 dB (0.24)	-8.55 dB (0.08)	-19.02 dB (1.75)	-13.32 dB (0.67)
Unshaded	-10.02 dB (0.06)	-6.85 dB (0.23)	-12.43 dB (0.61)	-10.74 dB (0.59)

Table 2.2. Average RSL for both arrays in failure mode 1 with 10 sensors missing, and mode 2 with 30 sensors missing.

In our proposed method the configuration of the damaged array is used as a constraint in the optimisation, with the weights of missing sensors set to zero. This is an important problem as the replacement or repair of damaged sensors can be extremely difficult and expensive, particularly in the case of underwater hydrophone arrays. We demonstrate that in the challenging task of improving performance when blocks of sensors are missing from the array, our proposed optimisation improves the array response.

3.5.3 Joint Sparsity Optimisation for Simultaneous Sensor Selection and DOA Estimation

Source localisation, such as direction of arrival (DoA) estimation, is an important issue in applications such as underwater acoustic detection, target tracking and environmental monitoring (Benesty et al., 2008, Bai et al., 2013). Traditionally, DoA estimation is addressed by methods, such as Capon beamformer, high-resolution and multiple signal classification (MUSIC) algorithm (Handel et al., 1993, Totarong, and El-Jaroudi, 1992, Hakam et al. 2013). Recently, Spatial sparsity based optimisation, which aims at extracting meaningful lower-dimensional information from high-dimensional data (Knee, 2012), has attracted great interests. A novel solution for spatial sparsity optimisation is to use a full array based compressive sensing (CS) theory (David, 2006), where the activity of source is assumed to be sparse and the sparsity is enforced by a constraint based on ℓ_1 norm of a vector of the coefficients corresponding to the source activities in the spatial domain (Malioutov et al., 2005). However, in practical applications, only partial sensors from the array may be available due to the constraints induced by the manufacturing costs of the sensors, physical space limits and the problem of sensor failure.

Motivated by the aforementioned problems, we have proposed a joint optimisation of sparse array and spatial sparsity, to achieve source detection in a subset of space with as few sensors as possible (Chen et al., 2016). The method is operated in a two-step iterative process, where the first step is to find the minimum number of sensors to be used in array and the second step is to perform source localisation based on the least absolute shrinkage and selection operator (LASSO) algorithm with the selected sensors. Both stationary and moving sources are considered as shown in Fig. 3.10. The approach can be initialised at a random direction and eventually find the DoA after it converges. An extension from narrowband to broadband has also been studied by reshaping the broadband signal in a narrowband-like manner, as well as the corresponding desired beam response and dictionary matrix. In Fig. 3.11, we show the spectrogram of wideband DoA estimates for the last frequency band and the 3D graph illustrates the simulations at the final time step where 69 of 300 sensors are used.

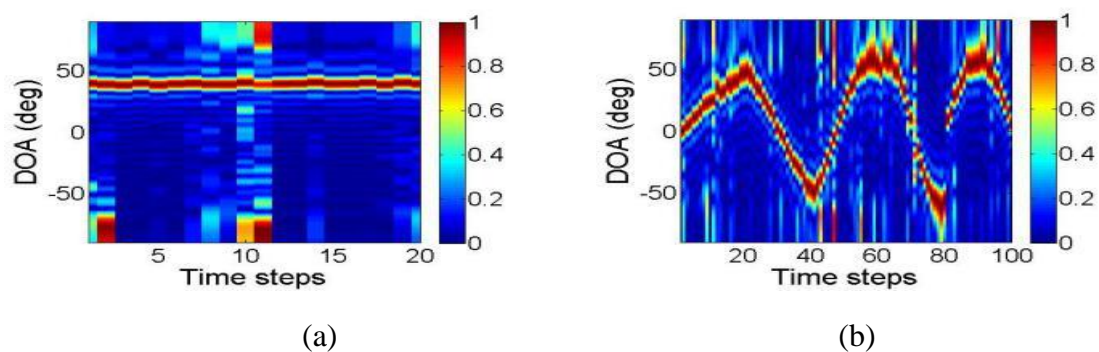


Fig. 3.10. Narrowband DoA estimations for (a) stationary source (SNR=20dB) with 37/100 active sensors and for (b) moving source (SNR=20dB) with 22/100 active sensors.

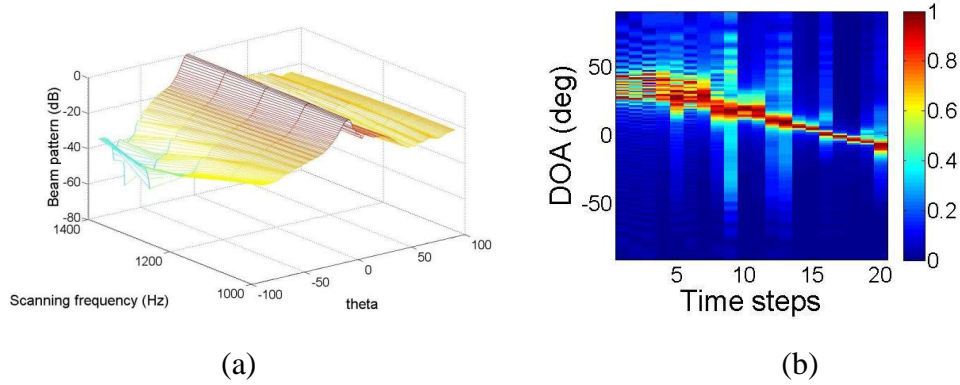


Fig. 3.11. Wideband DoA estimations for the moving source, the 3D graph (a) illustrates the simulation result at the 20-th time step and the spectrogram (b) is the DoA estimation for the last frequency band, 69/300 active sensors.

In order to further improve the DoA estimation result, we have considered the use of statistical constraints in joint array and spatial sparsity based optimisation framework, where the Fisher Information Matrix (FIM) is used to express the Maximum Likelihood Estimation (MLE) of the source signal (Nandi, 1994, Kay, 1993). In the step of sparse array optimisation, a constraint with FIM is considered to reduce the error before scaling the observed signal by the weight coefficients. In the spatial sparsity reconstruction step, the difference between the reconstructed result and the desired beam response is also constrained with a statistical term. Fig. 3.12 shows the results of narrowband DoA estimation with FIM constrained joint approach for the moving sources without and with noise. An example of tracking from 50 degrees to -50 degrees is shown to demonstrate the performance of the proposed method. For the future work, we will extend the FIM constraints from the narrowband to the broadband scenario. A more detailed study will be conducted for the use of FIM, including the process to calculate MLE through FIM, the possible convex optimization problem, and the problem of computing the expectation.

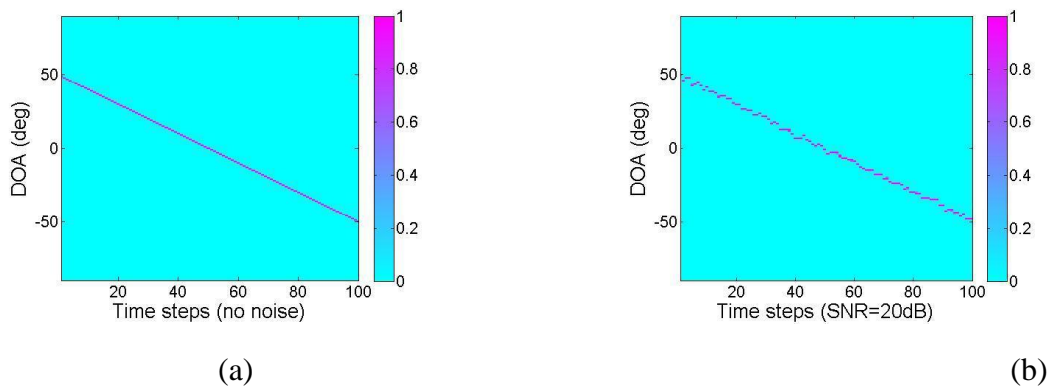


Fig. 3.12. Narrowband DoA estimation with FIM constrained joint array sparsity and spatial sparsity based approach for moving sources (a) without noise and (b) with noise (SNR=20dB).

3.5.4 Acoustic Reflector Localisation and Its Use to Improve Source Separation

The work undertaken by Luca Remaggi can be categorized into four main tasks. The first task regards the evaluation of an epoch detector algorithm, the clustered dynamic programming

projected phase-slope algorithm (C-DYPSA), which we proposed as times of arrival (TOAs) estimator. Secondly, several simulated room impulse responses (RIRs) have been produced and utilized to test the acoustic reflector localization methods proposed, comparing them with the state of the art. Both these tasks were included in the journal article that has been published this February 2017 (Remaggi et al., 2017). The acoustic reflector has been incorporated into a blind source separation as side information for further improving the performance of source separation in reverberant environment.

Starting with the C-DYPSA evaluation, this novel TOA estimator C-DYPSA was evaluated and compared against its previous version, the DYPSA algorithm (Naylor et al. 2007), on the four recorded datasets. In addition, the experiments to compare DYPSA and C-DYPSA with the algorithm in (Kuster, 2008) were performed, applying the same datasets. DYPSA estimated the peak positions in each RIR singularly, detecting zero crossings in the group delay function. C-DYPSA improved it, by exploiting the information given by multiple microphones, by clustering different microphone results and deleting outliers. On the other hand, the peak detector utilized in (Kuster, 2008) employed an adaptive threshold based on the time domain amplitudes averaged over neighbouring samples.

The fine errors produced were calculated as root mean square error (RMSE) and confidence interval (CI). These results are reported in the bottom of Table 3.3. C-DYPSA performed better in every dataset, since outliers produced by DYPSA for single RIRs are discarded in C-DYPSA, generating a final estimate more robust and accurate. In fact, the top part of Table 3.3 shows the gross errors decreasing for every dataset, applying C-DYPSA. Regarding the Kuster’s method (Kuster, 2008) preliminary results showed a gross error rate close to 100%. Therefore, a couple of improvements were applied on it: the first peak detected was forced to correspond to the RIR peak having greater energy (in other words all the peaks detected before the direct sound were deleted); since the Kuster’s method observes the RIRs by dividing them in temporal windows, it was improved by not allowing multiple peaks inside the same time interval (the only peak selected for each window is the one corresponding to the local maximum of energy). However, as can be seen in Table 3.3, C-DYPSA produced higher performance than (Kuster, 2008), both in terms of fine and gross errors.

	Gross Error (%)					RMSE (mm)				
	AudioBooth	Studio1	VML	Vislab	AVG	AudioBooth	Studio1	VML	Vislab	AVG
Kuster	16.9	26.7	57.5	26.7	31±9	89	194	227	94	151±34
DYPSA	2.3	0.5	27.1	0.5	11±11	54	100	194	110	115±50
C-DYPSA	0.7	0.0	21.1	0.0	8±9	48	99	192	95	109±51

Table 3.3. TOA estimation, C-DYPSA evaluation and comparison.

The second topic is the simulations made to evaluate the reflector localization algorithm proposed (i.e. ISDAR-LIB, mean-ISDAR-LIB, median-ISDAR-LIB, and ETSAC) together with two state-of-the-art methods. Both these results and the one provided by the C-DYPSA analysis have been published through a journal (Remaggi et al., 2017). The aim of these simulations was to evaluate the proposed reflector localization methods, over a wide variety of controlled scenarios, highlighting potential strengths and weaknesses. The metrics utilized were RMSE and CI to evaluate the fine errors, and the gross errors. Two different sets of

simulations were performed. First, the 100 datasets produced by varying size and average absorption coefficient α , with direct sound 70dB louder than the additive noise, and microphone perturbation of 7mm maximum, were evaluated, with results reported in Table 3.4.

Gross Error (%)	Size			α			Overall
	Small	Medium	Large	0.2	0.5	0.8	
ISDAR-LIB	29.7	0.5	0.0	3.6	19.1	6.6	9.9 ± 8.7
Median-ISDAR-LIB	14.0	0.0	0.0	2.0	11.4	1.0	4.7 ± 4.6
Mean-ISDAR-LIB	9.7	0.0	0.0	1.0	8.2	1.0	3.3 ± 3.2
ETSAC	8.1	0.0	0.0	0.1	5.9	0.4	2.4 ± 2.6

RMSE (mm)	Size			α			Overall
	Small	Medium	Large	0.2	0.5	0.8	
ISDAR-LIB	61	13	13	13	31	44	29 ± 15
Median-ISDAR-LIB	27	34	34	30	29	34	31 ± 2
Mean-ISDAR-LIB	207	34	24	60	151	109	98 ± 52
ETSAC	145	13	14	13	107	71	61 ± 41

Table 3.4. Simulations for varying size and absorption coefficient of the rooms.

Then, the 300 datasets obtained by varying the direct to noise ratio (DNR) were considered, and the results are shown in Table 3.5. Starting from the first set of simulations (Table 3.4, top), the direct localization ETSAC gives the best performance, with the lowest gross error over the 100 datasets. The multiple-loudspeaker methods (i.e. median-ISDAR-LIB and median-ISDAR-LIB) outperformed the single-loudspeaker method (i.e. ISDAR-LIB). Mean-ISDAR-LIB was the better image-source reversion reflector locator, among those tested. Grouping by room size, we note that every method suffers when the room dimensions become too small. This is due to the fact that, in really small environments, the loudspeakers, which are perfectly omnidirectional for the simulated datasets, can happen to be closer to different reflectors, raising an ambiguity on which reflector is under investigation. ETSAC, the direct locator, is still better under these conditions. On the other hand, organizing the results considering the three different α , when $\alpha=0.5$ all the methods seem to deteriorate. However, the smallest room generated has been coincidentally selected to have $\alpha=0.5$, and there is no clear trend between $\alpha=0.2$ and $\alpha=0.8$ under these conditions. The methods are more affected by the room size rather than α . Again, the direct localization ETSAC is the best method under every condition. The RMSE reported on the bottom of the table, should be read with the related gross error, as the RMSE of the fine error values depends on the amount of gross errors eliminated from the calculation. First, median-ISDAR-LIB has consistent results over all the conditions: although it produces gross errors with more datasets than mean-ISDAR-LIB, if the setup gives fine errors it is more robust on identifying outliers over the estimated image sources. Compared to the image-source reversion method with lowest gross

error, ETSAC's fine error is better. There is also a tendency for higher α s to produce higher fine errors with every method.

For the second set of simulations, observing the gross error reported in the top part of Table 3.5, the only two methods that are not strongly affected by lower DNRs are mean-ISDAR-LIB and ETSAC. ETSAC is, in general the best method here tested, however, it faces small issues with DNR=30dB. Here, mean-ISDAR-LIB has comparable performance, showing a high robustness over DNR variations. Nevertheless, looking at the fine errors on the right side of the table, a general trend of improving performance with increasing DNR can be noted. The only one that does not follow that trend is ETSAC. However, it has the lowest gross error for DNR=40dB and DNR=50dB, which includes more samples in its RMSE calculation. Compared to mean-ISDAR-LIB, ETSAC has lower RMSE, showing ETSAC to be the best method tested in these simulations.

	Gross error (%)			RMSE		
	Small	Medium	Large	0.2	0.5	0.8
ISDAR-LIB	11.8	9.4	9.3	41 ± 2	28 ± 2	30 ± 2.6
Median-ISDAR-LIB	19.3	5.1	5.7	45 ± 2	33 ± 1	33 ± 2.6
Mean-ISDAR-LIB	3.3	3.9	3.6	128 ± 6	107 ± 6	109 ± 2.6
ETSAC	3.7	2.1	2.2	65 ± 1	80 ± 1	80 ± 2.6

Table 3.5. Simulations varying the DNRs.

Finally, we consider the use of the acoustic reflector information to improve source separation performance. To this end, we use Mandel's method (Mandel et al., 2010) as a baseline, by including interaural phase difference (IPD) cues related to the first reflection. This allows the generation of a Gaussian Mixture model that is able to determine, for each time-frequency bin, the probability of a specific source that is dominant in the time-frequency point of the mixture, together with its first reflection. Experiments have been performed to evaluate the SDR produced by the proposed method. In Figure 3.13, the signal to distortion ratios (SDRs) are reported for every dataset and every position of the target signal. These results were calculated as the RMS over all the possible positions of the interferer. It is clear from Figure 3.13 that, for every dataset, the proposed blind source separation method, considering one interferer, performs better than Mandel's method. This implies that the use of the acoustic reflector information is helpful in improving source separation performance.

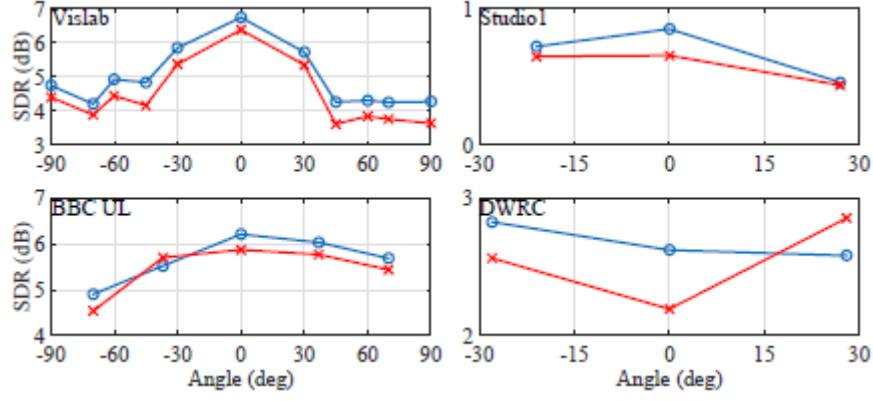


Figure 3.13. SDR obtained for different target positions. The blue lines with circular marks refer to our proposed method, whereas the red ones with crossed marks refer to (Mandel et al., 2010).

3.5.5 Source Tracking with PHD Filters

1) SFM-MCMC-PHD

The focus of the work by Pengming Feng is mainly on the social force model based MCMC-OVSCM particle PHD filter for multiple human tracking. This method is briefly summarised below.

After the prediction step of the particle PHD filter, the weights for each particle are calculated by the energy based social force model, which contains energy function for distance $E_{k,d}^{m,i}$, energy function for changing of angle $E_{k,\varphi}^{m,i}$, energy function for changing of velocity $E_{k,U}$ and energy function for changing of destination $E_{k,W}$:

$$E_{k,d}^{m,i}(n) = e^{-\frac{\|p_k^{m,i} + tv_k^{m,i} - p_k^n - tv_k^n\|}{2\sigma_d^2}} \quad E_{k,\varphi}^{m,i}(n) = \left(1 + \frac{(v_k^{m,i})^T v_k^n}{\|v_k^{m,i}\| \|v_k^n\|}\right)^\beta \quad (3.7)$$

$$E_{k,U}(m,i) = e^{-\frac{\|v_k^{m,i} - u^m\|}{2\sigma_v^2}} \quad E_{k,W}(m,i) = e^{-\frac{(p_k^{m,i} - p_0^m)^T v_k^{m,i}}{\|p_k^{m,i} - p_0^m\| \|v_k^{m,i}\|}} \quad (3.8)$$

then the energy based social force for each particle is calculated as:

$$s_k^{m,i} = \prod_{n \neq m} E_{k,d}^{m,i}(n) E_{k,\varphi}^{m,i}(n) E_{k,U}(m,i) E_{k,W}(m,i) \quad (3.9)$$

After calculating the social force for each particle, all particles are fed into an MCMC resampling step to achieve more accurate prediction. In the measurement model, the OCSVM classifier is employed to calculate the likelihood for particles, which is also aided by background subtraction. At last, the weights for the particles are updated by the update step of the particle PHD filter, and resampled in order to avoid the computational complexity growing exponentially. The proposed system is evaluated on the selected sequences from the CAVIAR, PETS2009 and TUD datasets. Results are presented in Figure 3.14 which shows that the proposed method improves the tracking performance over the baseline PHD methods. This work has been accepted to publish in a journal (Feng et al., 2017).

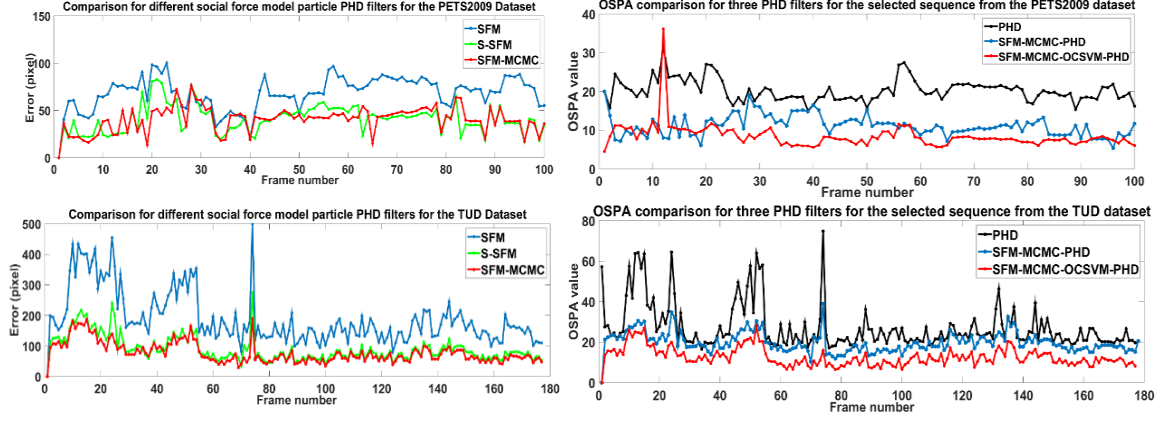


Fig. 3.14. Tracking performance of the proposed social force model based MCMC-OVSCM particle PHD filter as compared with baseline methods including PHD and SFM-MCMC-PHD.

2) Adaptive Retrodiction PHD

Following the idea of combination of adaptive filters, this work employs the forward and backward process adaptively, where the backward process is achieved from the backward retrodiction step. Instead of using the term of PHD smoother, the term of retrodiction is employed because of the non-Gaussian and nonlinear of the state and measurement model. Fig. 3.15 shows the flowchart of the proposed system.

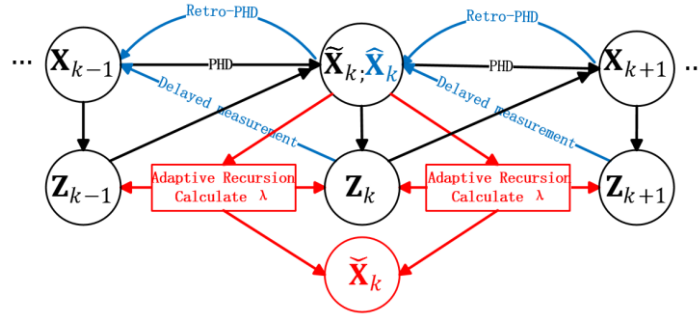


Fig. 3.15. Graphical comparison between PHD filtering, Retro-PHD filtering and the proposed adaptive Retro-PHD filtering algorithm.

Assuming the time lag to be L , the backward weight $\hat{w}_{t|k}^i$ is calculated as:

$$\hat{w}_{t|k}^i = \tilde{w}_t^i [e(\tilde{x}_t^i) \sum_{q=1}^N \frac{\tilde{w}_{t+1|k}^q f_{t+1|k}(\tilde{x}_{t+1}^q | \tilde{x}_t^i)}{\mu_{t+1|t}^q} + (1 - e(\tilde{x}_t^i))] \quad (3.10)$$

where

$$\mu_{t+1|k}^q = \gamma_{t+1}(\tilde{x}_{t+1}^q) + \sum_{r=1}^N \tilde{w}_t^r \times \{e(\tilde{x}_{t+1}^r) f_{t+1|t}(\tilde{x}_{t+1}^q | \tilde{x}_t^r)\} \quad (3.11)$$

and

$$f_{t|t-1}(\tilde{x}_t^i | \tilde{x}_{t-1}^i) = \frac{\exp\left(-\frac{(\tilde{x}_t^i - F(\tilde{x}_{t-1}^i))^T (\tilde{x}_t^i - F(\tilde{x}_{t-1}^i))}{2\sigma_f^2}\right)}{\sqrt{\det(2\pi\sigma_f^2)}} \quad (3.12)$$

After calculating the weight for particles from both the forward and backward process, the convex weights for the adaptive step are calculated as

$$\lambda_{filtering} = \frac{\sum_{i=1}^{M_k} \sum_{r=1}^{M_{k-1}} \exp\left(-\frac{(z_k^i - z_{k-1}^r)^T (z_k^i - z_{k-1}^r)}{2\sigma_\lambda^2}\right)}{M_{k-1}} \lambda_{retrodition} =$$

$$\frac{\sum_{i=1}^{M_k} \sum_{r=1}^{M_{k+1}} \exp\left(-\frac{(z_k^i - z_{k+1}^r)^T (z_k^i - z_{k+1}^r)}{2\sigma_\lambda^2}\right)}{M_{k+1}} \quad (3.13)$$

$$\lambda = \frac{\lambda_{filtering}}{\lambda_{filtering} + \lambda_{retrodition}} \quad (3.14)$$

And the tracking position from the adaptive step is found by using a convex combination of results from both filtering and retrodition as:

$$\tilde{x}_k^m = \begin{cases} \tilde{x}_k^m & \text{if target } m \text{ disappears at } k + 1 \\ \lambda \tilde{x}_k^m + (1 - \lambda) \hat{x}_k^m & \text{otherwise} \end{cases} \quad (3.15)$$

When evaluated on the selected sequences from the CAVIAR and PETS2009 datasets, the results are presented in Figure 3 which shows that the proposed method improves the tracking performance over the baseline methods. This work has been published as (Feng et al., 2016).

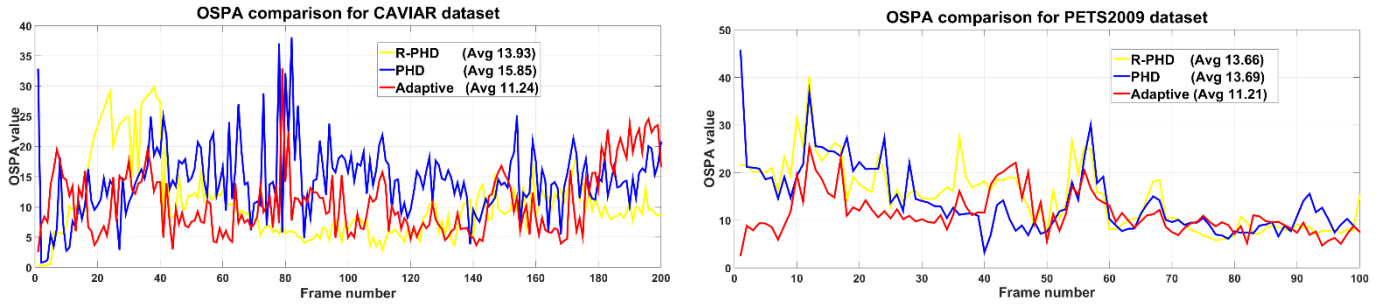


Fig. 3.16. Tracking performance of the proposed adaptive retrodition particle PHD filter as compared with the baseline methods.

3.5.6 IVA Based Source Separation with the Multivariate Model

The work of Waqas Rafique has been on source separation based on independent vector analysis (IVA) algorithms. IVA provides a different way for addressing the permutation problem by using a dependent multivariate source prior instead of independent univariate source prior as in the case of the ICA algorithm (Kim et al., 2007). Using a dependent multivariate source prior, the dependency between different frequency bins of each source can be retained, whilst independence between each source vector can be maximised. Therefore, selecting an appropriate multivariate source prior is crucial for the separation performance of the IVA algorithm. Two methods have been developed recently, as explained below.

1) Multivariate Mixed Source Prior for IVA Algorithm

The separation performance of the IVA algorithm depends on the nonlinear score function which is used to preserve the inter-frequency dependency. We have introduced a new mixed source prior to be used in both the IVA and the fast fixed point IVA (FastIVA) algorithm. Recently a mixture of multivariate Student's t and the super Gaussian distribution is adopted

as a source prior for the IVA and the Fast version of the IVA (FastIVA) algorithm. The multivariate Student's t distribution has heavier tails which can be useful in modelling high amplitude components in speech signals, such as in voiced signals (Rafique et al., 2015). At the same time, the dependent super Gaussian distribution can be used to model the rest of the signals. The performance of the proposed multivariate mixed source prior was tested in real room environments with reverberation time of 565ms. This work is published in IET Intelligent Signal Processing conference, London, UK 2015 (Rafique et al., 2015) and in IEEE Sensor Array and Multichannel Signal Processing Workshop, Rio de Janeiro, Brazil, 2016 (Rafique et al., 2016).

In order to further enhance separation performance of the mixed multivariate source prior, the ratio of the Student's t distribution and the super Gaussian source prior were adjusted automatically according to the energy of the speech signals. Importantly, the method is found to be successful only with access to the mixtures not the original sources. Again, the separation performance of the IVA algorithm is evaluated in different realistic scenario with very high reverberation time and results are shown in Figure 3.17. This work is published in EUSIPCO 2016 (Rafique et al., 2016).

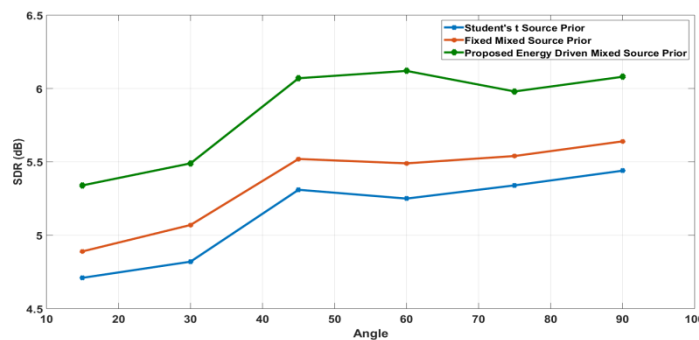


Fig. 3.17. The graph provides performance of the fixed mixed and energy driven mixed source prior at six different angles using BRIRs. Results were averaged over twelve mixtures at each angle.

2) Expectation Maximisation Framework for IVA Algorithm

Previously, identical source priors were used. However, different speech sources will generally have different statistical properties. The properties of natural speech vary from person-to-person and depend on which language being spoken as the pronunciation rates and phonemes can be totally different in different parts of the world. The recorded speech is dependent on variations in room acoustics and microphone characteristics e.g. different rooms will have different reverberation effects and different microphones will have variable frequency responses. All of these factors can change the observed human speech signal and therefore different speech signals generally have different statistical properties. It is important that the BSS algorithms can adapt their statistical structure according to the characteristics of the observed speech signals.

A novel IVA algorithm was proposed by using the Student's t mixture model (SMM) which is adopted as a source prior for the IVA algorithm, instead of the conventional identical multivariate distributions. The Student's t mixture model as a source prior can adapt to statistical properties of different speech mixtures. The unknown parameters of the source prior and unmixing matrices are estimated by deriving an efficient expectation maximization

(EM) algorithm. Improvement in the separation performance in realistic scenarios is confirmed by simulation studies on real datasets. A journal article is in preparation for this study.

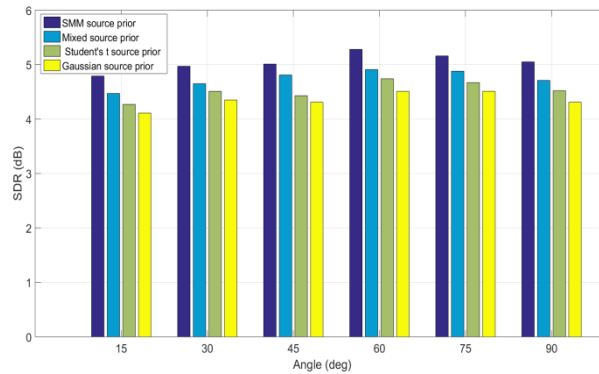


Fig. 3.18. Comparison between different source priors for the IVA algorithm for BRIRs (RT60 = 565ms). The separation performance at each angle is averaged over eighteen different speech mixtures. The IVA algorithm with proposed mixture model Student's t source prior performs better at all the separation angles in comparison to the use of identical source prior for all the sources.

3.6 Future Plans

- We will continue to improve the computational efficiency of the MS-SBR2 algorithms. We will also provide more theoretical studies to the behaviour of the SBR2 and MS-SBR2 algorithms. We will perform comprehensive evaluations for the MS-SBR2 algorithm. Different types of dataset will be used to test the algorithm, such as large size random matrices, simulated MIMO data, and defence related data such as Portland 03 dataset.
- We are extending the spatial sparsity based DoA estimation method by incorporating ship pose/direction information into the optimisation. We are currently testing this new algorithm on both synthetic data as well as Portland 03 dataset. We plan to submit a journal paper in the next two months.
- We will link further the sparse array work with automated sensor selection and the scenario for dealing with sensor failures. More experiments will be performed to evaluate its behaviour in a variety of situations including the sidelobe, array gain, and SNR. A journal submission is planned in the next six months.
- We will extend the evaluation of the joint sparsity model based method using both simulated data with an acoustic model, and real data underwater acoustic data e.g. Portland 03 dataset. The evaluations include different noise levels, different frequency overlaps between frequency bands, stationary and moving sources, and multiple sources.
- We will include statistical constraints into the joint sparsity model to improve the performance of the algorithm to account for uncertainties in the noisy measurements from the array. Currently, we are performing experimental studies on this new algorithm.

- We intend to use the dictionary learning method to enhance the measurements of the particle PHD filter, including the method of hierarchical dictionary learning method to improve the tracking accuracy and reduce the computational complexity. Moreover, an online dictionary will be utilized to further improve the accuracy of the measurement model.
- We will extend the experimental study of the acoustic reflector based source separation for more real acoustic data in room environment. Exploring the potentials of this algorithm for underwater acoustic data such as the Portland 03 dataset will also be an interest.

3.7 Selected Activities and Engagements

Engagement with industry partners and Dstl:

- Atlas Elektronik has been acting as a partner for the work package L_WP3.
- A joint project (of seven months) under the MoD MarCE scheme between Atlas and Surrey has been conducted. The project is titled "Array processing exploiting sparsity for submarine hull mounted arrays". Simulations have been performed for studying the performance of an array in terms of array gain and SNR under sparse array configuration. We have completed a report and submitted to Atlas and also shared with Dstl.
- Interactions with Julian Deeks and Nick Goddard on the 1st Polynomial Matrix Decomposition Workshop in August 2016 about the potential exploitation and development of the sparse array work.

Engagement between partners:

- Joint work between Surrey University and Newcastle University has been conducted on sparse analysis model based dictionary learning and its use for signal recovery from noisy signals e.g. for image denoising and audio super-resolution, as well as for multiplicative noise removal, and on PHD filter for multi-source tracking.
- Some informal discussions have been taken between Surrey and Cardiff on polynomial dictionary learning method based on polynomial matrix decomposition techniques.

3.8 Outputs

During the past year, we have generated the following publications.

Published/accepted:

- Z. Wang, J. G. McWhirter, J. Corr, and S. Weiss (2016), "Order-Controlled Multiple Shift SBR2 Algorithm for Para-Hermitian Polynomial Matrices," in Proc. 9th IEEE Sensor Array and Multichannel Signal Processing Workshop, Rio de Janeiro, Brazil, 2016.
- J. G. McWhirter and Z. Wang (2016), "A Novel Insight to the SBR2 Algorithm for Diagonalising Para-Hermitian Matrices," in Proc. 11th IMA International Conference on Mathematics in Signal Processing, Birmingham, England, 2016.

- Z. Wang, A. Sandmann, J. G. McWhirter, and A. Ahrens (2016), "Multiple Shift SBR2 Algorithm for Calculating the SVD of Broadband Optical MIMO Systems," in Proc. 39th Int. Conf. on Telecommunications and Signal Processing, Vienna, Austria, 2016.
- M. Chen, M. Barnard, and W. Wang. (2016). "Joint Array and Spatial Sparsity Based Optimisation for DoA Estimation." in Proc. IEEE Sensor Signal Processing for Defence (SSPD), pp. 1-5, 2016.
- L. Remaggi, P. J. B. Jackson, P. Coleman and W. Wang (2017), "Acoustic reflector localization: novel image source reversion and direct localization methods", IEEE/ACM Transactions on Audio, Speech and Language Processing, vol. 25, no. 2, 2017.
- P. Feng, W. Wang, S. Dlay, S. M. Naqvi and J. A. Chambers (2017), "Social force model based MCMC-OCSVM particle PHD filter for multiple human tracking," IEEE Transactions on Multimedia, December, 2017.
- P. Feng, W. Wang, S. M. Naqvi and J. A. Chambers (2016), "Adaptive particle PHD smoother for multiple human tracking," IEEE Signal Processing Letters, vol. 23, no. 11, 2016.
- Z. Fu, P. Feng, S. M. Naqvi and J. A. Chambers (2016), "Robust particle PHD filter with sparse representation for multi-target tracking," in Proc. IEEE International Conference on Digital Signal Processing (DSP), 2016.
- Z. Fu, P. Feng, S. M. Naqvi and J. A. Chambers (2017), "Particle PHD filter with hierarchical dictionary learning for multi-target tracking," in Proc. IEEE International Conference of Acoustics, Speech and Signal Processing (ICASSP), 2017.
- W. Rafique, S. Erateb, S. M. Naqvi, S. S. Dlay and J. A. Chambers (2016), "Independent vector analysis for source separation using an energy driven mixed student's T and super Gaussian source prior," 2016 24th European Signal Processing Conference (EUSIPCO), Budapest, pp. 858-862, 2016.
- W. Rafique, S. M. Naqvi and J. A. Chambers (2016), "Mixed source prior for the fast independent vector analysis algorithm," in Proc. IEEE Sensor Array and Multichannel Signal Processing Workshop (SAM), Rio de Janeiro, pp. 1-5, 2016.

Submitted/under review/under preparation:

- Z. Wang, A. Sandmann, J. G. McWhirter and A. Ahrens (2017), "Multiple Shift SBR2Algorithm for Calculating the SVD of Broadband Optical MIMO Systems," International Journal of Advances in Telecommunications, Electrotechnics, Signals and Systems, 2017. (under review)

3.9 References:

- J. G. McWhirter, P. D. Baxter, T. Cooper, S. Redif, and J. Foster (2007), "An EVD algorithm for para-Hermitian polynomial matrices," IEEE Trans. Signal Process., vol. 55, no. 5, pp. 2158–2169, 2007.
- S. Redif, S. Weiss, and J. G. McWhirter (2015), "Sequential matrix diagonalization algorithms for polynomial EVD of parahermitian matrices," IEEE Trans. Signal Process., vol. 63, no. 1, pp. 81–89, 2015.

- J. Benesty, J. Chen, and Y. Huang. (2008). *Microphone Array Signal Processing*. Springer Science & Business Media, 2008, vol. 1.
- M. R. Bai, J.-G. Ih, and J. Benesty. (2013). *Acoustic Array Systems: Theory, Implementation, and Application*. John Wiley & Sons, 2013.
- P. Handel, P. Stoica, and T. Soderstrom. (1993). "Capon method for doa estimation: accuracy and robustness aspects." in *Proceedings of The IEEE Winter Workshop on Nonlinear Digital Signal Processing*. IEEE, 1993, pp. P - 7.
- P. Totarong, and A. El-Jaroudi. (1992). "A novel approach for robust high-resolution doa estimation." in *Proceedings of The IEEE Sixth SP Workshop on Statistical Signal and Array Processing*. IEEE, 1992, pp. 366 - 369.
- A. Hakam, R. M. Shubair, and E. Salahat. (2013). "Enhanced DOA estimation algorithms using MVDR and MUSIC." in *2013 International Conference on Current Trends in Information Technology (CTIT)*. IEEE, 2013, pp. 172 - 176.
- P. Knee. (2012). "Sparse representations for radar with matlab® examples." *Synthesis Lectures on Algorithms and Software in Engineering*, vol. 4, no. 1, pp. 1 - 85, 2012.
- D. L. David. (2006). "Compressed sensing." *IEEE Transactions on Information Theory*, vol. 52, no. 4, pp. 1289 - 1306, 2006.
- D. Malioutov, M. Çetin, and A. S. Willsky. (2005). "A sparse signal reconstruction perspective for source localization with sensor arrays." *IEEE Transactions on Signal Processing*, vol. 53, no. 8, pp. 3010 - 3022, 2005.
- A. K. Nandi (1994). "Higher order statistics for digital signal processing." in *IEE Colloquium on Mathematical Aspects of Digital Signal Processing*, pp. 6-1, 1994.
- S. M. Kay. (1993). *Fundamentals of statistical signal processing, volume I: estimation theory* , 1993.
- P. A. Naylor, A. Kounoudes, J. Gudnason and M. Brookes (2007), "Estimation of Glottal Closure Instants in Voiced Speech Using the DYPSA Algorithm", *IEEE Transactions on Audio, Speech and Language Processing*, vol. 15, no. 1, 2007.
- M. Kuster (2008), "Reliability of estimating the room volume from a single room impulse response", *Journal of Acoustical Society of America*, vol. 124, no. 2, 2008.
- M. I. Mandel, R. J. Weiss and D. P. W. Ellis (2010), "Model-based expectation-maximization source separation and localization", *IEEE Transactions on Audio, Speech and Language Processing*, vol. 17, no. 8, 2010.
- W. Rafique, S.M. Naqvi, P.J.B. Jackson and J.A Chambers (2015), "Independent vector analysis with multivariate Student's t distribution source prior for speech separation in real room environments," in *Proc. IEEE ICASSP, Brisbane, Australia*, pp. 474-478, 2015.
- T. Kim, H. Attias, S. Lee, and T. Lee (2007), "Blind source separation exploiting higher-order frequency dependencies," *IEEE Transactions on Audio, Speech and Language Processing*, vol. 15, pp. 70-79, 2007.
- W. Rafique, S. M. Naqvi and J. A. Chambers (2015), "Speech source separation using the IVA algorithm with multivariate mixed super Gaussian Student's t source prior in real room environment," in *Proc. 2nd IET International Conference on Intelligent Signal Processing, London*, pp. 1-5, 2015.

L_WP4: MIMO and Distributed Sensing

End of Year Report April 2016– Mar 2017.

Staffing

Work Package Leaders: Prof John J. Soraghan (ST) and Prof Ian K. Proudler (LU).

Other Academics Involved: Dr Stephan Weiss (ST), Prof Sangarapillai Lambotharan (LU), Dr Carmine Clemente (ST).

Research Associates: Mr Christos Ilioudis (PDRA6a-ST), Mr Domenico Gaglione (PDRA6b-ST).

UDRC Research students:

Affiliated Research Students: Mr Jianlin Cao (ST), Mr Yixin Chen (ST), Mr Adriano Rosario Persico (ST), Mr Alessio Izzo (ST).

Lead Project Partner: Leonardo, Edinburgh.

Dstl contact: Stephen Moore (Sensors & Countermeasures Dept.), Brian Barber (Sensors & Countermeasures Dept.).

Aims and the lists of the original L_WP4 in the case for support:

To develop novel paradigms for Distributed MIMO Radar Systems (DMRS). Links to L_WP1 & L_WP2 through anomalies; L_WP3 through exploiting sparsity and L_WP5 for decentralised processing. Advanced signal processing methods for active/passive DMRS will be investigated. The approaches aim to improve performance, reduce system requirements with the result of producing a set of algorithms suitable for robust applications in a cluttered networked battlespace (T1, T3, T5, T8).

Progress made in the fourth year in addressing the original objectives

Staffing

Dr Carmine Clemente was promoted as Lecturer in April 2016.

Mr Christos Ilioudis and Mr Domenico Gaglione are near to completing their PhDs and were appointed as Research Assistants for WP4 since June 2016.

Mr William Coventry started his PhD in October 2016. His studentship is co-sponsored by the Electronic Support Measures of Leonardo. The student will be working on Fine-Time Resolution of Passive RF imaging.

Mr Ilias Theodorou started his PhD in December 2016. The student will be working on Space Debris detection based on passive CubeSAT radar systems.

L_WP4.1 progress

The work developed at ST on WP4.1 focuses on the development of novel signal processing techniques, paradigms and systems for high performance distributed sensing. The work includes the development of new cognitive radars that are able to fuse together intelligently different radar technologies and information sources in a distributed sensing framework. To this end, the work has concentrated in the following sub-areas during the fourth year.

- D. Gaglione is currently working on the extension of POMP based algorithm for helicopter

classification in the multi-target/multi-sensor scenario. Moreover, the Student Research Highlight paper was published; **L_WP4.1-3**

- Journal paper accepted regarding the use of Krawtchouk moments for target classification on SAR images.
- Hardware implementation of the Krawtchouk based approach for classification of human gait from micro-Doppler signatures. This work also generated a paper entitled “Efficient Micro-Doppler based pedestrian activity classification for ADAS systems using Krawtchouk moments” presented in the 11th IMA conference; **L_WP4.1-4**
- Investigation of classification of unmanned aerial vehicles (UAVs) using global navigation satellite system (GNSS) passive radars, and two proposal submissions one for CDE and one for the ESNC; **L_WP4.1-5**

L_WP4.2

The work developed at ST on L_WP4.2 focuses on the development of novel signal processing techniques and algorithms for distributed systems. To this end, we have concentrated in the following sub-areas in the fourth year.

- Journal paper accepted on modelling, algorithms and evaluation of micro-Doppler based recognition of ballistic targets; **L_WP4.2-1**
- The review of the Journal paper on CFAR Detection in Foliage Penetrating SAR images was completed; **L_WP4.2-2**
- Journal paper accepted on Oil Spill detection using Multi-family GLRT from SAR images; **L_WP4.2-2**
- Journal paper accepted on Covariance Matrices Symmetries based Polarimetric SAR image Classification;
- A paper on Co-Radar experimental validation was accepted and was presented at SSPD 2016. Additionally, a Journal paper on the proposed system is nearly completed. The proposed system was presented at the CDE marketplace (26th April); while two proposals, to Huawei and NXP for the application of the technique in vehicular communication were also submitted with the latter being accepted; **L_WP4.2-5**

Technical Highlight

Ambiguity Function for MIMO Radar Systems

Design and performance analysis of MIMO radar systems is a subject of high interest and relation to L_WP4. The most commonly used tool performance evaluation tool in radar systems is the *ambiguity function* (AF). Although the AF for monostatic radar systems is well defined by the so called *Woodward* AF, various definitions regarding the MIMO AF have been proposed in the literature.

Recently, a new AF definition based on the Kullback Leibler divergence and applied to a narrowband distributed MIMO signal model was proposed in [1]. Theoretical analysis showed that the proposed AF, similarly to the traditional definition, is maximally stretched between 0 and 1 while also being flexible for various system assumptions. Moreover, the performance of the proposed AF compared to the commonly applied approach of summing

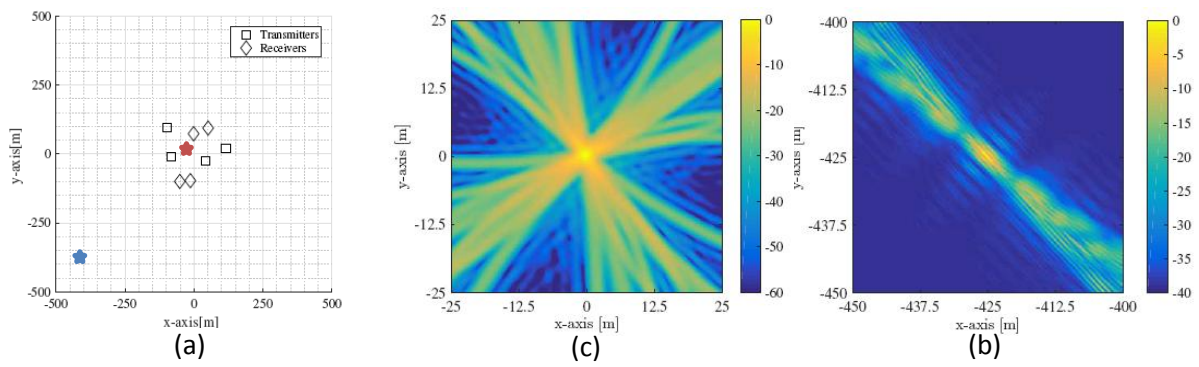
the matched filter outputs of all transmitter receiver pairs was examined. The simulation results demonstrated that the proposed method performs significantly better for varying energy parameter and offers lower floor levels when a constant energy parameter is assumed [1].

An extension of the MIMO AF in [1] was also held in [2] offering a more generalised definition. Here the proposed MIMO AF covers a broader signal model accounting for arbitrary system geometry configurations. Moreover, theoretical analysis showed that the KLD and therefore the proposed MIMO AF can be factorised into signal and channel correlation matrices. The derived expression of the KLD between the probability measures of the received signal indexed by real spatial/velocity position of the target θ_0 and an estimated one θ is as follows:

$$\begin{aligned}
I(\theta_0: \theta) = & \frac{1}{2} \left(-\text{tr} \left[\mathbf{\Psi}(\theta_0, \theta)^\dagger \frac{\mathbf{C}(\theta_0)}{\sigma_n^2} \mathbf{\Psi}(\theta_0, \theta) \frac{\mathbf{C}(\theta)}{\sigma_n^2} \left[\mathbf{\Phi}(\theta) \frac{\mathbf{C}(\theta)}{\sigma_n^2} + \mathbf{I}_{MN_R} \right]^{-1} \right] \right. \\
& + \text{tr} \left[\mathbf{\Phi}(\theta_0) \frac{\mathbf{C}(\theta_0)}{\sigma_n^2} \right] - \text{tr} \left[\mathbf{\Phi}(\theta) \frac{\mathbf{C}(\theta)}{\sigma_n^2} \left[\mathbf{\Phi}(\theta) \frac{\mathbf{C}(\theta)}{\sigma_n^2} + \mathbf{I}_{MN_R} \right]^{-1} \right] \\
& \left. - \ln \left| \mathbf{\Phi}(\theta) \frac{\mathbf{C}(\theta)}{\sigma_n^2} + \mathbf{I}_{MN_R} \right| + \ln \left| \mathbf{\Phi}(\theta_0) \frac{\mathbf{C}(\theta_0)}{\sigma_n^2} + \mathbf{I}_{MN_R} \right| \right)
\end{aligned}$$

where $\mathbf{\Psi}(\theta_0, \theta)^\dagger$ is the correlation between the real and expected received signal from each transmitter, and $\mathbf{\Phi}(\theta)$ and $\mathbf{C}(\theta)$ are the expected signal and channel correlation matrices assuming a target at θ . This formulation allows for higher flexibility and potentially more simplified optimisation process. The behaviour of the proposed AF was investigated in a 4×4 MIMO radar system using orthogonal waveforms. The geometry of the system for the examined scenario is illustrated in Figure 1a. The behaviour of the proposed AF for two different target placements: $[0,0]$ (see red star in Figure 1a) and $[-425, -425]$ (see blue star Figure 1a) is illustrated in Figure 1b and Figure 1c respectively. As it can be seen in Figure 1a, assuming the target at $[0,0]$ corresponds to a distributed system approximation as the target is “viewed” by the sensors from different directions. The main characteristic of this configuration is that the different transmitter-target-receiver channels will be uncorrelated [2] and therefore the AF can be described by the constructive summation of 16 ellipsoid ridges associated with each transmitter receiver pair (see Figure 1b). On the other hand, when the target is placed at $[-425, -425]$ the system can be considered as collocated as the target is “viewed” from a narrower span of directions (see Figure 1a). This geometry results in correlated transmitter-target-receiver channels [2] meaning that the ellipsoid ridges can be added constructively or destructively depending on their phase and channel correlation (see Figure 1c). A further investigation on the proposed definition is currently being performed to involve non-orthogonal and non-narrowband signal models. The research outcomes are planned to generate a journal paper.

Figure 1 Illustration of (a) geometry of system and MIMO AF behaviour assuming a target at (b) [0,0] and (c) [-425,-425] Cartesian [x,y] coordinates



Fractional Fourier Based Waveform for a Joint Radar-Communication System – Comparison Analysis with OFDM and Experimental Validation

The activity regarding the joint radar-communication (CoRadar) system based on the Fractional Fourier Transform (FrFT) [3] has been further investigated, through an extensive comparison analysis with OFDM and with the validation of the concept by means of a prototype of the system [4].

Compared to an OFDM waveform, the FrFT waveform presents lower range and Doppler sidelobes, as shown in Figure 2(a)-(b), and this is reflected in their performance in terms of Probability of Detection (P_D) and Probability of False Alarm (P_{FA}) when used with common detectors, as shown in Figure 2(c). Indeed, the FrFT shows performance very close to a Linear Frequency Modulated (LFM) pulse, while for the OFDM waveform, once the P_D is fixed to a certain desired level, the P_{FA} results are higher compared to FrFT and LFM waveforms.

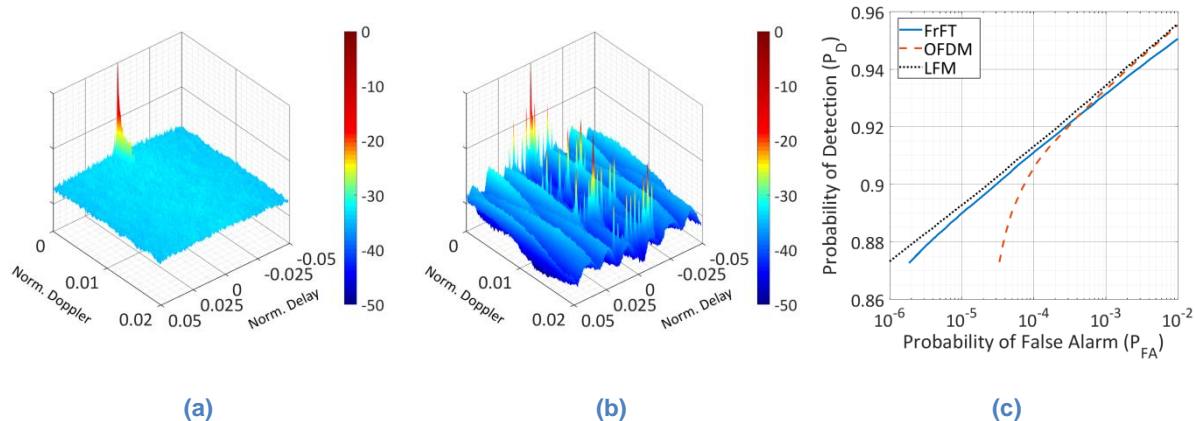


Figure 2. (a) and (b) Ambiguity Functions (AFs) of the FrFT and OFDM waveforms, respectively. (c) Receiver Operating Characteristic (ROC) of a square law detector when FrFT, OFDM and LFM waveforms are used and $SNR = 20$ dB.

Comparison is also made in terms of communication performance as shown in Figure 3, from which it is observable that the Bit Error Ratio (BER) presents the same trend on varying the energy per bit to noise power spectral density (γ_b) for both FrFT and OFDM, and for all the channel models considered.

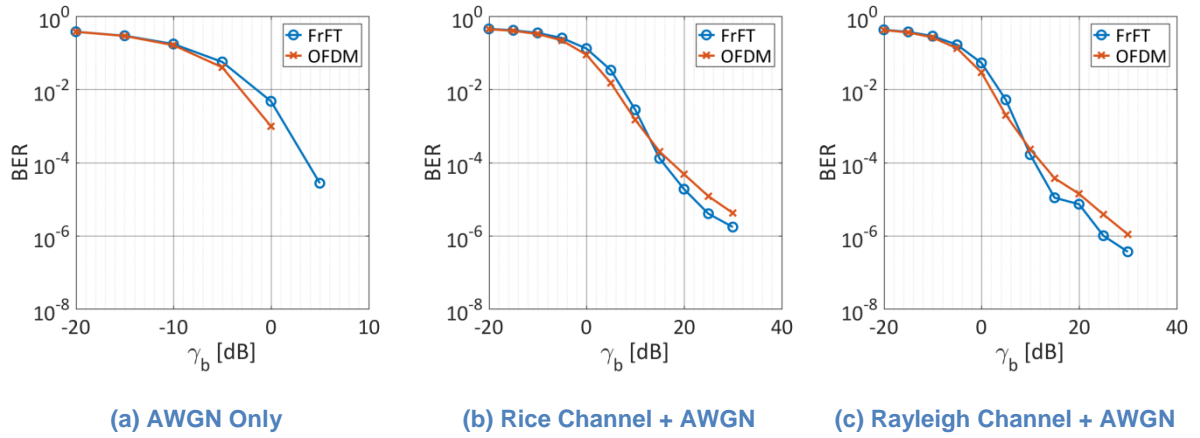


Figure 3. Communication performance. Comparison between FrFT waveform and OFDM on varying the energy per bit to noise power spectral density, for (a) AWGN noise only, (b) Rayleigh channel plus AWGN and (c) Rice channel plus AWGN.

The prototype of the proposed FrFT CoRadar system consists of a mono-static radar that generates the FrFT waveforms, sends the pulses and performs basic radar tasks, and a separate communication receiver that demodulates the pulses. The entire system is implemented by means of an SDR device, namely the NI-USRP 2943r. Figure 4(a) shows the communication performance of the FrFT CoRadar in different configurations evaluated on real data (solid lines), and compared to simulated data (dashed lines) assuming an indoor Rice channel, while Figure 4(b) shows a spectrogram when FrFT CoRadar pulses with 8 sub-carriers are used. The Doppler and micro-Doppler signature of the person walking towards and away from the radar is clearly visible.

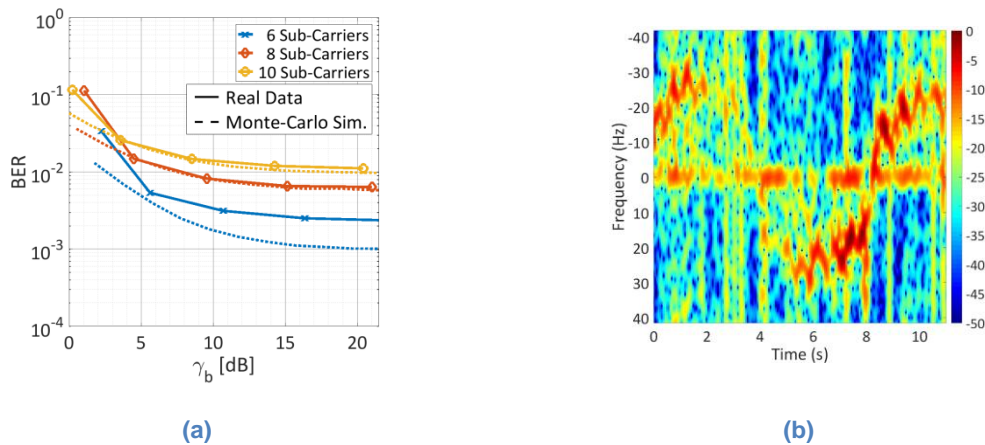


Figure 4. (a) Communication performance on real data, on varying γ_b and for different number of sub-carriers. (b) Spectrogram obtained from FrFT CoRadar pulses with 8 sub-carriers: person walking towards the radar approximately between 4-8 seconds, and away from it between 0-4 seconds and 8-11 seconds.

Model-Based Multi-Sensor Multi-Target Identification of Helicopters

The Micro-Doppler (mD) effect identifies the time-varying characteristic of the Doppler frequency shift due to secondary motions, also called micro-motions, that a target may exhibit. The mD may be due to swinging arms and legs of a human being while walking or

running, or due to moving legs or flapping wings of animals. The source of micro-motions can also be a rotating propeller of a fixed-wing aircraft, or rotating rotor blades of a helicopter. All these micro-motions are peculiar to each target, and generate different mD signatures that may be used for classification purposes.

The capability to identify the model of a helicopter by analysing its mD signature was first investigated in [5], after that in [6] it was demonstrated that the theoretical return signal from propeller blades depends on the number, K , the length, ρ , and the rotation speed ω , of the blades themselves. Moreover, since the Radar Cross Section (RCS) from the tail blades is smaller than the RCS from the main rotor blades [7], the majority of the methods only relies on the mD information extracted from the main rotor blades.

In this task, the previously proposed automatic mD model-based algorithm for helicopters identification [8] was refined and extended to:

1. operate in a multi-sensor scenario and
2. to be able to classify multiple targets present in the radar cell of interest.

The algorithm relies on a parametric sparse representation of the model of the signal scattered from a helicopter's rotor hub; the recovery of the sparse signal from the received one through the resolution of an optimisation problem, allows the estimation of K , ρ and ω , and then the classification of the target. However, the estimate of the length of the blades is strongly biased by the aspect angle with which the target is seen, making it unreliable in the final classification stage. The employment of multiple distributed sensors that observe the target from different points of view, leads to a more accurate and reliable estimate for ρ , which can then be exploited as a discriminative feature. The enhanced capability of identifying multiple targets, as well as recognising the number of targets, is achieved by estimating the mD parameters from a set of chunks of data extracted from the received signal, rather than just one. The no. of chunks is initialised to a maximum value, & then iteratively reduced until the no. of targets is estimated.

The algorithms were tested with both simulated and real data. Concerning the synthetic one, signals scattered from 10 helicopter models in different configurations were generated, and processed in a Monte-Carlo framework to assess the performance of the algorithm. Figure 5 shows the performance for the single-target algorithm in terms of identification accuracy and unknowns on varying the SNR.

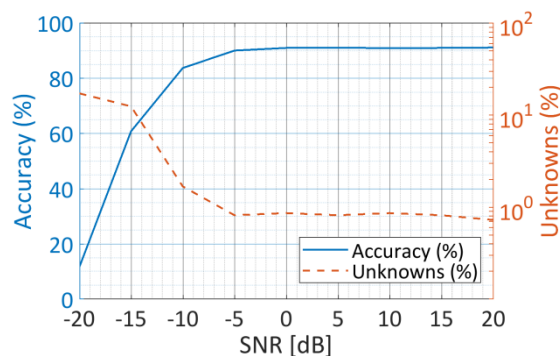


Figure 5. Performance for the single-target algorithm in terms of identification accuracy and unknowns.

The accuracy reaches 83.91 % for $SNR = -10$ dB, and it is above 90 % for SNR greater than -5 dB, while the percentage of unknowns is below 1 %.

Figure 6 shows the results obtained with the multi-target algorithm when one target is assumed to be in the region of interest. The detection rate, namely the ratio of the Monte-Carlo tests in which the number of helicopters has been correctly estimated to the total number of tests, is close to 1.00 across all the values of SNR, while the maximum accuracy is about 90 % in agreement with the performance achieved with the single-target algorithm.

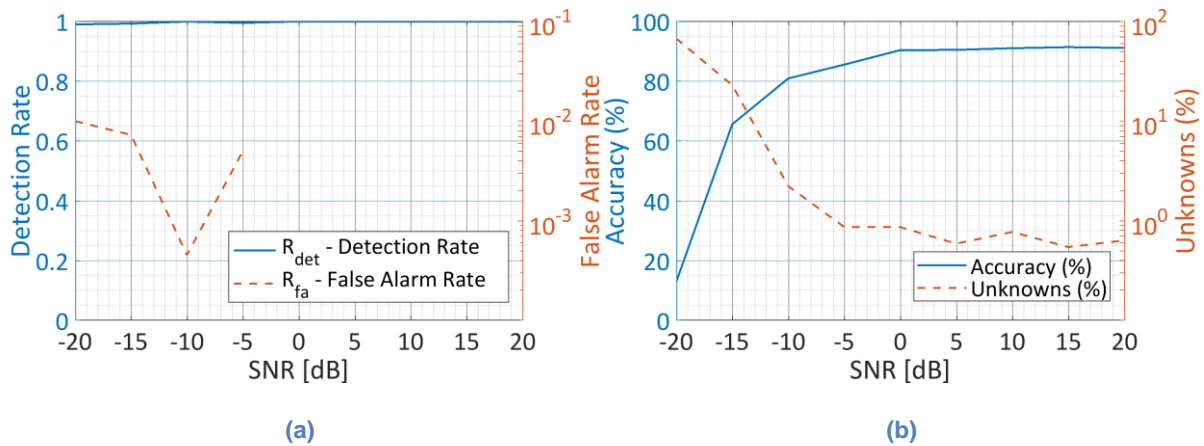


Figure 6. Performance for the multi-target algorithm tested in the presence of one target in the scene, in terms of (a) detection and false alarm rate, (b) identification accuracy and unknowns, on varying the SNR.

Tests are also performed assuming that two and three targets are present in the region of interest. Figure 7 shows the results in the first case: the rate of detection is above 0.80 for values of the SNR greater than 0 dB, while the false alarm, that is the ratio of the number of Monte-Carlo tests in which the number of helicopters has been overestimated to the total number of tests, is always below 0.01. Moreover, the accuracy in correctly identifying both the helicopters or at least one of them is 77 % and 98 %, respectively, for SNR above 10 dB.

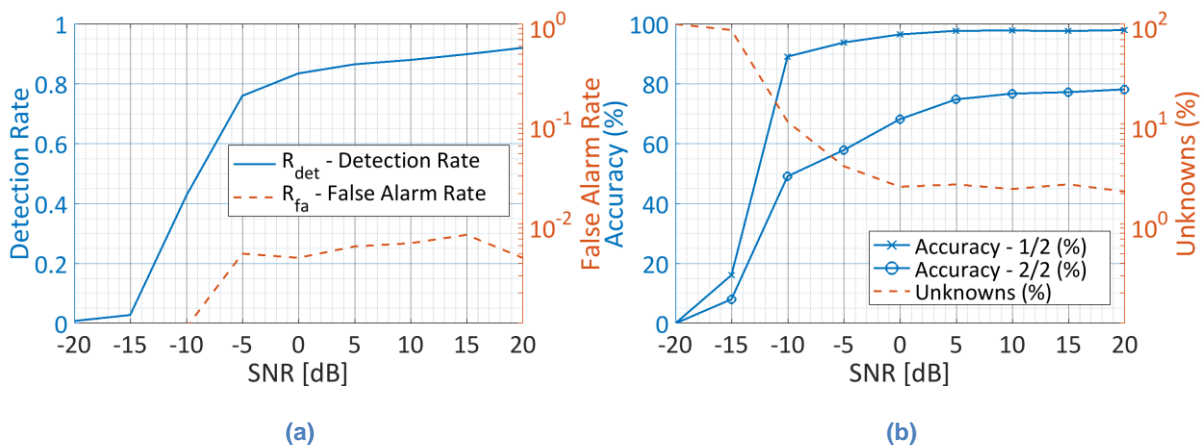


Figure 7. Performance for the multi-target algorithm tested in the presence of two targets in the scene, in terms of (a) detection and false alarm rate, (b) identification accuracy and unknowns, on varying the SNR.

The performance of the multi-target algorithm when three targets are in the region of interest is shown in Figure 8. The maximum detection rate is 0.74, while the false alarm rate is below 0.004. In 99 % of the cases and for SNR greater than 5 dB, at least one target is correctly identified. This percentage reduces to 90 % and 58 % when correctly identifying at least two, or all the three targets, respectively.

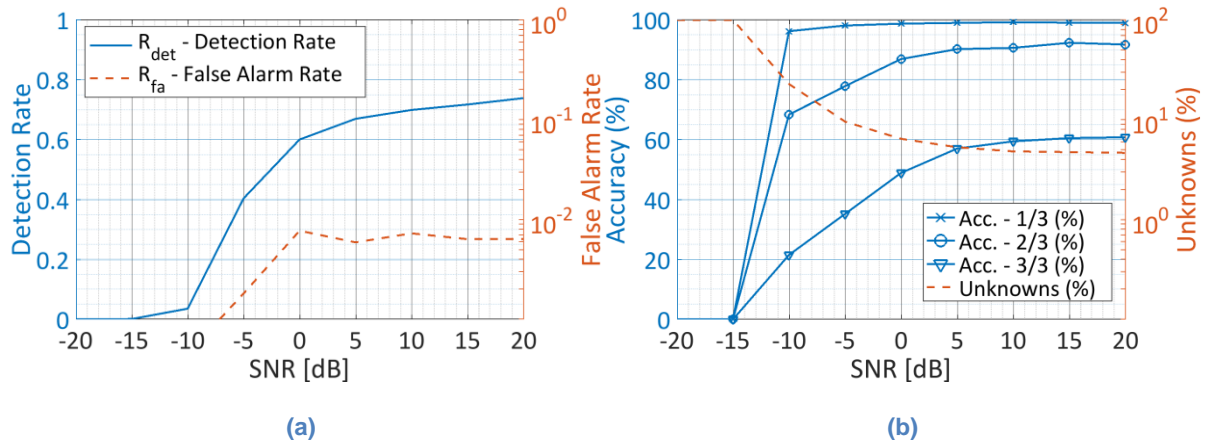


Figure 8. Performance for the multi-target algorithm tested on the presence of three targets in the scene, in terms of (a) detection and false alarm rate, (b) identification accuracy and unknowns, on varying the SNR.

Concerning the assessment on real data, a set of signals acquired with a 24 GHz CW radar and scattered from a two-bladed helicopter scale model GAUI X3 was used. Signals were acquired with four different aspect angles and with three different rotation speeds of the blades, in order to simulate as many targets H_1 , H_2 and H_3 . Both the single-target and the multi-target algorithms were tested, even if the latter was only evaluated in presence of single helicopters to assess the accuracy in estimating the number of targets. The results for the single-target algorithm are summarised in Table 1. The overall accuracy is above 95 % and the worst performance is obtained with signals acquired with aspect angle of 0° . This is probably due to the small RCS of the blades in this geometry.

Table 1. Real data performance evaluation. Single-target algorithm, accuracy (%).

Target	Aspect Angle			
	0°	15°	30°	45°
H_1	85.6	100	96.7	100
H_2	98.9	100	100	100
H_3	67.8	100	97.8	97.8

Table 2 and Table 3 show the results for the multi target algorithm, in terms of detection rate and percentage of accuracy, respectively. The detection rate is above 0.90 in all the analysed case, while the overall accuracy is of about 96.7 %.

Table 2. Real data performance evaluation. Multi-target algorithm, detection rate.

Target	Aspect Angle			
	0°	15°	30°	45°
H_1	0.94	0.89	0.89	0.89
H_2	0.82	0.85	0.86	0.97
H_3	0.92	0.94	0.90	1.00

Table 3. Real data performance evaluation. Multi-target algorithm, accuracy (%).

Target	Aspect Angle			
	0°	15°	30°	45°
H_1	83.8	100	98.4	100
H_2	98.3	100	100	100
H_3	81.8	100	97.8	98.6

Passive CubeSat

Space debris represents a real threat for new and existing space missions, because collisions with even very small objects (few cm size) at the orbital velocity (e.g. speeds of 10 km/s in LEO) can cause catastrophic impacts. Therefore, the new space missions have to be designed considering the presence of the orbital space debris avoiding the risk of collision. The challenge to detect and track space debris by radar is of fundamental importance to increase safety for online space mission.

A new system for space debris detection and monitoring is presented by using a bistatic passive radar deployed on a CubeSAT flying in low earth orbit. The two principal components composing the sensing platform are a Software Defined Radio (SDR) and a passive antenna. Moreover, a Low Noise Amplifier (LNA) can be used in order to increase the sensing capacities. Any satellite transmitting radio waves towards the Earth within the frequency band of the antenna on the sensing platform poses a suitable illuminator of opportunity (IO). The IOs can be statically or dynamically selected among the available platforms (e.g., Iridium, GNSS, HY2A).

The analysis of radar system capabilities is conducted by investigating the minimum detectable target size. The capability of a radar to detect a target generally depends on the received power from the target. In particular, the radar equation describes how the SNR depends on transmitter, receiver and target parameters and the system geometry. Considering the incoherent integration of N radar pulses and the signal processing gain G_{sp} given by the matched filtering, the SNR is as follows:

$$SNR = \frac{P_r}{P_n} = \frac{P_t G_t G_r \lambda^2 \sigma L_s}{(4\pi)^3 R_T^2 R_R^2 k T_0 B_r F} \sqrt{N} G_{sp} \quad (1)$$

where P_t is the transmitted power, R_T and R_R are the distances of transmitter and receiver from the target, G_t and G_r are the transmitter and receiver gains, λ is the transmitted signal

wavelength, σ is the Radar Cross Section (RCS) of the target, T_0 is the reference temperature, F the receiver noise figure, and $L_s (\leq 1)$ is a loss factor which includes no free-space propagation and temperature related losses.

From (1) it is noted that the SNR is proportional to the target's RCS. In cases of very small RCS, particular advantage in terms of SNR can be achieved by exploiting the forward-scattering radar (FSR) configuration. In principle, FSR is obtained from a bistatic radar configuration in which the bistatic angle close to 180° . The FSR guarantees relative RCS enhancement since in this case the RCS depends only on the area and the shape of a target's silhouette. In the Fraunhofer diffraction zone the forward-scattering RCS can be written as:

$$\sigma_{FS} = \frac{4\pi A^2}{\lambda^2} = G_{FS}A \quad (2)$$

where G_{FS} represents the peak antenna gain of uniformly illuminated aperture whose area is equal to A .

The proposed system configuration aims to employ the advantages in terms of RCS achieved by the FSR, considering the received power as the figure of merit for the detection. As it can be seen in (2), the maximal FS RCS is achieved when the target crosses the LOS. This event can hence be used as a figure of merit for the target detectability evaluation. However, even in the case in which the bistatic angle never reaches 180° , the detection via FSR can take place considering the sidelobes effect of the diffracted field.

By rearranging (1), the RCS (in dB) can be written as function of the system parameters and SNR as follows

$$\begin{aligned} \sigma_{dB} = SNR_{dB} - G_{t_{dB}} - G_{r_{dB}} - G_{sp_{dB}} - 20 \log_{10} \lambda - P_{t_{dBm}}^* - L_{s_{dB}} \\ - 5 \log_{10} N + 30 \log_{10} 4\pi + 20 \log_{10} R_T + 20 \log_{10} R_R \quad (3) \\ + 10 \log_{10}(kT_0B_r) + F_{dB} \end{aligned}$$

In this way it is possible to define the minimum RCS of a detectable target by fixing the SNR at the receiver. For the performance analysis, the target altitude is set equal to 800 km which is the orbit height with the highest concentration of space debris.

Due to the vast advance in hardware technology, nowadays it is possible to assemble a cubeSAT with a total weight smaller than 3 kg and a low power consumption for a relative low cost. Specifically, for the numerical simulations in this analysis it is considered a cubeSAT composed by an SDR and an LNA which guarantee a receiver gain of 69 dB with a noise figure of 12.5 dB . The SNR for fixed probability of detection (PD) and probability of false alarm (PFA) is set equal to 10 dB . The loss factor L_s is set equal to 1, translating to no system losses which is the optimum case. The proposed system in fact solves the problem of atmosphere absorption which represents one of the most relevant loss factor. The considered IO is the satellite from the Global Star constellation which is a low Earth orbit (LEO) satellite constellation orbiting at 14000 km from the Earth and is used for a satellite phone and low-speed data communications. In order to perform the radar task, the 16.5 MHz bandwidth downlink from the satellite to the user in the 2483.5 to 2500 MHz band is employed. Figure 9

shows that for integration time of 5 seconds it is possible to detect objects (circular or square plats) whose dimensions are smaller than 25 cm for all the examined values of cubeSAT's altitude. This analysis shows that the proposed system allows the detection of very small space debris when the suitable design is considered. One of the most important aspects of the proposed system is that the relative shorter distances between the transmitter-target system and space based receiver compared to that of a ground based receiver guarantees higher SNR for the radar tasks. Moreover, thanks to system geometry, the performance of the proposed system is not affected by atmospheric absorptions. For the same reason the system functionality is independent from weather conditions.

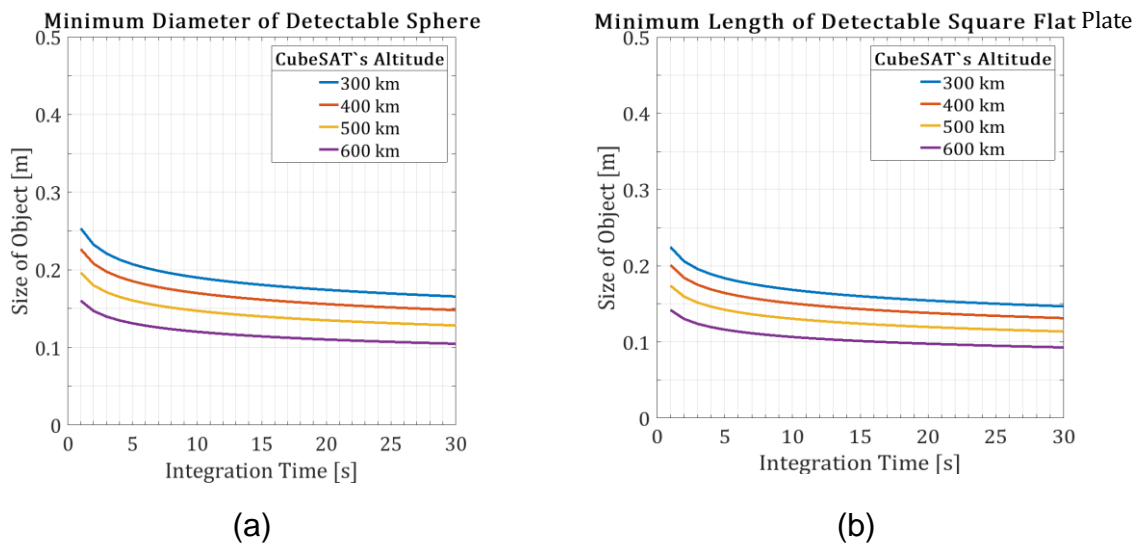


Figure 9: Minimum value for detectable (a) sphere (or circular plat) diameter and (b) square plat length by using Global Star payload as transmitter with carrier frequency 2.5 GHz.

GUAPO- GNSS based UAV monitoring system using Passive Observations

Professional large unmanned air vehicles (UAVs) are known to be used in several military and civilian applications nowadays, e.g. security, search and rescue, monitoring, disaster management. In addition, small UAVs have also recently attracted strong interest, especially among hobbyists and amateurs, due to their accessibility, potential and low cost. However, the lack of a clear regulation poses a real safety problem, as recently demonstrated by the crash between a small drone and a landing aircraft [9]. Moreover, small UAVs may end up being used in unconventional ways. For example drones could be deliberately used to interfere with common airport operations or their small size exploited to evade conventional radar systems [10] and border surveillance systems [11]. Even more alarming is the warning raised by world leaders about the use of drones to carry chemical weapons during a "dirty bomb" attack [12].

The Sensor Signal Processing & Security (SSP&S) Laboratories at the University of Strathclyde invented a Passive Bistatic Radar (PBR) system based on Global Navigation Satellite Systems (GNSS) for small UAVs' detection. The invention exploits the power drop

caused by UAVs when they cross the bistatic line of sight [13], between the GNSS transmitter and the receiver, for their detection and discrimination with other unwanted targets (i.e. birds). Use of multiple satellites and signal integration will help to deal with the typical small Radar Cross Section (RCS) of UAVs.

The forward scattering enhancement obtained facilitates improved detection capabilities, extending the minimum detectable range of the target thanks to the higher Signal to Noise Ratio (SNR) that is achieved. Figure 10 shows an example of power drop when an UAV crosses the LOS between transmitter and receiver. The profile of this drop is primary dependant to the silhouette of the target and therefore can be used as a feature to perform classification. In Figure 11 the Euclidian distance between the “shadowing” of three different UAVs in different acquisitions is illustrated. As it can be seen the received signals of the same type of UAV have a small distance to each other while received signals of different type of UAVs have much higher distance. These preliminary results demonstrate the high potential of the proposed system to achieve high detection and classification capabilities for small UAVs. Applications of this invention include but are not limited to, perimeter monitoring (for stadiums, sensitive buildings, prisons, etc.), base protection, restricted airfields monitoring, monitoring of UAVs’ dedicated flight paths (for delivery of goods).

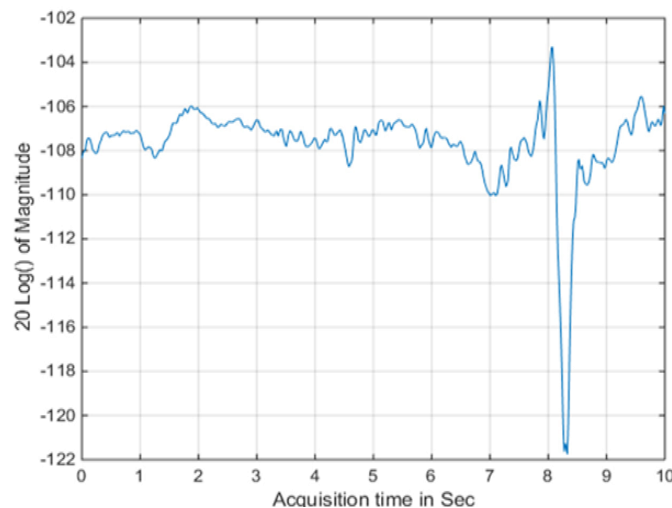


Figure 10. Example of power drop when an UAV crosses the LOS between transmitter and receiver

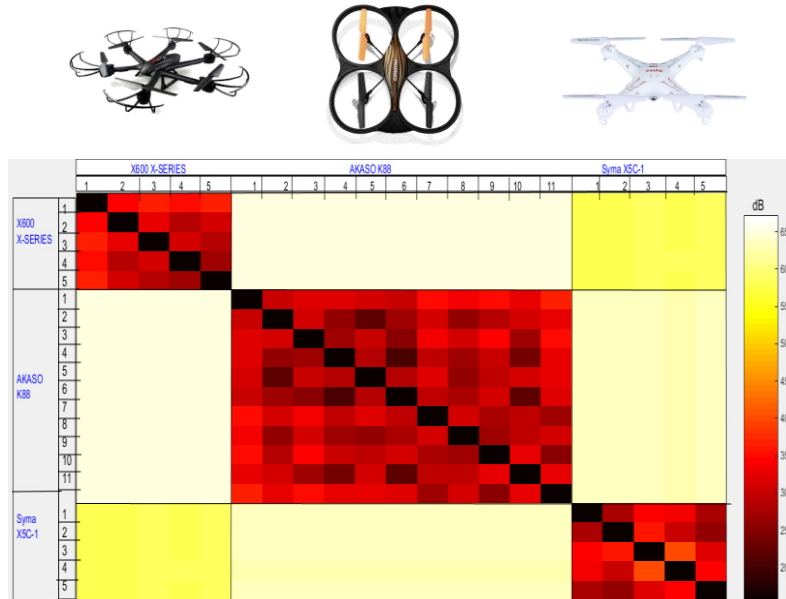


Figure 11 Euclidian distance between “shadowing” from different small UAV targets.

Other activities

- Granted the Regional (UK) and Overall European Winner award on European Satellite Navigation Competition (ESNC).
- Public dissemination of outcomes regarding advances on GNSS based UAV monitoring system through media (e.g. BBC Breakfast on Tuesday 29th November).
- Preparation of patent filing for GNSS based UAV monitoring system.
- Publication of a Case Study on the NI website entitled “Co-Radar: Combining Two Technologies to Increase Efficiency of Airborne, Space-Borne, and Ground-Based Platforms”;
- Guidance and Supervision of three MSc students on their final year projects associated with passive Radars;
- Knowledge exchange and expertise provision in the field of Micro-Doppler Signatures for Canon Research Centre France S.A.S.
- Attendance and presentation of three papers at the Sensor Signal Processing for Defence (SSPD) Conference 2016;
- Attendance and presentation of four papers for the Institute of Mathematics and its Application (IMA) conference.
- Attendance and presentation of a paper entitled “CubeSAT based passive bistatic radar for space debris detection and tracking” on the Stardust 2016 ESA-ESTEC.
- Attendance and presentation of group’s latest work in the UDRC LSSCN consortium CSG meeting.
- Attendance and presentation of “GUAPO: GNSS based UAV monitoring system for Air fields using Passive radar Observations” at the International Navigation Conference (INC) 2016.
- Attendance and presentation at the UDRC Themed Meeting on Space Surveillance and Tracking.

- Brian Barber from DSTL has visited the group and had individual discussions with members of the group regarding their current work and subjects of future interest.
- Meeting and knowledge exchange with George Matich and Steve Clark from Leonardo Finmeccanica.
- Knowledge exchange meeting with Dr Francesco Fioranelli from University of Strathclyde;
- Dr. Augusto Aubry from Università degli Studi di Napoli “Federico II” has visited the group and worked with it on a novel waveform design framework aiming at the mitigation of the clutter produced by wind turbines.

Plan for the fifth year

Communicating Radar in automotive applications

After successfully generating two conference and one journal paper, and a demonstrator showcased at the CDE marketplace, the concept of communicating radar will be further expanded in the 5th year. A PhD student starting in the month of March will investigate the adaptation and implementation of the proposed concept for automotive applications. The studentship is a part of the accepted NXP proposal.

Further investigation and field validation of GUAPO concept

Driven by the well-received introduction of the GUAPO concept through winning awards and public dissemination, further investigation of the proposed concept will be held in the 5th year. By successfully securing funds to support two full-time RA for 9 and 3 months using the impact acceleration support provided by the EPSRC, the system is scheduled to advance from its current TRL 2 state to a TRL 5 by the end of the 5th year. Potential funding from a Defence and Security Accelerator project can possibly further support the project.

Investigation of solution for Enhanced Space Situation Awareness

The research topic of Space Situation Awareness (SSA) will be expanded during year 5. Solutions able to provide enhanced capabilities for SSA will be investigated, including high range resolution profile and enhanced sensor systems. Extensive study on a Passive Bistatic Radar system on CubeSats for Space Debris monitoring will be held as a part of Mr Ilias Theodorou's PhD research. Moreover, feasibility study on Background modelling and constant false alarm rate (CFAR) Launch Detectors design will take place funded by MDC.

Investigation of novel signal processing techniques

Recently introduced signal processing techniques such as Partial Fast Fourier Transform, Random and Multi-Order Fractional Fourier transform, stochastic differential equations, and image moments appear to be very interesting and their potential in the network battlespace will be investigated.

References:

[1] C. V. Ilioudis, C. Clemente, I. Proudler, J. Soraghan, “Ambiguity Function for Distributed MIMO Radar Systems”, *IEEE International Radar Conference 2016*, Philadelphia, USA, 2-16 May 2016

[2] C. V. Ilioudis, C. Clemente, I. Proudler, and J. Soraghan, "Mimo radar ambiguity functions: A case study," *11th IMA International Conference on Mathematics in Signal Processing*, pages 1–5, Dec. 2016

- [3] D. Gaglione, C. Clemente, C. V. Ilioudis, A. R. Persico, I. K. Proudler and J. J. Soraghan, "Fractional Fourier based waveform for a joint radar-communication system," *2016 IEEE Radar Conference (RadarConf)*, Philadelphia, PA, 2016, pp. 1-6.
- [4] D. Gaglione, C. Clemente, A. R. Persico, C. V. Ilioudis, I. K. Proudler and J. J. Soraghan, "Fractional Fourier Transform Based Co-Radar Waveform: Experimental Validation," *2016 Sensor Signal Processing for Defence (SSPD)*, Edinburgh, 2016, pp. 1-5.
- [5] J. Misiurewicz, K. Kulpa and Z. Czekala, "Analysis of Recorded Helicopter Echo," *Radar 97 (Conf. Publ. No. 449)*, Edinburgh, 1997, pp. 449-453.
- [6] J. Martin and B. Mulgrew, "Analysis of the Theoretical Radar Return Signal from Aircraft Propeller Blades," *IEEE International Conference on Radar*, Arlington, VA, 1990, pp. 569-572.
- [7] P. Tait, "Introduction to Radar Target Recognition," ser. IEE Radar Series, Institution of Engineering and Technology, 2005.
- [8] D. Gaglione, C. Clemente, F. Coutts, Gang Li and J. J. Soraghan, "Model-Based Sparse Recovery Method for Automatic Classification of Helicopters," *2015 IEEE Radar Conference (RadarCon)*, Arlington, VA, 2015, pp. 1161-1165.
- [9] 'Drone' hits British Airways plane approaching Heathrow Airport, BBC News, retrieved from <http://www.bbc.co.uk/news/uk-36067591>.
- [10] White House Drone Crash Described as a U.S. Worker's Drunken Lark, The New York Times, retrieved from <http://www.nytimes.com/2015/01/28/us/white-house-drone.html>.
- [11] Drone carrying drugs crashes south of U.S. border, CNN, retrieved from <http://edition.cnn.com/2015/01/22/world/drug-drone-crashes-us-mexicoborder/>.
- [12] Isil plotting to use drones for nuclear attack on West, The Telegraph, retrieved from <http://www.telegraph.co.uk/news/2016/04/01/isil-plottingto-use-drones-for-nuclear-attack-on-west/>.
- [13] T. Martelli, F. Colone and P. Lombardo, "First experimental results for a WiFi-based passive forward scatter radar," *2016 IEEE Radar Conference (RadarConf)*, Philadelphia, PA, 2016, pp. 1-6.doi: 10.1109/RADAR.2016.7485108

Published Papers:

Journals

- 10-A. Izzo, M. Liguori, C. Clemente, C. Galdi, M. J. Di Bisceglie, J. and Soraghan, "Multi-Model CFAR Detection in Foliage Penetrating SAR Images", in *IEEE Transactions on Aerospace and Electronic Systems*, Jan 2017
- 9-C. Clemente; L. Pallotta; D. Gaglione; A. De Maio; J. J. Soraghan, "Automatic Target Recognition of Military Vehicles with Krawtchouk Moments," in *IEEE Transactions on Aerospace and Electronic Systems*, vol.PP, no.99, pp.1-1, 2017
- 8-A. R. Persico; C. Clemente; D. Gaglione; C. Ilioudis; J. Cao; L. Pallotta; A. De Maio; I. Proudler; J. J. Soraghan, "On Model, Algorithms and Experiment for Micro-Doppler based Recognition of Ballistic Targets," in *IEEE Transactions on Aerospace and Electronic Systems*, vol.PP, no.99, pp.1-1, 2017
- 7-V. Carotenuto, A. De Maio, C. Clemente, J. Soraghan, "Unstructured Versus Structured GLRT for Multi-Polarization SAR Change Detection", *IEEE Geoscience and Remote Sensing Letters*, vol.12, no.8, pp.1665,1669, Aug. 2015.
- 6-V. Carotenuto, A. De Maio, C. Clemente, J. Soraghan, G. Alfano, "Forcing Scale-

Invariance in Multi-Polarization SAR Change Detection”, IEEE Transactions on Geoscience and Remote Sensing, vol.54, no.1, pp.36-50, Jan. 2016.

5- C. Clemente, L. Pallotta, A. De Maio, J. Soraghan, A. Farina, “A Novel Algorithm for Radar Classification based on Doppler Characteristics Exploiting Orthogonal Pseudo-Zernike Polynomials”, IEEE Transactions on Aerospace and Electronic Systems, vol.51, no.1, pp.417,430, January 2015.

4- V. Carotenuto, A. De Maio, C. Clemente, J. Soraghan, “Invariant Rules for Multi-Polarization SAR Change Detection”, IEEE Transactions on Geoscience and Remote Sensing, vol.53, no.6, pp.3294,3311, June 2015

3- C. Clemente, L. Pallotta, A. De Maio, I. Proudler, J. Soraghan, A. Farina, “Pseudo-Zernike Based Multi-Pass Automatic Target Recognition From Multi-Channel SAR”, IET Radar Sonar and Navigation, vol.9, no.4, pp.457,466, 4 2015

2-C. Clemente, J. J. Soraghan, “GNSS Based Passive Bistatic Radar for micro-Doppler analysis of helicopter rotor blades”, IEEE Transactions on Aerospace and Electronic Systems, Vol. 50, issue 1, January 2014.

1-J. Zabalza, C. Clemente, G. Di Caterina, J. Ren, J. Soraghan, S. Marshall, “Robust Micro-Doppler Classification using SVM on Embedded Systems”, IEEE Transactions on Aerospace and Electronic Systems, vol.50, no.3, pp.2304,2310, July 2014

Conferences

37-P. Kirkland, C. Clemente, A. R. Persico, J. Soraghan, M. Vasile, "CubeSAT based passive bistatic radar for space debris detection and tracking," Final Stardust Conference, pages 1–3, Nov. 2016

36-A. Aßmann, A. Izzo, and C. Clemente, "Efficient Micro-Doppler based pedestrian activity classification for ADAS systems using Krawtchouk moments," 11th IMA International Conference on Mathematics in Signal Processing, pages 1–5, Dec. 2016

35-A. Izzo, L. Ausiello, C. Clemente, and J. Soraghan, "Partitioned Block Frequency Domain Prediction Error Method based Acoustic Feedback Cancellation for long feedback path," 11th IMA International Conference on Mathematics in Signal Processing, pages 1–5, Dec. 2016

34-A. R. Persico, C. V. Ilioudis, C. Clemente, S. Bruggenwirth, T. Bieker, and J. Soraghan, "Ballistic Targets Discrimination based on High Resolution Range Profiles," 11th IMA International Conference on Mathematics in Signal Processing, pages 1–5, Dec. 2016

33-C. V. Ilioudis, C. Clemente, I. Proudler, and J. Soraghan, "Mimo radar ambiguity functions: A case study," 11th IMA International Conference on Mathematics in Signal Processing, pages 1–5, Dec. 2016

32-M. B. Özcan, S. Z. Gürbüz, A. R. Persico, C. Clemente and J. Soraghan, "Performance analysis of co-located and distributed MIMO radar for micro-Doppler classification," 2016 European Radar Conference (EuRAD), London, 2016, pp. 85-88, Oct. 2016

31- L. Pallotta, C. Clemente, A. De Maio and D. Orlando, "A Multi-Family GLRT for Detection in Polarimetric SAR Images," 2016 Sensor Signal Processing for Defence (SSPD), Edinburgh, 2016, pp. 1-5, Sept 2016

30- Y. Chen, C. Clemente, J. Soraghan and S. Weiss, "Fractional Fourier Based Sparse Channel Estimation for Multicarrier Underwater Acoustic Communication System," 2016

Sensor Signal Processing for Defence (SSPD), Edinburgh, 2016, pp. 1-5, Sept 2016

29-D. Gaglione, C. Clemente, A. R. Persico, C. V. Ilioudis, I. K. Proudler and J. J. Soraghan, "Fractional Fourier Transform Based Co-Radar Waveform: Experimental Validation," 2016 Sensor Signal Processing for Defence (SSPD), Edinburgh, 2016, pp. 1-5, Sept 2016

28-A. R. Persico, C. Clemente, L. Pallotta, A. De Maio, J. Soraghan, "Micro-Doppler Classification of Ballistic Threats using Krawtchouk Moments", IEEE International Radar Conference 2016, Philadelphia, USA, 2-16 May 2016

27- D. Gaglione, C. Clemente, C. V. Ilioudis, A. R. Persico, I. K. Proudler, J. Soraghan, "Fractional Fourier Based Waveform for a Joint Radar-Communication System", - IEEE International Radar Conference 2016, Philadelphia, USA, 2-16 May 2016 - **Invited Paper - Special Session on Waveform Diversity in Modern Radar**

26- C. V. Ilioudis, C. Clemente, I. Proudler, J. Soraghan, "Ambiguity Function for Distributed MIMO Radar Systems", IEEE International Radar Conference 2016, Philadelphia, USA, 2-16 May 2016

25-M. Bugra Ozcan, A. R. Persico, C. Clemente, S. Zubeyde Gurbuz, J. Soraghan, "Performance Analysis of Co-Located and Distributed MIMO Radar for Micro-Doppler Classification", European Radar Conference 2016, EuRAD 2016 , London, United Kingdom, 5-7 October 2016

24-L, Pallotta, C. Clemente, A. De Maio, J. J. Soraghan, "On The Use of Image Moments for ATR from SAR Images", NATO SET on Radar Imaging and Target Identification, Pisa, Italy, 19-20 October 2015

23-R, Zhang , G. Li, C. Clemente, P. K. Varshney, "Helicopter Classification via Period Estimation and Time-Frequency Masks", IEEE workshop on Computational Advances in Multi-Sensor Adaptive Processing (CAMSAP 2015), 13-16 December 2015, Cancun, Mexico - **Invited Paper - Special Session on Sparse Time-Frequency Analysis**

22-C. V. Ilioudis, C. Clemente, M. H. Asghari, B. Jalali, John Soraghan, "Edge Detection in SAR images using Dispersive Phase Stretch Transform", 2nd IET International Conference on Intelligent Signal Processing, ISP2015, 1-2 December 2015, London UK,

21-A. Persico, C. Clemente, C. Ilioudis, D. Gaglione, J. Cao, J. Soraghan, "Micro-Doppler based Recognition of Ballistic Targets using 2-D Gabor Filters", Sensor Signal Processing for Defence 2015, 9-10 September 2015, Edinburgh

20-M. Liguori, A. Izzo, C. Clemente, C. Galdi, M. di Bisceglie, J. Soraghan, "A Location Scale Based CFAR Detection Framework for FOPEN SAR Images", Sensor Signal Processing for Defence 2015, 9-10 September 2015, Edinburgh

19-Y. Chen, C. Clemente, S. Weiss, J. Soraghan, "Fractional Cosine Transform (FrCT)-Turbo based OFDM for Underwater Acoustic Communication", Sensor Signal Processing for Defence 2015, 9-10 September 2015, Edinburgh

18-F. K. Coutts, D. Gaglione, C. Clemente, G. Li, I. Proudler, J. Soraghan, "Label Consistent K-SVD for Sparse Micro-Doppler Classification", 2015 IEEE International Conference on Digital Signal Processing (DSP), Singapore, 21-24 July 2015 - **Invited Paper - Special Session on Sparse and Compressive Sensing in Radar**

17-Y. Chen, C. Clemente, S. Weiss, J. Soraghan, "Partial Fractional Fourier Transform

(PFRFT)-OFDM for Underwater Acoustic Communication”, EUSIPCO 2015, European Signal Processing Conference 2015, 31 August-4 September, Nice, France

16-J. Cao, C. Clemente, G. Mingotti, J. Soraghan, C. McInnes, “A Novel Approach for Earth Remote Sensing Using FEMT-Satellites In Sun Synchronous Orbit”, International Astronautical Conference, IAC 2015, 12-16 October 2015, Jerusalem, Israel

15-D. Gaglione, C. Clemente, F. Coutts, G. Li, J. Soraghan, “Model-Based Sparse Recovery Method for Automatic Classification of Helicopters”, IEEE International Radar Conference 2015, Arlington, USA, 11-15 May 2015 - **1st Prize at the Best Student Paper Competition**

14-C. Clemente, T. Parry, G. Galston, P. Hammond, C. Berry, C. Ilioudis, D. Gaglione, J. Soraghan, “GNSS Based Passive Bistatic Radar for Micro-Doppler based Classification of Helicopters: Experimental Validation”, IEEE International Radar Conference 2015, Arlington, USA, 11-15 May 2015

13-C. Ilioudis, C. Clemente, I. Proudler, J. Soraghan, “Performance Analysis of Fractional Waveform Libraries in MIMO Radar Scenario”, IEEE International Radar Conference 2015, Arlington, USA, 11-15 May 2015 - **Invited Paper - Special Session on MIMO Radar- 3rd Prize at the Best Student Paper Competition**

12-V. Carotenuto, A. De Maio, C. Clemente, J. Soraghan, “Multi-polarization SAR change detection with invariant decision rules”, IEEE Radar Conference 2014, Cincinnati, USA, 19-23 May 2014

11-L. Pallotta, C. Clemente, A. De Maio, J. Soraghan, A. Farina, “Pseudo-Zernike Moments Based Radar Micro-Doppler Classification”, IEEE Radar Conference 2014, Cincinnati, USA, 19-23 May 2014

10-C. Clemente, I. Shorokhov, I. Proudler, J. Soraghan, “Radar Waveform Libraries Using Fractional Fourier Transform”, IEEE Radar Conference 2014, Cincinnati, USA, 19-23 May 2014

9-C. Clemente, C. Ilioudis, D. Gaglione, K. Thompson, S. Weiss, I. Proudler, J. Soraghan, “Reuse of Fractional Waveform Libraries for MIMO Radar and Electronic Countermeasures”, 6th International Symposium on Communications, Control, and Signal Processing (ISCCSP 2014), Athens, Greece, 21-23 May 2014

8-C. Clemente, L. Pallotta, I. Proudler, A. De Maio, J. Soraghan, A. Farina, “Multi-Sensor Full-Polarimetric SAR Automatic Target Recognition Using Pseudo-Zernike Moments”, International Radar Conference 2014, Lille, France, 13-17 October 2014

7-V. Carotenuto, C. Clemente, A. De Maio, J. Soraghan, “GLRT Based Scale-Invariant Multipolarization SAR Change Detection”, International Radar Conference 2014, Lille, France, 13-17 October 2014

6-C. Ilioudis, C. Clemente, I. Proudler, J. Soraghan, “Constant Envelope Fractional Fourier Transform based Waveform Libraries for MIMO Radar”, Sensor Signal Processing for Defence Conference 2014, 8-9 September 2014, Edinburgh, UK.

5-D. Gaglione, C. Clemente, L. Pallotta, A. De Maio, I. Proudler, J. Soraghan, “Krogager Decomposition and Pseudo-Zernike Moments for Polarimetric Distributed ATR”, Sensor Signal Processing for Defence Conference 2014, 8-9 September 2014, Edinburgh, UK.

4-V. Carotenuto, C. Clemente, A. De Maio, J. Soraghan, S. Iommelli, “Multi-Polarization

SAR Change Detection: Unstructured Versus Structured GLRT”, Sensor Signal Processing for Defence Conference 2014, 8-9 September 2014, Edinburgh, UK.

3-M. Asghari, C.Clemente, B.Jalali, J. Soraghan, “SAR Image Compression using DAST”, Global-SIP2014, 2-3 December 2014, Atlanta, GE, USA

2-C. Clemente, A. Miller, J. J. Soraghan, “Robust Principal Component Analysis for micro-Doppler based automatic target recognition”, 3rd IMA conference on Mathematics in Defence, 24- October 2013, Malvern (UK)

1-A. Miller, C. Clemente, A. Robinson, D. Greig, T. M. Kinghorn, J. J. Soraghan, “Micro-Doppler based target classification using multi-feature integration”, Intelligent Signal Processing (ISP) Conference, 2-3 December 2013, London (UK)

Magazine

1-D. Gaglione, "Student research highlights: MACHe - Model-based algorithm for classification of helicopters," in IEEE Aerospace and Electronic Systems Magazine, vol. 31, no. 8, pp. 38-40, Aug. 2016.

PhD projects Titles:

Mr Domenico Gaglione (PS6- ST) -*Automatic Target Recognition and Tracking from Radar*

Mr Christos Ilioudis (PS5- ST)– *Distributed MIMO Radar Systems*

Mr Jianlin Cao (ST)-*Spacecraft-on-a-chip concepts with application to Earth remote sensing*

Mr Yixin Chen (ST)-*Underwater acoustic Communication based on Multicarrier Scenario*

Mr Adriano Rosario Persico (ST)-*Radar signal processing for defence against airborne threats and space situation awareness*

Mr Alessio Izzo (ST)- *Acoustic MIMO Array Echo Cancellation Algorithms and Radar Technology based Audio Speakers Characterization*

Mr William Coventry (ST) - *Fine-Time Resolution of Passive RF imaging*

Mr Ilias Theodorou (ST) - *Space Debris Detection Based on Passive CubeSAT radar systems*

L_WP5 (EI): Low Complexity Algorithms and Efficient Implementation

1. Staffing

Work Package Leaders: Prof. Ian Proudler (LU), Dr. Stephan Weiss (ST)

Other Academics involved: Prof. John McWhirter (CU)

Research Associate: Dr. Keith Thompson (ST)

Other Research Associates: all other PDRAs (LU, SU, CU and ST) will be involved.

Contributing PhD Students: Jamie Corr (ST), Fraser Coutts (ST), Mohamed Alrmah (ST), and Ahmed Alzin (ST)

Project Partners: Mathworks and Texas Instruments,

Research Themes: T8 and T9

[dstl] Contacts: Dr David Nethercott, Dr George Jacob, and Dr Nick Goddard

2. Aims and Objectives of L_WP5

2.1 Lists of original aims in the case for support

To develop novel paradigms and implementation strategies for a range of complex signal processing algorithms operating in a networked environment. Links to L_WP1-L_WP4. (Relates to all themes)

Low complexity algorithms will be targeted by both generic efficient approaches to common themes across the consortium, such as high-dimensional array data, and application-specific low-cost implementations through collaborative research and active engagement with all other WPs.

L_WP5.1 Data reduction and distributed processing

Lower dimensional representation of data can lead to significant cost reduction, including data-independent techniques such as frequency domain, sub-band or subspace-based processing and thinning of sensor data. This work will exploit a combination of data dependent and independent techniques to achieve a significant data reduction, and will demonstrate how this can be exploited in low-cost algorithms. Due to operating in a networked environment, the efficient organisation of algorithms across a distributed processing platform will be considered. This work will explore algorithms and applications from across all work packages. Areas of study include (i) Polynomial decompositions leading to sparse representations through data-dependent optimal transformations (e.g. Karhunen-Loeve transform (KLT)), for dimensionality reduction in beamformers (ii) Parallel implementations of linear algebra functions and distributed processing methods (e.g. systolic array design, IP core implementations, vector-codebook methods) to minimise the communications bandwidth between processing nodes and (iii) Statistical signal processing problems will be utilised to map algorithms to distributed processors, whereby constraints on the communication bandwidth between nodes need to be set (e.g. Bayesian belief network (BBN) structures).

L_WP5.2 Hardware Realisations

Collaborating with Texas Instruments, PrismTech, and Steepest Ascent (now Mathworks), numerically efficient schemes are to be derived, with mappings onto suitable processing platforms to be investigated that demonstrate real-time algorithms in suitable test scenarios. Multi-core GPU-based platforms and programming environments such as CUDA are an enabling technology for massively parallel processing of data (facilitating real-time applications at low cost, but potentially high power consumption). In contrast, micro-controllers, DSP and FPGA based processing platforms are perfect candidates for low power, inexpensive sensor processing units. In collaboration with industrial partners, state-of-the-art Multicore DSP/FPGA embedded solutions are to emerge that are capable of matching the power performance-price constraints posed by the range of specific problems arising within all work packages of the consortium.

2.2 Modification to Aims and Objectives

Some tasks have changed during the project, as stipulated by quarterly meetings and the midterm review. Particularly w.r.t. the latter, L_WP5 objectives, sub-tasks and progress points were updated to the following:

Objectives

- L_WP5.1) Exploit recently developed spatio-temporal techniques based on polynomial matrix decompositions to generate sparse representations of broadband signals to aid in distributed signal detection and separation.
- L_WP5.2) Propose computationally efficient realizations based on parallel implementation.

2.3 Progress against Objectives and Subtasks

Overall Progress against Objective

The aim of WP5 is to develop novel paradigms and implementation strategies for complex signal processing algorithms in a networked environment. With a focus on polynomial matrix methods, we have made significant progress in terms of understanding the underlying theory, algorithm enhancement, further updating of a unique Matlab toolbox that supports a range of applications where we have demonstrated the method's benefits. We also took several steps to promote the uptake of polynomial matrix approaches by the wider community.

We now are fully equipped in terms of hardware processing platforms to undertake implementations, and have started to assist other WPs with algorithm implementation in hardware. For the remainder of the project, WP5 will continue to exploit the consortium's unique expanding expertise on polynomial methods and their applications, and work to enable hardware realisations by interacting with other WPs.

Progress against Sub-Tasks

L_WP5.1) Data reduction and distributed processing

- *Element completed* - A Matlab toolbox on polynomial matrix decomposition has been created and made available to the public with support from MathWorks. In the area of polynomial matrix decompositions fast converging algorithms have been developed. Numerical speed-up of implementations have been achieved using e.g. Jacobi sweeps instead of an eigenvalue decomposition (polynomial matrix methods were adopted as an example implementation and area of focus at the 2nd quarterly LSSC meeting).
- *Ongoing* - Review of Bayesian belief networks; further development of polynomial matrix methods, with applications to beamforming and sonar.

- *Future* - Activities will be directed towards distributed beamforming, the application of polynomial matrix methods to sonar dataset; general assistance with numerical optimisation for WP1-4.

L_WP5.2) Hardware realisations

- *Element completed* - Hardware kits for FPGA, multicore DSP and CPU processing have been acquired, with an FPGA implementation of a wideband transceiver completed; attendance of TI training courses; some sample implementations on FPGA platforms have been completed and published.
- *Ongoing* – Continued development of sample implementations for all three platforms; and hardware implementation of a polynomial matrix decomposition algorithm are currently undertaken.
- *Future* - Assistance to WP1-4 for hardware realisation of workpackage-specific solutions.

In the following sections of this report more details are included to elaborate on the technical progress made.

3. Progress made in the 4th year in addressing the original objectives

In the 4th year of the project, L_WP5.1 has further driven the progress of numerically efficient algorithms of interest to the consortium. In particular, polynomial matrix decompositions capable of formulating and providing novel solutions to broadband multichannel problems have been further pursued in a number of directions, ranging from the underlying theoretical understanding to algorithm development, provision of enhanced routines in our PEVD Matlab toolbox, to exploring new applications.

In L_WP5.2, hardware realisations have been driven forward, and demonstrator kits for FPGA, DSP, and GPU computing platforms are now available and operational. Some sample implementations have been pursued in collaboration with WPs 1 and 4, and in tandem with L_WP5.1, hardware implementation of some the latest developments in PEVD algorithms is in progress.

3.1 Progress of L_WP5.1 (Efficient Algorithms, Data Reduction and Distributed Processing)

In L_WP5.1 the focus of Keith Thompson has been on understanding complex signal processing algorithms, in particular Gaussian mixture models and techniques for distributed processing. The former is in particular to assist WP1 (Cardiff) with algorithm realisation. Keith is also involved in the ongoing development of PEVD algorithms through the co-supervision, with Dr. Stephan Weiss, of PhD students Jamie Corr, Fraser Coutts, and Ahmed Alzin, has been supervising a number of undergraduate projects in the area of WP5 (Radar implementation etc), and provides support in maintaining the PEVD Matlab Toolbox.

The focus of Stephan Weiss and Ian Proudler has been particularly in the context of L_WP5.1, with the aim of exploring theory, algorithms, applications and implementations of polynomial matrix approaches. A number of different iterative polynomial matrix eigenvalue decomposition (PEVD) algorithms have now been developed, and progress continues to be made in terms of algorithm performance, further enhancing accuracy and computational speed, and the cultivation of new application areas. The majority of these algorithms, together with a representative number of demonstrations, are contained in the PEVD Matlab toolbox.

These techniques have been promoted in a dedicated 1st International Workshop on Polynomial Matrix Decompositions, held at the Kavli International Centre at the Royal Society's Chicheley Hall, in August 2016, chaired by John McWhirter and Stephan Weiss. On behalf of the consortium, Stephan also presented a tutorial on polynomial matrices at the IEEE Sensor and Multichannel Signal Processing Conference (SAM 2016) in Rio de Janeiro in July 2016.

3.2 Progress of L_WP5.2 (Hardware Implementations)

The focus of Dr. Keith Thompson has been on further developing capability of implementing complex algorithms across a range of different computing platforms and devices. To support this objective, recent hardware development options acquired by the group in Strathclyde are detailed below. Access to computational resources and supporting training materials has been made available to consortium partners. Not all algorithms are suitable for full implementation in hardware (FPGA/ASIC), therefore different options for developing solutions with suitable hardware/software partitions are desirable.

- Xilinx Kintex-7 FPGA Digilent Genesys2 (50,950 slices, 16mb BRAM, 840 DSPs, 1Gb DR3)

<http://www.digilentinc.com/Products/Detail.cfm?NavPath=2,719,1488&Prod=GENESYS2>

- Xilinx Zync-7000-based Zedboard (Dual-Core ARM Cortex A9, 13300 logic slices, 512mb DDR3, 220 DSP slices)
<http://www.xilinx.com/support/university/boards-portfolio/xup-boards/XUPZedBoard.html>
- TI Multicore DSP 66AK2L06 (2x ARM Cortex A15, 4x C66x DSP cores, 2x FFT Co-processor, 2GB DDR3)
<http://www.ti.com/tool/xevmk2lx>
- GPU Laptop – Quad-core Intel i7, Nvidia GTX 970M with 1280 CUDA Cores, 3Gb DDR5,
<http://www.geforce.co.uk/hardware/notebook-gpus/geforce-gtx-970m/specifications>
- Qualcomm Snapdragon - Intrinsic's Open-Q™ 805 Embedded Development Kit incorporates quad-core ARM-based CPUs each 2.5 GHz, with 16GB eMMC 5.0, & 3GB PoP LPDDR3 RAM
<https://www.intrinsic.com/snapdragon-embedded-development-kits/openq-805-development-kit/>

The Qualcomm Snapdragon development kit has recently been acquired with support from Leonardo (formerly Selex ES) for the development of suitable image processing algorithm implementations (to involve MSc industrial project students). The Snapdragon processing architecture has been selected as the basis for the new Firefly IR camera from Leonardo <http://www.leonardocompany.com/en/-/firefly>, a power efficient imaging sensor designed for use on a variety of airborne/ground platforms. Initially, the goal is to identify various video analytics algorithms of interest, and look to adapt them toward deployment on the Snapdragon embedded processor. As a smartphone platform, the Snapdragon SoC has been designed with the Android OS in mind, with the Snapdragon 820 Development Kit from

Intrinsyc delivered with this pre-loaded (with a potential option for Linux) facilitating Java-based algorithm development.

Current implementation work is focused on FPGA implementation of a video image segmentation algorithm for Anomaly Detection, in collaboration with WP1, FPGA implementation of Polynomial EVD algorithms, and SAR image formation algorithms implemented on Multicore ARM & DSP device. Further details are provided in Section 4.2.

4. Technical Details

4.1 L_WP5.1 Polynomial EVD Theory, Implementations and Applications

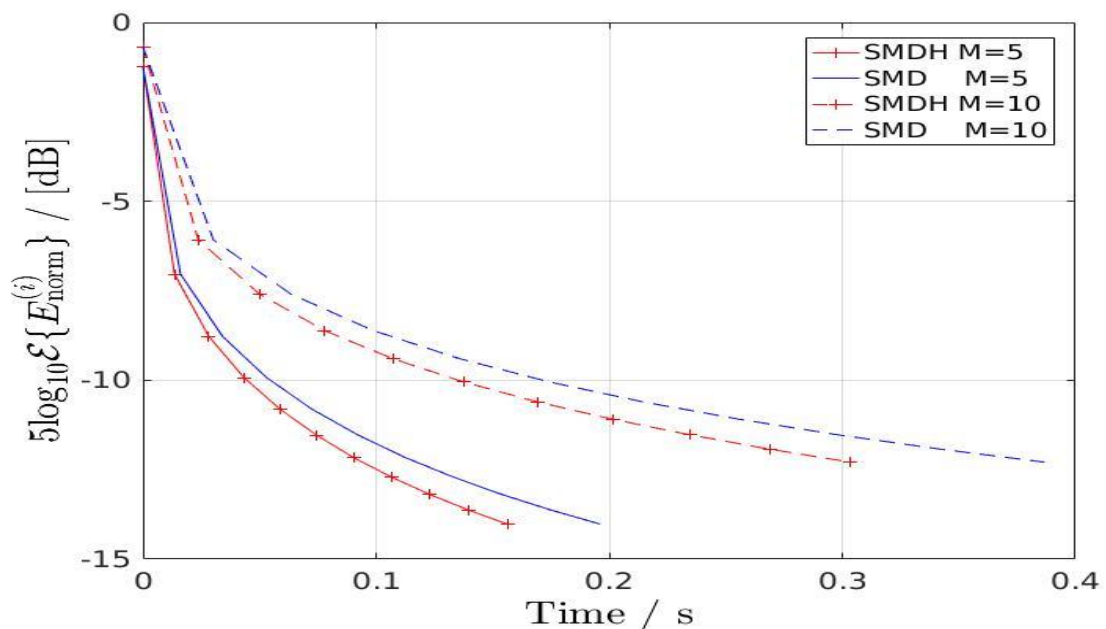
Further development of polynomial matrix algorithms have remained a core part of the work carried out in WP5. These methods have been found to have great utility across both WP3 and WP5, and are of particular interest to Dstl in the Sonar domain. The novelty and wide-ranging implications of the work have also been recognised by hosting dedicated events: the 1st International Workshop on Polynomial Matrix Decompositions and Applications, held from 24th to 26th of August 2016 at the Royal Society's Chicheley Hall chaired by John McWhirter and Stephan Weiss, a tutorial session on 'Polynomial Matrix Decompositions with Applications' at the IEEE Sensor Array and Multichannel Signal Processing Workshop in Rio de Janeiro, Brazil in July 2016, organised by Stephan Weiss and John McWhirter, and delivered with support from Zeliang Wang and Jamie Corr, two research students working at Cardiff and Strathclyde Universities. A potential special session – given sufficient participation – has been accepted for the forthcoming European Signal Processing Conference in Kos, Greece, in August 2017. A further special session proposal has also been submitted to a linear algebra conference to be held in Glasgow in summer 2017, organised by Jennifer Pestana from Strathclyde's Department of Mathematics and Statistics in conjunction with Stephan Weiss, Ian Proudler and John McWhirter. Particularly the Chicheley workshop has been a transformative event, and the research in this area is now advancing rapidly our theoretical understanding of the general approach, and will lead to improved numerical and computational efficiency, to new application domains, and to practical implementations in hardware.

Improved Computational Performance and Algorithm Speed-Up

Complexity and Search Space Reduction in Cyclic-by-Row PEVD Algorithms [Coutts 2016a]. Further investigation into previously defined Cyclic-By-Row PEVD algorithms has yielded significant gains in computational efficiency. The SMD PEVD algorithms first reported in WP5 have been shown to provide the twin benefit of greater diagonalisation performance together with a much reduced implementation cost, i.e. a reduced order of filters defined by the polynomial factors that algorithm yield. The Cyclic-by-Row approximation was later identified as providing a significant benefit in terms of reducing the computational cost of the SMD approach by replacing an 'exact' EVD step with a Cyclic-By-Row approximation. New methods developed have allowed the complexity (in terms of MACs) of this algorithm to be reduced by approximately 50%. This has been achieved by collecting the

rotations to be applied to the zero-lag of the Parahermitian matrix into a concatenated unitary matrix. This allows all rotations to be applied in one single step rather than successively applying individual sparse rotations across the entire polynomial matrix on each iteration. An innovative ‘Reduced Search Space’ strategy has also been defined to provide further computational cost savings through limiting the search region around the zero-lag where maximum off-diagonal elements are identified. The exact size of this search space can be adapted as the iterative process is executed by maintaining an understanding of the overall distribution of energy in the parahermitian matrix being diagonalised. Measured cost reductions for some arbitrary 5x5 and 10x10 matrices are detailed in Fig.1.

Figure 1:



Caption: Algorithmic cost reduction in terms of execution time when only operating on one half of a Parahermitian matrix [Coutts 2016a].

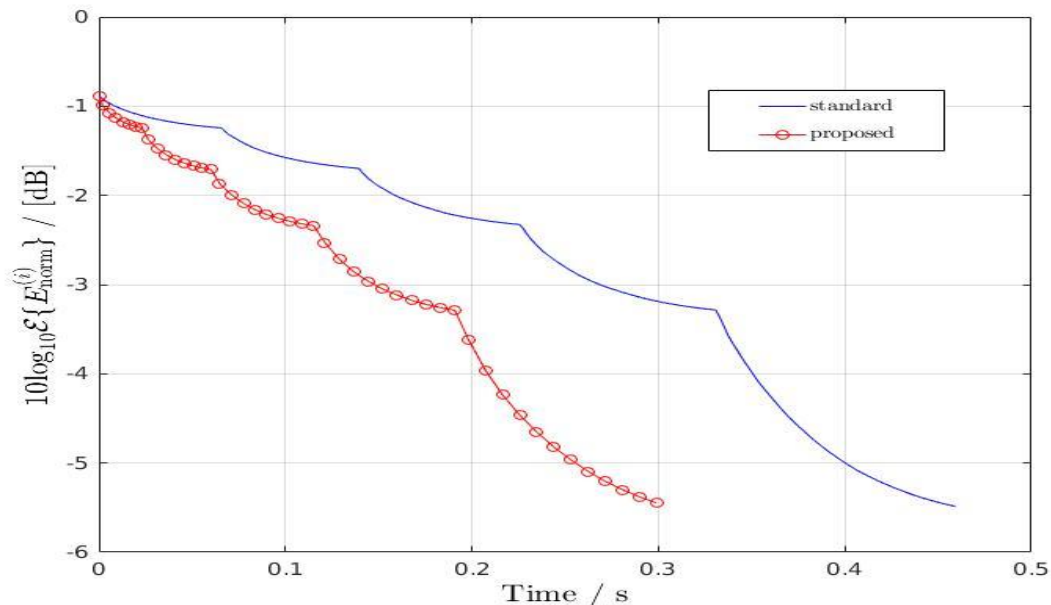
Multiple-Shift Algorithms for Polynomial Matrices

In the development of computationally faster PEVD algorithms such as the sequential matrix diagonalisation approach, the general concept of shifting more off-diagonal energy per algorithm iteration (multiple-shift) has been found to be advantageous when factorising a Parahermitian matrix by means of a polynomial matrix EVD. This has led to the consideration of tackling other useful matrix decompositions using a similar approach. One very useful matrix decomposition is the QR decomposition of a matrix into $A = QR$, where Q is orthogonal matrix, and R is upper triangular, which is found in many matrix-inversion based problems. A multiple-shift QR decomposition for polynomial matrices has therefore been defined which demonstrates a significant increase in computational efficiency, as measured by transfer of energy from lower-triangular to upper-triangular space against time.

This work [Coutts 2016c] extends research that had previously been conducted at the University of Cardiff. Fig. 2 shows the reduction of this polynomial QRD compared to the initial work proposed at Cardiff.

Meanwhile, the idea of a multiple-shift algorithm has been applied to the original PEVD algorithm, the second order sequential best rotation (SBR2) method at Cardiff in [Wang 2015].

Figure 2:



Caption: *Reduction of algorithm complexity for a polynomial QRD algorithm, showing the remaining energy in the lower left triangular matrix vs the algorithm execution time [Coutts 2016c]. The benchmark is the original polynomial QRD algorithm by Joanne Foster et al. [Foster 2010].*

Parallelisation through Partitioning of Covariance Matrix

An important recent aspect of the work on polynomial matrix techniques is to consider how larger scale problems may be tackled, along with how the algorithms can be parallelised. The PEVD algorithms operate on a space-time covariance matrix that is estimated through computing the correlation of sensor array inputs, where the number of sensor inputs (N) thus dictates the size of the matrix to be decomposed (N×N). Therefore, for large arrays of sensors, such as found in towed sonar array applications, this will result in a very large data structures to be handled. Furthermore, as this matrix is parahermitian in nature, i.e. conjugate-symmetric across the zero-lag, the potential for partitioning of data to perform a conventional single-Instruction-Multiple-Data (SIMD) parallel processing approach is not immediately clear. This has clear implications for the potential exploitation of the algorithms in custom parallel hardware. Nevertheless, recent outcomes have identified the potential for a larger-scale parahermitian covariance matrix to be partitioned effectively to allow PEVD algorithms to be applied in parallel (i.e. multiple PEVD threads). The optimisation of this approach is

considered for submission to EUSIPCO 2017, and is to form the basis for the development of a PEVD hardware demonstrator.

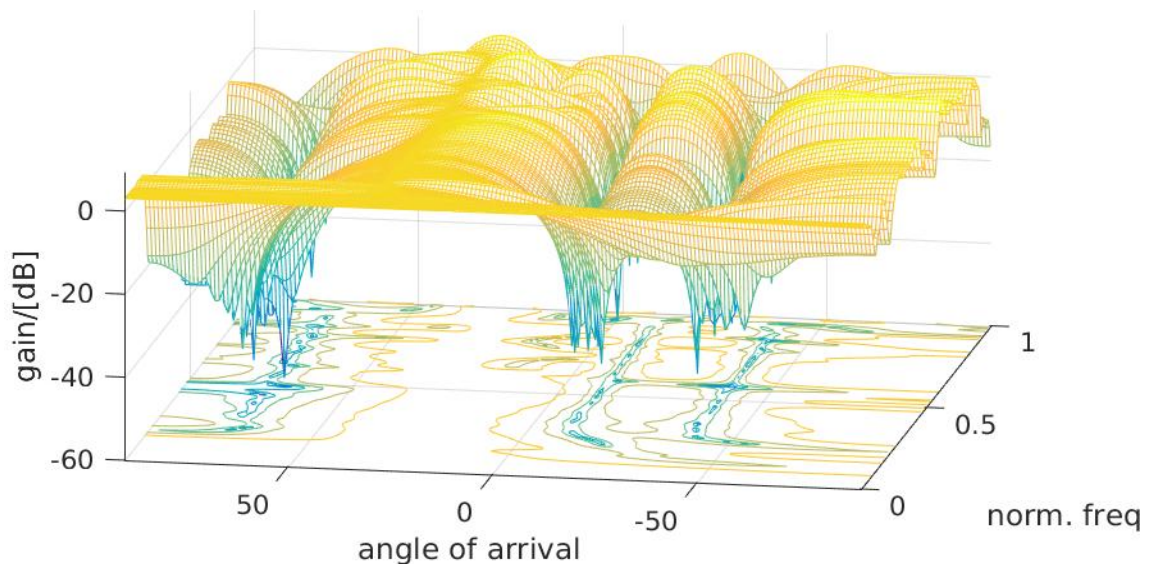
Extension to other polynomial matrix factorisation

An important development that extends the potential utilization of polynomial matrix techniques to new applications has been the extension of an existing narrowband technique, the generalized EVD (GEVD) to the broadband case using polynomial matrices. This work is a fruit of collaboration with Prof. Marc Moonen's group at KU Leuven where a GEVD algorithm has been successfully developed to tackle Multichannel Wiener Filtering (MWF) problems, such as noise cancellation in distributed sensor applications. To extend to the broadband case, a polynomial GEVD technique has been defined that solves a joint diagonalisation problem, where covariance matrices from multiple arrays are decomposed using a two-step Cholesky decomposition ($A = LL^*$) approach [Corr 2016]. Research on an enhanced polynomial QR decomposition algorithm using multiple-shifts per iteration has already been outlined earlier [Coutts 2016c].

Polynomial matrix formulations for broadband beamforming

Broadband beamforming had been successfully targetted as an application of polynomial matrix factorisations, where a broadband generalised sidelobe canceller could be easily extended from the narrowband to the broadband case, and solved in a fashion that decoupled the complexities of the quiescent vector, the blocking matrix and the adaptive process, which yielded significant reduction in computational complexity. In the meanwhile, we have extended this work to formulate and solve for a polynomial matrix-based Capon beamformer [Alzin 2016]. The gain response of a Capon beamformer design with look direction towards 30 degrees in the presence of three interferers is shown in Fig. 3.

Figure 3:



Caption: *Array gain vs angle of arrival and normalised operating frequency for a bradoand capon beamformer design detailed in [Alzin 2016].*

Broadband Blind Source Separation

Collaboratively with the University of Cardiff and a former colleague, Prof Soydan Redif, applications of polynomial EVD methods to the problem of broadband blind source separation have been summarised in [Redif 2017]. This includes various approaches, such as domain-weighted filtering, in order to extract a signal of interest from various interfering sources. This work is currently extended to include a polynomial GEVD approach to BSS, by Soydan Redif and Ian Proudler, submitted to EUSIPCO. Further, an investigation into the existence and uniqueness is likely to yield important results on the well-known permutation problem in BSS, which typically limits the performance of BSS algorithms,

4.2 L_WP5.2 Technical Details for WP5.2

WP5.2 is to develop novel computationally efficient hardware realizations using the latest hardware options. In this section we highlight the work currently underway in support of developments in WP5.1 and to support colleagues from other work packages.

Evolving GMM for Image Segmentation – FPGA Implementation

In collaboration with Dr. Ioannis Kaloskampis (WP1, Cardiff) a custom FPGA implementation is in development to help accelerate the main computational bottleneck identified in the ‘Evolving Gaussian Mixture Model (GMM) for Online Video Segmentation’ techniques completed for Anomaly Detection [Kaloskampis 2014]. The algorithm development by Ioannis builds on earlier algorithm developments from Figueiredo and Jain (2002) where an Unsupervised Learning approach to the problem of mixture modelling was outlined. The algorithm avoids particular well-known drawbacks of the standard Expectation-Maximization (EM) approach to density estimation through mixture modelling. In particular, the EM approach is very sensitive to initialization conditions where the number of components in the mixture must be selected a priori. The algorithm from Figueiredo and Jain [Figueiredo 2002] moves away from this approach by adopting a Minimum Message Length (MML) criterion where the number of components is first initialised as an arbitrarily large number and the algorithm seeks to then infer an appropriate structure from data to effectively merge the components. This unsupervised approach is particularly valuable in terms of image segmentation in video as consecutive frames can be subject to abrupt changes (where anomalies are of interest).

In order to implement the algorithm on FPGA hardware, a fundamental reworking of the algorithm has been required. The learning algorithm defined by Figueiredo and Jain (2002), and modified by WP1 with further adaptive parameters, is an iterative algorithm (composed of nested While loops) which has been converted into a more hardware-friendly Finite-State-Machine model of computation. Whilst it is possible to model and simulate iterative algorithms (composed of conditional while loops) after conversion to RTL language (vhdl), the process of logic synthesis demands that the number of loop iterations to be performed

must be bounded (as the logic synthesizer tools seek to unroll loops detected in RTL level code into individual parallel logic components, the number loop iterations must be pre-determined).

In order to increase the speed of computation and take advantage of the innate parallelisation capability of the FPGA, computational bottlenecks and areas for potential parallelisation have been identified. In particular, the algorithm repeatedly computes a measure (Bhattacharya distance) of the distance (dissimilarity) between the modified component densities with previously held versions stored in memory. A VHDL entity module has been defined to carry out this computation, where an approximation to the exponential function (trading-off approximation by Look-Up Table and iterative Cordic block) must be computed. This module has been instantiated multiple times to provide a parallel mechanism to compute these functions (with a further FSM to test whether number of components exceeds this number of modules, and thus reverting to a more serial execution if required). Further hyperbolic function approximation has been necessary to compute the natural log functions (\ln) required to evaluate the log-likelihood functions utilised by the algorithm to assess the success of and update conditional variables. The implementation has been designed using fixed-point numerical representation with a combination of Xilinx System Generator (Simulink) block-based design tools along with manual coding in vhdl. Final performance results are to be published in a forthcoming paper, and the utilisation of the implementation with surrounding pre- and post-processing stages also of interest in terms of delivering a more fully-featured demonstrator.

Polynomial EVD Algorithms – FPGA Implementation

The proposed FPGA implementation (outlined in previous updates) is in the process of being completed. The development was paused in order to complete the necessary work outlining the potential for the Divide-and Conquer (DC-DMD) algorithm to be applied in parallel through judiciously partitioning of the space-time covariance matrix (to be submitted). Key sub-modules of the implementation have been defined with the overall implementation now able to be completed. The pause in this development has been the need to diversify from an existing publication detailing the implementation of the original SBR2 algorithm on FPGA [Kasap 2014], where a well-established parallel Jacobi algorithm (limited to handling 2x2 submatrices in parallel) was modified for the polynomial matrix case. In the parallel approach to be adopted, we are no longer limited by the size of the submatrices to be computed in parallel, as the algorithm may now be applied independently to larger partitions of the overall matrix. The result should see significant improvement in computational performance.

SAR Image Formation – Multicore DSP

Synthetic Aperture Radar (SAR) data collection typically results in very large sets of complex data (temporal and spatial data capture, large dynamic range, etc.), with image formation a well-known computationally complex task. Numerous algorithms have been proposed in literature to tackle the task of SAR image formation, including the Range-Doppler and Backprojection algorithms. A number of researchers have identified significant

parallelism within such algorithms and have sought to accelerate the computation through leveraging many-core architectures such as GPUs [Clemente 2009] and reconfigurable FPGA hardware [Cordes 2009]. In this work we are evaluating the potential of our recently acquired multicore Texas Instruments Multicore ARM and DSP SoC device (66AKK2L06) for SAR image formation. This device has been promoted as a suitable candidate solution for SAR processing with significant benefits in terms of power efficiency versus GPU-based alternative approaches. The multicore DSP is integrated with multiple onboard hardware FFT co-processors to specifically accelerate the Range compression tasks utilised by the algorithms. A Strathclyde undergraduate project student is currently developing some suitable Matlab code that is to be converted into C code for implementation on the Multicore DSP device.

5. Linkages With Industry

Dstl

L_WP5 has maintained regular contact with David Nethercott, George Jacob, Nick Goddard at Dstl.

In the summer of 2016, Dr. George Jacob approached all WPs requesting further information about how LSSC(N) research could be adapted for exploitation as real-time algorithms (within an FPGA-based framework). L_WP5 is to coordinate this effort with support from the other WPs to attempt to collect the following information into a general survey:

- 1) Identify ‘Potential Algorithms that could be implemented in real-time
- 2) Performance of Algorithms in fixed-point form (after quantization)
- 3) Effort required to transform fixed-point algorithms toward HDL code generation

Overall, the ideal would be to extract some working code examples in Matlab, perform some numerical analysis using profiler and fixed-point conversion software tools, a literature search to identify similar existing implementation, and to reformulate the most suitable candidate algorithms into a realisable form for HDL Code-Generation (e.g. Simulink & System Generator).

Leonardo (formerly Selex ES)

Together with Strathclyde colleagues from L_WP4, L_WP5 has been heavily engaged in developing a relationship with Leonardo with regard to investigating the potential for new Neuromorphic Computing platforms to enable signal processing and machine learning techniques to be performed at very-low power. The initial stages of this work have been to complete a detailed literature and technology review of underlying computational concepts, available hardware and potential algorithms of interest. Further stages of the project are in the process of being determined. In tandem with this effort, Leonardo have initiated interest in

supporting industrial MSc projects based upon developing suitable image processing algorithms on a Qualcomm Snapdragon development kit.

Mathworks

L_WP5 has benefitted greatly from continued excellent support from our industrial partner Mathworks from contacts at both Mathworks Cambridge (Dr Marc Willerton) and Mathworks Glasgow (Dr Garrey Rice).

6. Future Plans

Carrying forward into the 5th and last year of this project, we aim for the following research to be completed:

Existence and Uniqueness of Polynomial Matrix EVD

A number of polynomial matrix algorithms have emerged over the past decade, and enabled a number of otherwise problems that had previously not been possible to solve. While many algorithms can be proven to converge in terms of minimising off-diagonal energy, it has been uncertain to what solution algorithms converge. Particularly for the paraunitary matrix factors, different algorithms often return different solutions. We will therefore characterise the existence of the decomposition, and the uniqueness of the polynomial eigenvalues and -vectors. Besides theoretical value, this is expected to have an impact on the creation of a new family of parahermitian matrix EVDs (as opposed to a polynomial EVD, which assumes a representation by finite power series), as well as a potential solution to the long-standing problem of source permutation in blind source separation.

PEVD Algorithms Operating in the Frequency Domain

Based on our theoretical investigations to date, enforcing spectral majorisation is detrimental to the order of factors in a polynomial matrix EVD (and by association, for polynomial QRD and polynomial GEVD). We will aim to extract analytic factors, which can be shown to exist and would yield maximally smooth solutions of hence lower order when either solved exactly or approximated by a polynomial.

Broadband Blind Source Separation

A polynomial EVD can be used for blind source separation in isolating decorrelated signals. However, there is ambiguity of how to associate eigenvalues in dependency of frequency, which is commonly known as the permutation problem in the BSS community. We believe that by enforcing maximally smooth eigenvalues and -vectors, we can address this problem adequately.

Broadband Beamforming

Based on various contributions in this area over the past year, we would like to wrap-up the application of polynomial matrix methods to broadband beamforming by considering robust methods. This can be achieved by setting up the constraint equation appropriately [Lorenz 2005]. Based on discussions with Sam Somasundaram at Thales, we will also be using a more realistic and state-of-the-art benchmark to which we can compare a polynomial solution.

PEVD Toolbox Evolution

Our toolbox will continue to expand, in terms of functions and algorithms to be included, but also in terms of the application examples and demonstrations that are incorporated.

Distributed Processing

Following Jamie Corr's visit to KU Leuven (Belgium) in 2016, we aim to continue this link and expand our current work on the polynomial generalised EVD to develop robust distributed beamforming and multichannel filtering algorithms.

Applications and Working With Real Data

Discussions with Nick Goddard (Dstl) and Sam Somadundaram (Thales) have taken place to address open problems in underwater data processing, as well as the application of polynomial matrix methods to sonar data sets. Jamie Corr is now likely to complete his PhD before an internship with Thales will materialise, but it is hoped that this activity can be carried forward with another researcher, such as Fraser Coutts who has only just started his 2nd year.

Hardware Realisations

With a number of systems in place, it is anticipated that during the last year of this project, a number of algorithms across the consortium can be implemented – at least in parts – in hardware, or the common algorithmic components can be demonstrated to be feasible in real time, therefore underpinning some of the scientific claims of the consortium by demonstrations of technical feasibility.

7. Academic Outputs

UDRC Output with Dstl Clearance: Journal and Conference Publications

[Alrmah 2014] M. Alrmah, J. Corr, A. Alzin, K. Thompson, and S. Weiss. Polynomial subspace decomposition for broadband angle of arrival estimation. In *Sensor Signal Processing for Defence*, pages 1–5, Edinburgh, Scotland, Sept. 2014.

[Alzin 2015] A. Alzin, F. Coutts, J. Corr, S. Weiss, I. K. Proudler, and J. A Chambers. Adaptive broadband beamforming with arbitrary array geometry. In *IET/EURASIP Intelligent Signal Processing*, London, UK, December 2015.

[Alzin 2016] A. Alzin, F. Coutts, J. Corr, S. Weiss, I. K. Proudler, and J. A Chambers. Polynomial Matrix Formulation-Based Capon Beamformer, *IMA International Conference on Mathematics in Signal Processing*, Birmingham, UK, December 2016.

[Corr 2014a] J. Corr, K. Thompson, S. Weiss, J. McWhirter, S. Redif, and I. Proudler. Multiple shift maximum element sequential matrix diagonalisation for parahermitian matrices. In *IEEE Workshop on Statistical Signal Processing*, pages 312–315, Gold Coast, Australia, June 2014.

[Corr 2014b] J. Corr, K. Thompson, S. Weiss, J.G. McWhirter, and I.K. Proudler. Maximum energy sequential matrix diagonalisation for parahermitian matrices. In *48th Asilomar Conference on Signals, Systems and Computers*, Pacific Grove, CA, USA, November 2014.

[Corr 2014d] J. Corr, K. Thompson, S. Weiss, J. McWhirter, and I. Proudler. Cyclic-by-row approximation of iterative polynomial EVD algorithms. In *Sensor Signal Processing for Defence*, pages 1–5, Edinburgh, Scotland, Sept. 2014.

- [Corr 2015a] J. Corr, K. Thompson, S. Weiss, I.K. Proudler, and J.G. McWhirter. Row-shift corrected truncation of paraunitary matrices for PEVD algorithms. In 23rd European Signal Processing Conference, pages 849–853, Nice, France, August/September 2015.
- [Corr 2015b] J. Corr, K. Thompson, S. Weiss, I.K. Proudler, and J.G. McWhirter. Shortening of paraunitary matrices obtained by polynomial eigenvalue decomposition algorithms. In Sensor Signal Processing for Defence, Edinburgh, Scotland, September 2015.
- [Corr 2015c] J. Corr, K. Thompson, S. Weiss, I.K. Proudler, and J.G. McWhirter. Impact of source model matrix conditioning on PEVD algorithms. In IET/EURASIP Intelligent Signal Processing, London, UK, December 2015.
- [Corr 2015d] J. Corr, K. Thompson, S. Weiss, I.K. Proudler, and J.G. McWhirter. Reduced search space multiple shift maximum element sequential matrix diagonalisation algorithm. In IET/EURASIP Intelligent Signal Processing, London, UK, December 2015.
- [Corr2015e] J. Corr, K. Thompson, S. Weiss, J.G. McWhirter, and I.K. Proudler. Performance trade-offs in sequential matrix diagonalisation search strategies. In IEEE 6th International Workshop on Computational Advances in Multi-Sensor Adaptive Processing, pages 25–28, Cancun, Mexico, December 2015.
- [Corr2016] J. Corr, J. Pestana, S. Weiss, I.K. Proudler, S. Redif, M. Moonen. Investigation of a Polynomial Matrix Generalised EVD for Multi-Channel Wiener Filtering. In Asilomar Conference on Signals, Systems and Computers, Pacific Grove, CA, November 2016.
- [Dowell 2014a] J. Dowell, S. Weiss, D. Infield, and S. Chandna. A widely linear multi-channel Wiener filter for wind prediction. In *IEEE Workshop on Statistical Signal Processing*, pages 29–32, Gold Coast, Australia, June 2014.
- [Elliot 2015] R. A. Elliot, A. Nagy, L. H. Crockett, K. Thompson, S. Weiss, and R. W. Stewart. Low-cost frequency-agile filter bank-based multicarrier transceiver implementation. In IET/EURASIP Intelligent Signal Processing, London, UK, December 2015.
- [Elliot 2016] R.A. Elliot, M.A. Enderwitz, K. Thompson, L.H. Crockett, S. Weiss, and R.W. Stewart. Wideband TV white space transceiver design and implementation. *IEEE Transactions on Circuits and Systems II: Express Briefs*, 63(1):24–28, January 2016.
- [Redif 2015] S. Redif, S. Weiss, and J. McWhirter. Sequential matrix diagonalization algorithms for polynomial EVD of parahermitian matrices. *IEEE Transactions on Signal Processing*, 63(1):81–89, January 2015.
- [Redif 2017] S. Redif, S. Weiss, and J.G. McWhirter. Relevance of polynomial matrix decompositions to broadband blind signal separation. *Signal Processing*, vol. 134, pp. 76-86, May 2017.
- [Wang 2015] Z. Wang, J.G. McWhirter, J. Corr, and S. Weiss. Multiple shift second order sequential best rotation algorithm for polynomial matrix EVD. Submitted to *European Signal Processing Conference*, Nice, France, September 2015.
- [Weiss 2013] S. Weiss, M. Alrmah, S. Lambotharan, J. McWhirter, and M. Kaveh. Broadband angle of arrival estimation methods in a polynomial matrix decomposition framework. In *IEEE 5th International Workshop on Computational Advances in Multi-Sensor Adaptive Processing*, pages 109–112, Dec. 2013.
- [Weiss 2015] S. Weiss, S. Bendoukha, A. Alzin, F.K. Coutts, I.K. Proudler, and J.A. Chambers. MVDR broadband beamforming using polynomial matrix techniques. In 23rd European Signal Processing Conference, pages 839–843, Nice, France, September 2015.

Software Output:

[Weiss 2014] S. Weiss, J. Corr, K. Thompson, J.G. McWhirter, and I.K. Proudler: PEVD Toolbox. Published online at pevd-toolbox.eee.strath.ac.uk, last updated December 2014.

Related Output (without Dstl Clearance):

[Allan 2016] D. Allan, L.H. Crockett, S. Weiss, K. Stuart and R.W. Stewart. FPGA Implementation of a Cyclostationary Detector for OFDM Signals. In 24th European Signal Processing Conference, Budapest, Hungary, pp. 642-646, August 2016.

[Alrmah 2013a] M. Alrmah, S. Weiss, S. Redif, S. Lambbotharan, and J. McWhirter. Angle of arrival estimation for broadband signals: A comparison. In *IET Intelligent Signal Processing*, London, UK, December 2013.

[Alrmah 2013b] M. Alrmah and S. Weiss. Filter bank based fractional delay filter implementation for widely accurate broadband steering vectors. In *5th IEEE International Workshop on Computational Advances in Multi-Sensor Adaptive Processing*, Saint Martin, December 2013.

[Alrmah 2013c] M. Alrmah, S. Weiss, and J.G. McWhirter. Implementation of accurate broadband steering vectors for broadband angle of arrival estimation. In *IET Intelligent Signal Processing*, London, UK, December 2013.

[Alshammary 2016] A. Alshammary and S. Weiss. Low-cost and accurate broadband beamforming based on narrowband sub-arrays. In International ITG Workshop on Smart Antennas, Munich, Germany, to appear, March 2016.

[Corr 2014c] J. Corr, K. Thompson, S. Weiss, J. G. McWhirter, and I. K. Proudler. Causality-Constrained multiple shift sequential matrix diagonalisation for parahermitian matrices. In 22nd European Signal Processing Conference, pages 1277–1281, Lisbon, Portugal, September 2014.

[Coutts 2016a] F.K. Coutts, J. Corr, K. Thompson, S. Weiss, I.K. Proudler, and J.G. McWhirter. Memory and Complexity Reduction in Parahermitian Matrix Manipulations of PEVD Algorithms. In 24th European Signal Processing Conference, Budapest, Hungary, September 2016.

[Coutts 2016b] F. Coutts, J. Corr, K. Thompson, S. Weiss, I.K. Proudler, J.G. McWhirter. Complexity and Search Space Reduction in Cyclic-by-Row PEVD Algorithms. In Asilomar Conference on Signals, Systems and Computers, Pacific Grove, CA, November 2016.

[Coutts 2016c] F. Coutts, J. Corr, K. Thompson, S. Weiss, I.K. Proudler, J.G. McWhirter. Multiple Shift QR Decomposition for Polynomial Matrices. In IMA International Conference on Mathematics in Signal Processing, Birmingham, UK, December 2016.

[Dowell 2013] J. Dowell, S. Weiss, Short-term prediction using Fraser Coutts, Jamie Corr, Keith Thompson, Stephan Weiss, Ian K. Proudler, John G. McWhirter: “Multiple Shift QR Decomposition for Polynomial Matrices”, IMA International Conference on Mathematics in Signal Processing, Birmingham, UK, Dec. 2016. an ensemble of particle swarm optimised FIR filters, *IET Conference on Intelligent Signal Processing*, London, 2013.

- [Dowell 2014b] J. Dowell, S. Weiss, D. Hill, and D. Infield. Short-term spatio-temporal prediction of wind speed and direction. *Wind Energy*, 17(12):1945–1955, December 2014.
- [Dowell 2014c] J. Dowell, S. Weiss, and D. Infield. Spatio-temporal prediction of wind speed and direction by continuous directional regime. In *13th International Conference on Probabilistic Methods Applied to Power Systems*, Durham, UK, July 2014. (Best student paper award)
- [Dowell 2015] J. Dowell, S. Weiss, D. Infield, Kernel Methods for Short-term Spatio-Temporal Wind Prediction. *IEEE PES General Meeting*, Denver, CO, 2015.
- [Karagiannakis 2013a] P. Karagiannakis, K. Thompson, J. Corr, S. Weiss, and I. K. Proudler. Distributed processing of a fractal array beamformer. In *IET Intelligent Signal Processing*, London, UK, December 2013.
- [Karagiannakis 2013b] P. Karagiannakis and S. Weiss. Analysis of a purina fractal beamformer. In *Asilomar Conference on Signals, Systems and Computers*, pages 466–470, November 2013.
- [Karagiannakis 2013c] P. Karagiannakis, S. Weiss, G. Punzo, M. Macdonald, J. Bowman, and R. Stewart. Impact of a Purina fractal array geometry on beamforming performance and complexity. In *21st European Signal Processing Conference*, pages 1–5, Marrakech, Morocco, September 2013.
- [McGuire 2013] C. McGuire and S. Weiss. Power-optimised multi-radio network under varying throughput constraints for rural broadband access. In *21st European Signal Processing Conference*, Marrakech, Morocco, September 2013.
- [McGuire 2014] C. McGuire and S. Weiss. Multi-radio network optimisation using Bayesian belief propagation. In *22nd European Signal Processing Conference*, pages 421–425, Lisbon, Portugal, September 2014.
- [Punzo 2014] G. Punzo, P. Karagiannakis, D. Bennet, M. Macdonald, and S. Weiss. Enabling and exploiting self-similar central symmetry formations. *IEEE Transaction on Aerospace and Electronic Systems*, 50(1):789–803, January 2014.
- [Wang 2016] Z. Wang, J.G. McWhirter, J. Corr, and S. Weiss. Order-Controlled Multiple Shift SBR2 Algorithm for Para-Hermitian Polynomial Matrices. In *IEEE Sensor Array and Multichannel Signal Processing Workshop*, Rio de Janeiro, Brazil, pp. 1-5, July 2016.
- [Weiss 2013] S. Weiss, M. Alrmah, S. Lambbotharan, J. McWhirter, and M. Kaveh. Broadband angle of arrival estimation methods in a polynomial matrix decomposition framework. In *IEEE 5th International Workshop on Computational Advances in Multi-Sensor Adaptive Processing*, pages 109–112, Dec. 2013.
- [Weiss 2015] S. Weiss, S. Bendoukha, A. Alzin, F.K. Coutts, I.K. Proudler, and J.A. Chambers. MVDR broadband beamforming using polynomial matrix techniques. In *23rd European Signal Processing Conference*, pages 839–843, Nice, France, September 2015.

8. References

- [Alrmah 2013a] M. Alrmah, S. Weiss, S. Redif, S. Lambbotharan, and J. McWhirter. Angle of arrival estimation for broadband signals: A comparison. In *IET Intelligent Signal Processing*, London, UK, December 2013.

- [Alrmah 2013b] M. Alrmah and S. Weiss. Filter bank based fractional delay filter implementation for widely accurate broadband steering vectors. In *5th IEEE International Workshop on Computational Advances in Multi-Sensor Adaptive Processing*, Saint Martin, December 2013.
- [Alrmah 2013c] M. Alrmah, S. Weiss, and J.G. McWhirter. Implementation of accurate broadband steering vectors for broadband angle of arrival estimation. In *IET Intelligent Signal Processing*, London, UK, December 2013.
- [Alrmah 2014] M. Alrmah, J. Corr, A. Alzin, K. Thompson, and S. Weiss. Polynomial subspace decomposition for broadband angle of arrival estimation. In *Sensor Signal Processing for Defence*, pages 1–5, Edinburgh, Scotland, Sept. 2014.
- [Alzin 2015] A. Alzin, F. Coutts, J. Corr, S. Weiss, I. K. Proudler, and J. A Chambers. Adaptive broadband beamforming with arbitrary array geometry. In *IET/EURASIP Intelligent Signal Processing*, London, UK, December 2015.
- [Alzin 2016] A. Alzin, F. Coutts, J. Corr, S. Weiss, I. K. Proudler, and J. A Chambers. Polynomial Matrix Formulation-Based Capon Beamformer, *IMA International Conference on Mathematics in Signal Processing*, Birmingham, UK, December 2016.
- [Carotenuto 2014] V. Carotenuto, A. De Maio, C. Clemente, J. Soraghan. “Multi-Polarization SAR Change Detection with Invariant Decision Rules”. In *IEEE Radar Conference*, 2014.
- [Cetin 2006] M. Cetin, L. Chen, J.W. Fisher III, A.T. Ihler, R.L. Moses, M.J. Wainwright, and A.S. Willsky. “Distributed Fusion in Sensor Networks”, In *IEEE Signal Processing Magazine*, volume 23, number 4, 2006.
- [Clemente 2009] C. Clemente, M. Di Bisceglie, M. Di Santo, N. Ranaldo, M. Spinelli. Processing of Synthetic Aperture Radar Data with GPGPU. In *IEEE Workshop on Signal Processing Systems (SiPS)*, 2009.
- [Cordes 2009] B. Cordes, M. Leeser. Parallel Backprojection: A Case Study in High-Performance Reconfigurable Computing. In *EURASIP Journal on Embedded Systems*, vol. 2009, p.1 2009.
- [Corr 2014a] J. Corr, K. Thompson, S. Weiss, J. McWhirter, S. Redif, and I. Proudler. Multiple shift maximum element sequential matrix diagonalisation for parahermitian matrices. In *IEEE Workshop on Statistical Signal Processing*, pages 312–315, Gold Coast, Australia, June 2014.
- [Corr 2014b] J. Corr, K. Thompson, S. Weiss, J.G. McWhirter, and I.K. Proudler. Maximum energy sequential matrix diagonalisation for parahermitian matrices. In *48th Asilomar Conference on Signals, Systems and Computers*, Pacific Grove, CA, USA, November 2014.
- [Corr 2014c] J. Corr, K. Thompson, S. Weiss, J. G. McWhirter, and I. K. Proudler. Causality-Constrained multiple shift sequential matrix diagonalisation for parahermitian matrices. In *22nd European Signal Processing Conference*, pages 1277–1281, Lisbon, Portugal, September 2014.
- [Corr 2014d] J. Corr, K. Thompson, S. Weiss, J. McWhirter, and I. Proudler. Cyclic-by-row approximation of iterative polynomial EVD algorithms. In *Sensor Signal Processing for Defence*, pages 1–5, Edinburgh, Scotland, Sept. 2014.
- [Corr 2015a] J. Corr, K. Thompson, S. Weiss, I. Proudler, and J. McWhirter. Row-shift corrected truncation of paraunitary matrices for PEVD algorithms. Submitted to *European Signal Processing Conference*, Nice, France, September 2015.

- [Corr 2015b] J. Corr, K. Thompson, S. Weiss, I.K. Proudler, and J.G. McWhirter. Shortening of paraunitary matrices obtained by polynomial eigenvalue decomposition algorithms. In *Sensor Signal Processing for Defence*, Edinburgh, Scotland, September 2015.
- [Corr 2015c] J. Corr, K. Thompson, S. Weiss, I.K. Proudler, and J.G. McWhirter. Impact of source model matrix conditioning on PEVD algorithms. In *IET/EURASIP Intelligent Signal Processing*, London, UK, December 2015.
- [Corr 2015d] J. Corr, K. Thompson, S. Weiss, I.K. Proudler, and J.G. McWhirter. Reduced search space multiple shift maximum element sequential matrix diagonalisation algorithm. In *IET/EURASIP Intelligent Signal Processing*, London, UK, December 2015.
- [Corr2015e] J. Corr, K. Thompson, S. Weiss, J.G. McWhirter, and I.K. Proudler. Performance trade-offs in sequential matrix diagonalisation search strategies. In *IEEE 6th International Workshop on Computational Advances in Multi-Sensor Adaptive Processing*, pages 25–28, Cancun, Mexico, December 2015.
- [Corr2016] J. Corr, J. Pestana, S. Weiss, I.K. Proudler, S. Redif, M. Moonen. Investigation of a Polynomial Matrix Generalised EVD for Multi-Channel Wiener Filtering. In *Asilomar Conference on Signals, Systems and Computers*, Pacific Grove, CA, November 2016.
- [Coutts 2016a] F.K. Coutts, J. Corr, K. Thompson, S. Weiss, I.K. Proudler, and J.G. McWhirter. Memory and Complexity Reduction in Parahermitian Matrix Manipulations of PEVD Algorithms. In *24th European Signal Processing Conference*, Budapest, Hungary, September 2016.
- [Coutts 2016b] F. Coutts, J. Corr, K. Thompson, S. Weiss, I.K. Proudler, J.G. McWhirter. Complexity and Search Space Reduction in Cyclic-by-Row PEVD Algorithms. In *Asilomar Conference on Signals, Systems and Computers*, Pacific Grove, CA, November 2016.
- [Coutts 2016c] F. Coutts, J. Corr, K. Thompson, S. Weiss, I.K. Proudler, J.G. McWhirter. Multiple Shift QR Decomposition for Polynomial Matrices. In *IMA International Conference on Mathematics in Signal Processing*, Birmingham, UK, December 2016.
- [Dowell 2013] J. Dowell, S. Weiss, Short-term prediction using an ensemble of particle swarm optimised FIR filters, *IET Conference on Intelligent Signal Processing*, London, 2013.
- [Dowell 2014a] J. Dowell, S. Weiss, D. Infield, and S. Chandna. A widely linear multi-channel Wiener filter for wind prediction. In *IEEE Workshop on Statistical Signal Processing*, pages 29–32, Gold Coast, Australia, June 2014.
- [Dowell 2014b] J. Dowell, S. Weiss, D. Hill, and D. Infield. Short-term spatio-temporal prediction of wind speed and direction. *Wind Energy*, 17(12):1945–1955, December 2014.
- [Dowell 2014c] J. Dowell, S. Weiss, and D. Infield. Spatio-temporal prediction of wind speed and direction by continuous directional regime. In *13th International Conference on Probabilistic Methods Applied to Power Systems*, Durham, UK, July 2014. (Best student paper award)
- [Dowell 2015] J. Dowell, S. Weiss, D. Infield, Kernel Methods for Short-term Spatio-Temporal Wind Prediction. *IEEE PES General Meeting*, Denver, CO, 2015.
- [Elliot 2012] R. Elliot, M.A. Enderwitz, L.H. Crockett, S. Weiss, and R.W. Stewart. “Efficient TV White Space Filter Bank Transceiver”. In *20th European Signal Processing Conference*, Bucharest, Romania, September 2012.

- [Figueiredo 2002] M.A.T. Figueiredo, A.K. Jain. Unsupervised Learning of Finite Mixture Models. In *IEEE Transactions on Pattern Analysis and Machine Intelligence*, Volume: 24, Issue: 3, March 2002.
- [Foster 2010] Foster JA, McWhirter J, Davies MR, Chambers JA, An algorithm for calculating the QR and singular value decompositions of polynomial matrices, *IEEE Transactions on Signal Processing*, 58(3):1263-1274, March 2010.
- [Kalokampis 2014] I. Kaloskampis, Y. Hicks. Estimating Adaptive Coefficients of Evolving GMMs for Online Video Segmentation. In 6th International Symposium on Communications, Control and Signal Processing (ISCCSP), 2014.
- [Karagiannakis 2013a] P. Karagiannakis, K. Thompson, J. Corr, S. Weiss, and I. K. Proudler. Distributed processing of a fractal array beamformer. In *IET Intelligent Signal Processing*, London, UK, December 2013.
- [Karagiannakis 2013b] P. Karagiannakis and S. Weiss. Analysis of a purina fractal beamformer. In *Asilomar Conference on Signals, Systems and Computers*, pages 466–470, November 2013.
- [Karagiannakis 2013c] P. Karagiannakis, S. Weiss, G. Punzo, M. Macdonald, J. Bowman, and R. Stewart. Impact of a Purina fractal array geometry on beamforming performance and complexity. In *21st European Signal Processing Conference*, pages 1–5, Marrakech, Morocco, September 2013.
- [Koller 2009] D. Koller and N. Friedman. “Probabilistic Graphical Models - Principles and Techniques”, MIT Press, 2009.
- [Lorenz 2005] R.G. Lorenz and S.P. Boyd. Robust minimum variance beamforming. In *IEEE Transactions on Signal Processing*, vol. 53, no. 5, pp. 1684-1696, May 2005.
- [McEliece 1998] R.J. McEliece, D.J.C. Mackay, and J-F. Cheng: “ Turbo Decoding as an Instance of Pearl’s ‘Belief Propagation’ Algorithm,” *IEEE Journal on Selected Areas in Communications*, 16(2):140-152, 1998.
- [McGuire 2013] C. McGuire and S. Weiss. Power-optimised multi-radio network under varying throughput constraints for rural broadband access. In *21st Europea Signal Processing Conference*, Marrakech, Morocco, September 2013.
- [McGuire 2014] C. McGuire and S. Weiss. Multi-radio network optimisation using Bayesian belief propagation. In *22nd European Signal Processing Conference*, pages 421–425, Lisbon, Portugal, September 2014.
- [McWhirter 2007] J.G. McWhirter, P.D. Baxter, T. Cooper, S. Redif, and J. Foster: “An EVD Algorithm for Para-Hermitian Polynomial Matrices,” *IEEE Transactions on Signal Processing*, 55(5):2158-2169, 2007.
- [Proudler 2007] I.K. Proudler, S. Roberts, S. Reece, and I. Rezek: “An Iterative Signal Detection Algorithm Based on Bayesian Belief Propagation Ideas,” *15th International Conference on Signal Processing*, 2007.
- [Punzo 2014] G. Punzo, P. Karagiannakis, D. Bennet, M. Macdonald, and S. Weiss. Enabling and exploiting self-similar central symmetry formations. *IEEE Transaction on Aerospace and Electronic Systems*, 50(1):789–803, January 2014.
- [Raynal 2013] M. Raynal. “Distributed Algorithms for Message-Passing Systems”, Springer-Verlag, 2013.

- [Redif 2015] S. Redif, S. Weiss, and J. McWhirter. Sequential matrix diagonalization algorithms for polynomial EVD of parahermitian matrices. *IEEE Transactions on Signal Processing*, 63(1):81–89, January 2015.
- [Redif 2017] S. Redif, S. Weiss, and J.G. McWhirter. Relevance of polynomial matrix decompositions to broadband blind signal separation. *Signal Processing*, vol. 134, pp. 76-86, May 2017.
- [Üney 2014] M. Üney and M. Cetin. “Optimization of decentralized random field estimation networks under communication constraints through Monte Carlo methods”, In *Digital Signal Processing*, 34, 16–28, 2014.
- [Wang 2015] Z. Wang, J.G. McWhirter, J. Corr, and S. Weiss. Multiple shift second order sequential best rotation algorithm for polynomial matrix EVD. Submitted to *European Signal Processing Conference*, Nice, France, September 2015.
- [Wang 2016] Z. Wang, J.G. McWhirter, J. Corr, and S. Weiss. Order-Controlled Multiple Shift SBR2 Algorithm for Para-Hermitian Polynomial Matrices. In *IEEE Sensor Array and Multichannel Signal Processing Workshop*, Rio de Janeiro, Brazil, pp. 1-5, July 2016.
- [Weiss 2013] S. Weiss, M. Almah, S. Lambotharan, J. McWhirter, and M. Kaveh. Broadband angle of arrival estimation methods in a polynomial matrix decomposition framework. In *IEEE 5th International Workshop on Computational Advances in Multi-Sensor Adaptive Processing*, pages 109–112, Dec. 2013.
- [Weiss 2015] S. Weiss, S. Bendoukha, A. Alzin, F. Coutts, I.K. Proudler, and J.A. Chambers. MVDR broadband beamforming using polynomial matrix techniques. In *European Signal Processing Conference*, Nice, France, September 2015.